Design and Experimental Performance Test of Vapor Compression Refrigeration System Using Isuzu Cargo Space as Cabin for Fruit Transportation

Eyerusalem Samuel Abushe

A Thesis Submitted to

The department of Mechanical Engineering

School of Mechanical, Chemical and Materials Engineering

Presented in Partial Fulfillment of the Requirement for Degree of Master of Science in Automotive Engineering

Office of Graduate Studies

Adama Science and Technology University

November, 2022

Adama, Ethiopia

Design and Experimental Performance Test of Vapor Compression Refrigeration System Using Isuzu Cargo Space as Cabin for Fruit Transportation

Eyerusalem Samuel Abushe

Advisor**:** Gezahegn Habtamu Tafesse (PhD)

A thesis Submitted to

The department of Mechanical Engineering

School of Mechanical, Chemical and Materials Engineering

Presented in Partial Fulfillment of the Requirement for the Degree of Master of Science in Automotive Engineering

Office of Graduate Studies

Adama Science and Technology University

November, 2022

Adama, Ethiopia

DECLARATION

I declare that this thesis entitled "Design and Experimental Performance Test of Vapor Compression Refrigeration System Using Isuzu Cargo Space as Cabin for Fruit Transportation" is my original work. That is, it has not been submitted for the award of any academic degree, diploma or certificate in any other university. All sources of material that are used for this thesis have been duly acknowledged through citation.

______________________ ______________________ ______________________

Name of student Signature Date

RECOMMENDATION

I, the major advisor/supervisor of this thesis, hereby certify that I have read the revised version of the thesis entitled "Design and Experimental Performance Test of Vapor Compression Refrigeration System Using Isuzu Cargo Space as Cabin for Fruit Transportation" prepared under my guidance by Eyerusalem Samuel submitted in partial fulfillment of requirement for Master of Science in automotive engineering. Therefore, I recommend the submission of revised version of the thesis to the department following the applicable procedures.

______________________	______________________	______________
Major Advisor/Supervisor	Signature	Date

APPROVAL PAGE

I the advisor of the thesis entitled "Design and Experimental Performance Test of Vapor Compression Refrigeration System Using Isuzu Cargo Space as Cabin for Fruit Transportation" developed by Eyerusalem Samuel, here by certify that the recommendation and suggestion made by the board of examiners are appropriately incorporated into the final version of the thesis.

______________________	______________________	________________
Major Advisor	Signature	Date

We, the undersigned, members of the Board of Examiners of the thesis by Eyerusalem Samuel have read and evaluated the thesis entitled entitled "Design and Experimental Performance Test of Vapor Compression Refrigeration System Using Isuzu Cargo Space as Cabin for Fruit Transportation" and examined the candidate during open defense. This is, therefore, to certify that the thesis is accepted for partial fulfillment of the requirement of the degree of Master of Science in Automotive Engineering.

______________________	______________________	________________
Chairperson	Signature	Date
______________________	______________________	________________
Reviewer 1	Signature	Date
______________________	______________________	________________
Reviewer 2	Signature	Date

Finally, approval and acceptance of the thesis is contingent upon submission of its final copy to the Office of Postgraduate Studies (OPGS) through the Department Graduate Council (DGC) and School Graduate Committee (SGC).

______________________	______________________	________________
Department Head	Signature	Date
______________________	______________________	________________
School Dean	Signature	Date
______________________	______________________	________________
Office of Postgraduate Studies	Dean Signature	Date

ACKNOWLEDGMENT

I would like to start by extending my deepest gratitude to my Lord Jesus Christ enabling me to undertake my studies and this research. I would like to thank my husband Dr. Biniyam Yosef for his encouragement and deep support. I would like to sincerely thank my advisor Dr. Gezahegn Habtamu for his incredible contribution in shaping the foundation of this thesis. I would like to thank Dr. Addisu Bekele for sharing his materials during experimental work. At the end, I would like to dedicate this thesis project to my families whose complete support kept through the ups and downs of my academic life.

TABLE OF CONTENTS

CONTENTS PAGES

ACKNOWLEDGMENT....................iv

TABLE OF CONTENTS....................v

LIST OF TABLES....................ix

LIST OF FIGURES....................xi

ABBREVAITION....................xiv

LIST OF SYMBOLS....................xv

NOMENCLATURES....................xvi

GREEK LETTERS.................... xviii

DIMENSIONLESS NUMBER.................... xviii

ABSTRACT....................xix

CHAPTER ONE....................1

INTRODUCTION....................1

1.1. Background....................1

1.2 Statement of problem....................3

1.3. Objectives of the study....................4

1.3.1 General objective....................4

1.3.2 Specific objectives....................4

1.4 Significance of study....................5

1.5 Scope the study....................5
1.6 Limitation of study....................5
CHAPTER TWO....................6
LITERATURE REVIEW....................6
2.1 Different works in refrigerated vehicles....................6
2.2 Review on insulation material....................12
2.3 Different works on vapour compression refrigeration system....................15
2.4 Computational Fluid Dynamics (CFD) use for refrigerated vehicle body....................19
2.5 Conclusions from literature review....................21
2.6 Research gap....................22
CHAPTER THREE....................23
MATERIALS AND METHODS....................23
3.1 Introduction....................23
3.2 Materials....................23
3.3 Methodology....................24
CHAPTER FOUR....................29
DESIGN AND SELECTION OF THE REFRIGERATION SYSTEM MAIN COMPONENTS....................29
4.1 Introduction....................29
4.2 Selection of Main Components of the Vapor Compression Refrigeration System....................29

4.2.1 Compressor Selection 29

4.2.2 Condenser Selection 32

4.2.3 Evaporator selection 34

4.2.4 Selection expansion device 37

4.2.5 Refrigerant selection 38

4.2.6 Selection of Other essential components of refrigeration system 40

4.3 Cooling load demand estimation 42

4.4 Design of the major component 48

4.4.1 Sizing of the compressor 48

4.4.2 Sizing of Evaporator Coil 55

4.4.3 Sizing of the condenser 61

4.5 Design of insulation materials for cabin using ANSYS CFD Software 67

4.6 Analysis fuel consumption estimation 77

4.7 Summary of the design results 79

CHAPTER FIVE 80

SCALE DOWN PROTOTYPE DESIGN AND FABRICATION 80

5.1 Introduction 80

5.2 Scale down vapor compression refrigeration system 80

5.3 Fabrication and assembly of scale down refrigerator 83

5.3.1 Fabrication of evaporator 84

5.3.2 Fabrication of condenser 85

5.4 Other component of refrigerator..85

5.5 Assembly of refrigerator parts..85

5.6 Temperature measurement 88

CHAPTER SIX 91

EXPERMENTAL PERFORMANCE TEST OF REFRIGERATION SYSTEM....................91

6.1 Introduction 91

6.2 Experimental performance of the VCRS..92

6.3 Dimensional similarity 94

CHAPTER SEVEN 96

CONCLUSION AND RECOMMENDATION..96

7.1 Conclusions 96

7.2 Recommendation..97

REFERENCES 98

APPENDICES 103

Appendix A 103

Appendix B..104

Appendix C..106

Appendix D 108

Appendix E..109

LIST OF TABLES

Table 3.1 Material used for scale down prototype 23

Table 3.2 Material property 25

Table 3.3 Constituting of vehicle wall material from literature 25

Table 3.4 Constituting of vehicle wall material from literature 25

Table 3.5 Constituting vehicle wall from literature 26

Table 4.1 Ozone depletion factor of refrigerant 40

Table 4.2 Selected components of refrigeration system. 41

Table 4.3 Recommended temperature and relative humidity of different products 42

Table 4.4 Isuzu fruit transportation route cities starting from Arba minch to Adis Abeba and their maximum ambient temperature 43

Table 4.5 Common fruit that transported by Isuzu car in Ethiopia and their minimum storage temperature 43

Table 4.6 Summarized value of cooling load calculation 48

Table 4.7 Properties of R134a at evaporator temperature $\boldsymbol{Te = -2}$℃ and condenser pressure $\boldsymbol{Pc = 1000kPa}$ 53

Table 4.8 Properties of superheated R134a at condenser pressure $Pc = 1000kPa$ 54

Table 4.9 Based on the above equations, the mass flow rate, power of compressor and COP are achieved. 55

Table 4.10 Standard pipe size for evaporator and condenser 58

Table 4.11 C and M selection table for different Reynold value 61

Table 4.12 Simulation case 1 72

Table 4.13 Simulation case 2 73

Table 4.14 Simulation case 3 74

Table 4.15 Simulation case 4 75

Table 4.16 Simulation case 5 76

Table 4.17 Total power and brake specific fuel consumption 79

Table 5.1 Based on the above equations, the following results are achieved. 81

Table 5.2 Refrigerator system component description for scale down prototype 84

LIST OF FIGURES

Figure 1.1 Current fruits transportation system 2

Figure 1.2 The scale down vapor compression refrigeration system designed and tested in this thesis. 3

Figure 3.1 3D model of Refrigerated truck 27

Figure 3.2 Block diagram of methodology 28

Figure 4.1 Classification of compressor. 30

Figure 4.2 Classification of condenser 33

Figure 4.3 Evaporator classification 35

Figure 4.4 Classification of expansion valve 37

Figure 4.5 Temperatures vs. entropy diagram of an ideal VCRC 49

Figure 4.6 Pressures vs. enthalpy diagram of an ideal VCRC 53

Figure 4.7 Correction factor plot for single pass cross flow exchanger one fluid mixed the other unmixed 64

Figure 4.8 Insulation thickness 67

Figure 4.9 Back view of 3D model of Refrigerated truck 68

Figure 4.10 Side view of 3D model of Refrigerated truck 68

Figure 4.11 Top view of 3D model of Refrigerated truck 69

Figure 4.12 Front view of 3D model of Refrigerated truck 69

Figure 4.13 Mesh generation 71

Figure 4.14 Mesh quality 72

Figure 4.15 Wall temperature 72

Figure 4.16 Simulation result of case one..........73

Figure 4.17 Simulation result of case two..........74

Figure 4.18 Simulation result of case three..........75

Figure 4.19 Simulation result of case four..........76

Figure 4.20 Simulation result of case five 77

Figure 5.1 Evaporator 84

Figure 5.2 Condenser..........85

Figure 5.3 Compressor, capillary tube and filter drier..........85

Figure 5.4 Scale down prototype 87

Figure 5.5 Temperature measuring instrument (a) Digital thermocouple thermometer (b) k type thermometer (c) timer (d) k type thermocouple thermometer 87

Figure 5.6 Calibration temperature measuring instrument with ice..........88

Figure 5.7 Papaya fruit for experimentation..........88

Figure 5.8 Papaya inside refrigerator..........88

Figure 5.9 Papaya fruit used for on load test. 89

Figure 5.10 Papaya fruit used for full load test..........89

Figure 5.11 Papaya fruit with different depth for full load test. 89

Figure 5.12 Papaya fruit with different depth for on load test..........90

Figure 6.1 Temperature of evaporator at middle starting from atmospheric temperature.......92

Figure 6.2 Temperature of papaya at different depth for no load test 92

Figure 6.3 Temperature of papaya at different depth for full load test 93

Figure 6.4 Inlet temperature of evaporator with and without load 93

Figure 6.5 Middle temperature of condenser with and without load 94

Figure 6.6 Temperature of wall...95

ABBREVAITION

ASTU	Adama science and technology university	R12	Dichlorodifluoromethane
CFC	Chlorofluorocarbon	R11	Trichlorofluoromethane
COP	Coefficient of performance	R113	Trichloro-trifluoroethane
GWP	Global warming potential	R134a	Tetrafluoroethene
HCFC	Hydro chlorofluorocarbon	R152a	Difluoroethane
HCF	Hydrofluorocarbon	R22	Monochlorodifluoromethane
ODP	Ozone depletion potential		
BSFC	Brake specific fuel consumption		

LIST OF SYMBOLS

Capital letters

A	Area (m^2)
C	Heat capacity $(kj.kg^{-1})$
E	Energy (kJ)
F	Correction factor
G	Mass velocity $(kg.s^{-1}m^{-2}s)$
I	Irreversibility (kW)
K	Thermal conductivity$(W.m^{-1}K^{-2})$
L	Length (m)
P	Power (kW)
Q	Heat (kJ)
S	Entropy $(kJ.K^{-1})$
T	Temperature (K)
U	Overall heat transfer $(W.m^{-2}k^{-2})$
V	Volume (m^3)

Small letters

α	Diffusivity (m^2s^{-1})
c	Specific heat $(kg.kg^{-1}K^{-1})$
d	Diameter (m)
f	Coefficient rolling resistance
g	Gravity $(m.s^{-2})$
h	Specific enthalpy $(kJ.kg^{-1}K^{-1})$
m	Mass of products (kg)
r	Radius (m)
q	Specific heat $(kJ.kg^{-1})$
s	Specific entropy $(kJ.K^{-1}kg^{-1})$
t	Time (s)
v	Velocity $(m.s^{-1})$
x	Dryness factor

NOMENCLATURES

C_p	Specific heat capacity of the product $(kJ.kg^{-1}°C^{-1})$
ρ_{air}	Density of air$(kg.m^{-3})$
E_{in}	Energy entered to the system (kJ)
E_{out}	Energy leaves to the system (kJ)
F_w	Wheel force or total running resistance (N)
F_{grad}	Gradient force (N)
F_{ae}	Aerodynamic force (N)
F_a	Acceleration force (N)
F_R	Rolling resistance force (N)
h_f	Enthalpy at saturated liquid $(kJ.kg^{-1})$
h_{fg}	Enthalpy of super-heated vapor $(kJ.kg^{-1})$
h_g	Enthalpy saturated vapor $(kJ.kg^{-1})$
h_1	Specific enthalpy of refrigerant before compression $(kJ.kg^{-1})$
h_2	Specific enthalpy of refrigerant after compression$(kJ.kg^{-1})$
h_3	Specific enthalpy of refrigerant after cooling $(kJ.kg^{-1})$
h_4	Specific enthalpy of refrigerant after expansion $(kJ.kg^{-1})$
m_v	Mass of vehicle (kg)
T_{ebt}	Engine brake torque (Nm)
P_{ebt}	Engine brake power (kJ)
η_{tf}	Efficiency of tractive force
P_{comp}	Compressor power (kJ)
T_e	Temperature of evaporator (°C)
P_e	Suction pressure (kPa)
P_c	Discharge pressure (kPa)
T_c	Saturated temperature of condenser (°C)
T_2	Temperature at exit of compressor (°C)
T_{stor}	Storage temperature (°C)
T_i	Internal temperature or air temperature inside the room (°C)
T_o	External temperature or ambient air temperature (°C)
h_o	Heat transfer coefficient on the outer surface$(W.m^{-2}K^{-1})$
h_i	Heat transfer coefficient on the inner surface $(W.m^{-2}K^{-1})$
x_1, x_2	Thickness of wall insulating material (m)

k_1, k_2	Thermal conductivity of wall insulating materials $(W.m^{-1}K^{-1})$
T_{fru}	Product input temperature (℃)
Q_{tran}	Transmission heat load $(kWh.day^{-1})$
Q_{exra}	Extracted heat load $(kWh.day^{-1})$
Q_{inf}	Air infiltration heat load $(kWh.day^{-1})$
Q_{RES}	Fruit product respiration heat load $(kWh.day^{-1})$
Q_{in}	Heat gain by evaporator (kJ)
Q_{out}	Heat released by condenser (kJ)
s_1	Entropy at inlet of compressor $(kJ.kg^{-1}K^{-1})$
s_2	Entropy at exit of compressor $(kJ.kg^{-1}K^{-1})$
s_g	Entropy at saturated vapor $(kJ.kg^{-1}K^{-1})$
RESP	Respiratory temperature of the product $(kJ.kg^{-1})$
V_s	Vehicle speed $(km.hour^{-1})$
w_t	Weight of vehicle (kg)

GREEK LETTERS

σ	Entropy generated $(kW.K^{-1})$
τ	Time (s)
ρ	Density $(kg.m^{-3})$
π	Pi
ϵ	Emissivity
μ	Viscosity $kg.m^{-1}s^{-1}$

DIMENSIONLESS NUMBER

Nu	Nusselt number
Re	Reynold number
Pr	Prandtl number

ABSTRACT

Isuzu car is commonly used to transport perishable fruit freight in open cargo such as Tomato, potato, onion, cabbage, banana, and other perishable food stuffs without refrigeration and in open air transport. This mode of transportation exposes the fruit to fluctuating thermal stresses and excessive moisture losses before the fruits reach the market. This thesis focuses on designing vapor compression refrigeration system (VCRS) that can cool the Isuzu open loading space by enclosing it with a rectangular cabin space and testing the experimental performance of a scale down cabin. The dimension of the Isuzu cargo and the scale down cabin were 4.84m x 2.1 m x 2 m and 1.1 m x 0.6 m x 0.5m with cooling load of 4.319 kW and 0.4319 kW, respectively. The cooling load was estimated by considering transmission heat load through cabin, heat extracted from fresh fruit, respiration temperature load of product and entry of unconditioned air. The size of the condenser and evaporator were found to be 21.61m and 26.65m, for the actual cargo and 4.2m and 3.23m the scale down cabinet, respectively. The specific fuel consumption due to power of compressor and mass of cabin is studied. The estimated which increase fuel consumption on engine is 1.34 L/hour. Scale down model was tested for the cooling temperature without and with load of papaya fruit for three days. Infrared thermometer and thermocouple wires were used to measure temperature and surface of cabin. Experimental work result shows of free load and full load test it takes 45 minute and 1hour to becomes to storage temperature respectively. Using ANSYS WORKBENCH simulation of insulation material with different thickness and different cover material is done the result show fiber glass is the best cover material due thermal conductivity and density.

***Keywords**: Vapor Compression Refrigeration System, Isuzu cargo, scale down, Cold Chain, Transportation, insulation material*

CHAPTER ONE

INTRODUCTION

1.1. Background

A transport refrigeration system removes excess heat and provides temperature control for food products. The food products commonly transport by land transportation in Ethiopia are meat, dairy products, flowers and different fruits such as banana, orange, mango, tomato papaya and onion are the main ones by using unrefrigerated transports such as Isuzu cars. Global food losses are estimated to be as high as 45% for fruits and vegetables, 35% for seafood and fish, 30% for cereals, and 20% for dairy products and meat (Rech et al., 2020). As reported by (Rech et al., (2020) fruits and vegetables are highly perishable compared to the others. The main objective in the design of refrigerated transportation of fruits is to estimate the main components of the refrigeration system that maintain the product temperature at the optimum where metabolic and microbial deterioration are minimized so as to keep the freshness and to increase the shelf life. The main thermal conditions to be considered for design are the desired or ideal holding temperature & moisture control during storage and distribution (Brecht et al., 2019). and good hygienic state during transportation to avoid contaminants such as dust, (Jara et al.,2019). In general, these transportation systems are expected to maintain the temperature of the food within close limits to ensure its optimum safety and high-quality shelf-life and protect moisture loss due to solar heating during transportation.

Different kinds of fruit transportation systems are in use in the developed world. There are many technologies available for transport refrigeration like salt-water solution vapor absorption refrigeration system (VARS) (Venkataraman et al., 2020), cryogenic system using liquid nitrogen or liquid carbon oxide refrigerant (James, 2019), eutectic solution or phase change material (PCM) refrigerant systems suitable for short delivery (Tassou and De-Lille

2010) and the most common vapor compression refrigeration systems (VCRS) (Ahamed, Saidur, and Masjuki 2011). Some researchers attempt to use VARS for transportation (Garimella et al., 2011). This system's main components are binary mixture of absorber (salt) & water (or refrigerant), evaporator, heat driven refrigerant generator with rectifier, absorber, solution heat exchanger with pump that circulates the solution between the generator and absorber, condenser, expansion valve and refrigerant heat exchanger between the condenser & evaporator. In VARS, the mechanical compressor of VCRS is replaced by pump, generator and absorber (Venkataraman et al., 2020). Although this system operated with heat energy, it is not commonly used for transportation since it requires additional heat source that cannot be fulfilled using the car engine exhaust and occupies large space since it has many components. VCRS is better compared to VARS for Isuzu car fruit transportation used in Ethiopia but it requires external electric power. Figure 1.1 shows current fruit transportation system in Ethiopia.

Figure 1.1 Current fruits transportation system

Since it is easy to construct cabin over the Isuzu cargo space, it is possible to minimized fruit losses and deliver them to the market with preserved freshness. This thesis focuses on designing vapour compression refrigeration system (VCRS) that can cool the Isuzu open loading space by enclosing it with a rectangular cabin space theoretically and experimentally that can reduce expiration, wastage, deterioration of products and market lose.

Figure 1.2 The scale down vapor compression refrigeration system designed and tested in this thesis.

1.2 Statement of problem

In Ethiopia tomato, onion, avocado, banana, mangoes, oranges, papaya and other perishable food items transported to major city commonly adapting unrefrigerated vehicles and particularly Isuzu car is commonly used to transport freight in open cabin without refrigeration by exposing fruits and vegetables to sun and temperature fluctuation which will cause large tons of food product wastage/spoilage. These fruits have different desired delivery temperature as low as $5^{o}C$ and the weather condition they are exposed also depends on the areas of their production & destination and the design of the cabin. In this thesis, a refrigerated cabin for a medium sized Isuzu cargo and its one tenth scale down size was designed by estimating the cooling load that satisfies the cabin space and types of fruits to be transported. The major components of the refrigeration system for the cabin such as condenser and evaporator were designed using the standard correlations for both systems by considering transmission heat load through cabin, heat extracted from fresh fruit, respiration temperature load of product and entry of unconditioned air. During transportation of fruits using refrigerated cabin insulation material great impact on energy consumption of vehicle. CATIA Software for 3D model conceptual design of the refrigerated truck and ANSYS WORKBENCH were used for vary the insulation thickness and cover material. Experimentation were performance to identify the temperature distribution inside the cabin on the scale down model with papaya as a representative fruit and without load. The additional specific fuel consumption on the engine of the Isuzu car were also estimated using the cabin mass, compressor power requirement and its aerodynamic forces.

1.3. Objectives of the study

1.3.1 General objective

General objective of this work is designing a vapor compression refrigeration system for Isuzu car cargo space that can transport different fruits and carry out experimentation on a scale down refrigeration system.

1.3.2 Specific objectives

The specific objectives are

- To identify fruits items safe cold storage temperature ranges commonly transported by Isuzu car in Ethiopia,
- To identify the size (width and length) of the Isuzu cargo cars area for deciding the cooling chamber cabin for the fruits or estimate maximum cooling load requirement.
- To design a vapor compression refrigeration system that can cool a cabin constructed using an Isuzu car sizes for the estimated maximum cooling load.
- Estimate the increment in specific fuel consumption of the Isuzu car due to the added VCRS & cabin weight and aerodynamic drag,

- Varying insulation thickness and caver material insulated wall for best performance using ANSYS WORKBENCH.
- To develop a scale-down Isuzu freight cabin cooled by a vapor compression refrigeration system for experimentation

1.4 Significance of study

- food can be transported their destination without reducing nutritional value.
- freshness of food items is maintained and increase shelf life of foods.
- reduce wastage of food items and reduce market lose in the country.

1.5 Scope the study

Scope of this thesis work deals with design of VCRS which include the design of major component of VCRS condenser, evaporator and selecting other main component refrigeration system. Model of refrigerated truck designed by CATIA software and then transferred to ANSYS to study simulation of insulation thickness and cover material of insulation. Finally manufacturing of scale down prototype for experimental test of VCRS.

1.6 Limitation of study

Due to availability and cost the compressor used to expermenta1 work is take power from utility electric source. Solar heat gain during transportation of refrigerated truck is not considered in cooling load estimation due to color selected to refrigerated truck and speed of truck.

CHAPTER TWO

LITERATURE REVIEW

2.1 Different works in refrigerated vehicles

Glouannec et al., (2014) studied an experimental and numerical study of an insulation wall for a refrigerated panel van. The different experimental and numerical tools developed allowed the dynamic characterization of the thermal transfer within several multilayer insulation walls of the cabin. Reflective multi-foil insulation and aerogel layers gave good results, especially for limiting peak heat transfer and energy consumption during the daytime period. As a result, a 20% increase in the multilayer panel thickness resulted in a 36% reduction in energy when compared to the reference application. The use of a PCM layer to boost wall inertia yielded promising results as well. Nevertheless, for the experimental conditions tested, the layer could not fully melt or freeze during the eight-hour experimental periods. Work to optimize the size, emplacement and choice of the PCM layer are underway to increase the performances of the insulation wall.

Ilorkar et al., (2019) designed and developed e-vehicle that transport milk in controlled environment based on vapour compression refrigeration system (VCRS). By considering refrigeration load VCR system was designed and which include selection of compressor, refrigerant, power source to be used in VCR system for 100 liters capacity milk. Battery inverter combination has been used during running condition and AC power when stationary. To prevent heat transfer polyurethane foam (PUF) used as insulation. The heat load of milk, power of compressor and coefficient of performance (COP) calculated theoretically and also the performance of battery checked based on battery output, compressor input and output for every 15 minutes during 2h operation. The result of their work was theoretical COP is 3.46 at full load for 100 liters of milk and actual COP is 2.14 at full load for 100 liters of milk.

Jara et al., (2019) worked on the analysis of thermal behavior of refrigerated vehicle for food transportation to predict temperature distribution inside it. Computational fluid dynamics (CFD) used to model fluid flow situation. Temperature data is acquired using DS18B20 encapsulated sensor and ANSYS WORKBENCH for simulation of data obtained. MATLAB ARDUINO interface used also to facilitate the storage and analysis of data. In different range of climate condition refrigerated food transport vehicle performance was checked. The experimental temperature value was taken with the help of temperature sensors DS18B20, which have an accuracy of ±0. 5°C.The difference that occur between temperature value, measure, and simulated was acceptable.

Artuso et al., (2019) worked on dynamic modelling and thermal performance analysis of insulated box of refrigerated vehicle and validated it experimentally. A 0-D lumped parameter model is used to characterize the refrigerated box structure. The model is tuned and successively validated over experimental data. The cooling power required by the vehicle and the dynamic load that insists on the exterior surface of the structure are simulated after description and validation of the numerical model. Refrigerated cargo is modelled as the internal air volume of 9.75 m^3 has been considered and experimentally characterized. The truck body was first investigated under steady state conditions, to quantify its global heat transfer coefficient. The testing procedure is based on applying a known and controlled thermal load by electrical heating within the insulated box using fan-heat. The result of their work was best fit value of thermal capacity was found to be 47% higher than the one derived from stratigraphy while the best fit value of thermal resistance allowed by 23% lower than the one obtained by stratigraphy

Imtiaz et al., (2020) works also in refrigerated vehicle in their work numerical analysis carried out to assess the performance of refrigerated vehicle. Computational Fluid Dynamics (CFD) simulations are performed for each of the designs and crate arrangements along with the compartment design and product storage pattern for better air circulation and uniform temperature distribution which would result in an improved cooling and storage of goods. This study, ANSYS Fluent was used to perform the numerical analysis of different configurations. The result of assessment was the thermal performance improved more when vertical partitioning of the chamber was introduced. The percentage of products stored in the chamber within the acceptable temperature increased significantly when the chamber was vertically partitioned.

Adekomaya et al., (2017) studied a sustainable way of reducing energy consume in diesel engine driven vapor compression system of refrigerated vehicle. The best way to reduce energy consumption in refrigerated vehicles, according to the authors, is to find a material that is lightweight and has a low thermal conductivity to use for the exterior walls of the vehicles. All indications point to the thermal conductivity value (K) of the sandwiched insulation as the main factor influencing the performance of an insulated panel. The concept of energy demand in this medium of transportation is still not solved. Another possible area of exploration could be fiber reinforced polymer composite which is generally reported to be lighter in weight and have better dimensional and tensile properties.

Xiaofeng and Xuelai, (2020) presented research to couple cold storage materials and vacuum insulation panel technology to design multi-temperature zone cold chain logistics transportation equipment, namely a multi-temperature zone insulation box. A three-dimensional unsteady model was developed in their study to analyze the temperature fields in various parts of the box. Two different PCMs suitable for cold chain transportation were prepared. The experimental results reveal that the phase transition temperatures of PCM1 (n-octanoic acid-myristic acid composite) and PCM2 (potassium sorbate-water composite) are

7.1°C and -2.5°C, the latent heats of phase change are 146.1 and 256.2 J/g, and the thermal conductivities are 0.2832 and 0.9427 $W.m^{-1}K^{-1}$, respectively. The theoretical calculations reveal that 13.8 kg PCM1 is optimal for T2 and 12.1 kg PCM2 for T3. The multi-temperature insulation box can keep cold for 15 h. The experimental results show that the temperatures of T2 and T3 remained at 7°C and -2°C for 13 and 14h, respectively, and that of T1 was maintained at 19°C for these times.

Islam et al., (2019) studied transport refrigeration system and numerical simulation of refrigeration performance. Computational Fluid Dynamics (CFD) modeling is carried out to examine the effect of commonly practice storage pattern on performance of transport refrigeration system and the effect of goods loading pattern inside the refrigerated chamber of refrigeration vehicle on refrigeration performance. It is found that the commonly practiced storage pattern with crate causes considerable non-uniformity in the cold air and temperature distribution inside the refrigeration chamber. From the insight obtained from this study, it is recommended that a more detailed study should be carried out which would investigate the future prospect of integrating more energy conserving.

So et al., (2021) using experimental and numerical analysis techniques, it was studied how the loading patterns of the box affected the airflow and temperature change in the refrigerated body. CFD modelling with two different turbulence models (k-ϵ and SST k-w) was developed using COMSOL Multiphysics for predicting the temperatures inside boxes loaded with different patterns, and the predicted data were compared to the experimental data. Based on the experimental results, a temperature distribution model was developed for different loading patterns in the refrigerated body. For practical modelling, the k-ε model was selected as the turbulence model. In addition, the insulated walls and outside airflow were neglected in the modelling. In the developed model, the error increased when measurements were closer to the wall of the refrigerator body, but it was within an acceptable error range. This developed model can be applied in the future, taking into account the loading patterns, cargo, and box sizes for real transport environments.

Micheaux et al., (2016) worked on experimental and numerical investigation of heat and mass infiltration rates during the opening of a refrigerated truck body. The infiltration dynamics was found to involve two different ways: the first is buoyancy driven flow during this period, the density difference between the two volumes is the driving force. The volume flow rate reaches a peak value but quickly decays due to the temperature increase inside the truck body. The measured temperature and velocity profiles at the doorway and the CFD model, which assumes an instantaneous door opening, agree well. A very simple ODE model taking into account both mass and thermal inertia and the second a boundary layer flow. This is basically natural convection over the cold walls of the container. This phenomenon appears once the inside air has roughly reached a ceiling temperature of a few Kelvin below the outside temperature. Then, a quasi-steady-state heat transfer is observed until doors are closed, at a time that can reach 10 min in actual food deliveries.

Zhang et al., (2017) studied the stability of the temperature within a refrigerated vehicle during unloading has been studied using varied door geometries by examining how open doors of four different doors using computational fluid dynamics (CFD) models. The results show that, temperature inside the compartment increases due to large difference with respect to the ambient temperature, wind pressure and thermal pressure. The stability of the ambient temperature inside the refrigerated compartment affected by different door placement. The maximum root mean-square error for volume mean temperature and wind speed is 1.218℃ and 0.27 $m/_{s}$, respectively.

Getahun, (2018) studied the airflow distribution inside two types of refrigerated shipping containers (T-bar floor and flat floor) which used for transporting fresh fruit handling were investigated. (CFD) airflow model was created and experimentally confirmed. Then put into practice to investigate how container designs and operational circumstances affect airflow distribution and pattern. The two-reefer design's high and low evaporator speed possibilities were looked into. The result indicates that airflow distribution in the two container designs were markedly different. And reefer with T-bar floor design exhibited a noticeable reduction of air recirculation zone and enhanced uniform vertical air movement than reefer with flat floor design.

Senguttuvan et al., (2020) studied numerically analyzing the airflow patterns in the refrigerated container with Fifteen different design models of the refrigeration unit. By altering the refrigeration unit's effective dimensions and design criteria. By taking into account the pressure drops and flow characteristics of the refrigeration unit, the numerical simulation of the airflow inside the refrigerated container is carried out. By simulating the refrigeration unit's evaporator coil as a porous media, the pressure drop in the refrigeration unit is determined. In comparison to the refrigeration unit's base case design, the upgraded refrigeration unit's improved design offers much higher jet velocity, higher vertical velocity distributions, higher mass averaged velocity, and reduced areas of dead zones in the container. The mass averaged velocity in the refrigerated container with the improved refrigeration unit is 33.66% higher than that of the base case refrigerated container.

Oury et al., (2015) studied temperature distribution and air flow in the chamber of a refrigerated truck using CFD both with open door/cooling system on and closed door/ cooling system off. When the door is closed and the cooling system is turned on, the first way is applied, in which CFD and heat transport are somewhat decoupled. When the cooling system is turned off and the door is opened following a cooling period, the second (completely connected) technique calculates the natural convection that takes place. The simulation results are compared to experimental values. The result of their study shows that the COMSOL is a tool particularly well adapted for simulating non isothermal flow and it can be used for like to optimize the location or the power specifications of the cooling system as well as the design of the box walls and the associated materials.

2.2 Review on insulation material

Verma and Singh, (2020) studied by creating a system-level computer model of a household refrigerator, the impact of various insulation materials, with varied thickness, on the energy consumption, weight, inner-volume, and payback periods was evaluated. Polyurethane (PU) foam and vacuum insulation panels (VIPs) consisting of fumed silica, glass fiber, and alternative core materials are among the insulation materials. The results of their study were indicated that a fridge insulated with 10mm thick and the freezer with 20mm thick fumed silica VIP energy consumption decreased by 19.6% while increasing the inner volume by 148 liters and weight by 2.48 kg when compared with PU foam insulated refrigerator.

Sruti et al., (2020) studied the improvement of insulating material both theoretically and experimentally used in cool boxes. Theoretically three best insulating materials, polyurethane (PU), expanded polystyrene (EPS) and poly-glass fiber (PGF) selected out of six based on calculation and simulation. Then experimentally tested at three different room temperatures using thermal insulation test to determine the best insulating material for a cool box. The result of their study was, polyurethane recorded the best performing insulation material in terms of heat transfer and longest time taken for ice to change into water at the three different temperatures experimentally. Also resulting in better thermal insulation of the cool box.

Thiessen et al., (2018) study on the effectiveness of applying vacuum insulation panels in domestic refrigerator. Experimental analysis was done on the thermodynamic behavior of a normal home refrigerator that has vacuum insulation panels (VIPs) insulated in 16 different ways. Additionally, both the coverage area and the positioning of the panels have an impact on energy usage. The result observed from their study shows that the energy consumption is reduced by approximately 6% and 11 % when the doors and the rear wall are insulated with VIPs, respectively. It was also found that a coverage area of 56 % drops the energy consumption by 21%. refrigerated transport system by focusing on parameters such as the number and type of refrigerated vehicles, size, design, fuel consumption, type of refrigeration system, refrigeration performance, and energy efficiency. Some others also analysis thermal behavior.

Oludaisi et al., (2017) study to investigates the overall heat transfer coefficient of reinforced composite panel with the aim of being used as the internal and external cover sheet of the insulated panel. The result of their study shows that the overall heat transfer coefficient, U $(W.m^{-2}K^{-1})$value of the composite reinforced with 10%wt. of fiber at 0° orientation (G10E) offers the lowest U value of 0.386950 $(W.m^{-2}K^{-1})$ and 0.196680$(W.m^{-2}K^{-1})$ for 50mm and 100mm insulation thicknesses, respectively. This also shows their potential of being used as internal and external sublayer of insulation materials which may prolong the ageing period of insulation and increase the shelf life of fresh raw fruits.

Gupta et al., (2014) worked on optimum sizing of PV panel, battery capacity and insulation thickness for a photovoltaic operated domestic refrigerator. The PV-based refrigeration system is simulated using the transient simulation program (TRNSYS). and confirmed by data from experiments. The factors taken into consideration include the battery bank's capacity, the PV array's PV panel wattage, and the refrigerator's insulation variance. The result of their study indicates that 25 mm insulation thickness on solar photovoltaic (SPV) without grid power with 320 W panel arrays with 50 Ah battery capacity can operate refrigerator. At 50 mm thickness 200 W panel capacity is sufficient to drive the refrigerator.

Hammond and Evans, (2014) investigates the viability of using VIPs in the cold chain by incorporating VIPs into the polyurethane foamed walls of conventional refrigerator and freezer cabinets. With and without VIPs implanted in the insulating walls, thermal modelling of the insulation of a variety of typical refrigerator and freezer cabinets used throughout the cold chain was conducted. potential energy savings and payback times were then calculated; The result indicates that for refrigerators the average payback was 9.7 years, for freezers it was 4.5 years.

Taylor, (2007) studied the fundamental problem in design of insulation thickness. This study includes how incorporate the new generation of non-CFC (chlorofluorocarbons) materials in a composite layer which contains polyurethane foam and how to choose the thickness of each sublayer in the composite to reduce the overall cost over the refrigerator's lifetime. The second how distribute a given amount of insulation material around the refrigerator. The result shows non-CFC material can be used in a sandwich with polyurethane foam to provide thermal resistance and adequate mechanical stability. Insulation thicknesses for the freezer and cooler sections can be optimized so that the overall heat transfer rate is minimum.

Jae et al., (2012) study the optimization process for the insulation thickness to improve the energy efficiency of a total refrigerator-freezers (RF) system. which detailed the quantitative relationship between the COP and the individual compartment's insulation thickness. Additionally, the dual-loop cycle and the bypass two-circuit cycle performance of RF were examined for how the proposed optimization technique affected them. According to their research, using the suggested optimization technique resulted in energy consumption reductions of 5.7% and 6.1% for the bypass two circuit cycle and the dual-loop cycle, respectively.

2.3 Different works on vapour compression refrigeration system

Fikresendek, (2020) designed a domestic refrigerator that operates based on vapor compression refrigeration system (VCRS) and studied its experimental performance. The experimental performance was studied with and without integrating phase change material (PCM) at the condenser and refrigerator. Placing this PCM in condenser and evaporator to increase performance of refrigerator and to reduce temperature fluctuation. He designed major components of VCRS. Designed length of both evaporator and condenser and selected other component. SOLIDWORK software was used for design of refrigerator. Temperature measuring instrument used were like the digital thermocouple thermometer, mercury thermometer, and K type thermocouple wire. Refrigeration system designed was having cooling capacity of 0.433 kW with 0.186 kW compressor power input and cyclically operating R134a refrigerant working with -10 and 60 ℃ temperature of the condenser and evaporator, respectively in the pipe circuit. Finally assembled and manufactured the prototype. Experimental work was done with load and without load using water and by varying the thickness of PCM 2, 3 ,4 and 5 mm. The recommendation was Integration of a maximum 2 mm thick paraffin wax of on the condenser is recommended since the COP increase, on-off time reduces and on-off frequency increased.

Ajayi et al., (2019) worked to investigate experimentally the performance of the vapour compression refrigerator using Al2O3 nanoparticles dispersed with R-134a working fluid for single temperature domestic refrigerator. The outcome of their study indicates that the Al2O3 nanoparticle increase the performance of the refrigeration process with better efficiency. Addition to, the pH analyses indicate that the presence of the Al2O3 nanoparticles in the working fluid may have negative effects on the compressor walls and material. They recommended that for future better to determine anti-wear properties of the nano lubricant and ascertain the reliability of its application in a vapour compression refrigeration system.

Thavamani and Senthil, (2020) studied thermal performance of hydrocarbon blend refrigerant in a domestic refrigerator application. And domestic refrigerator designed for investigation purpose to work with HFC-R134a. The result of this study is the use of the HC blend refrigerant system faster rate of cooling by 7 min than that of the R134a refrigerant and the energy consumption of HC 17.86% lower than R134a refrigerant of the same cooling capacity with higher coefficient of performance.

Arora and Kaushik, (2008) studied theoretical analysis of a vapor compression refrigeration (VCR) cycle with R502, R404A, R507a. For R502, R404A, and R507A, a computational model has been created to calculate the coefficient of performance (COP), energy destruction, exegetic efficiency, and efficiency faults. This investigation has been done for evaporator and condenser temperatures in the range of -50°C to 0°C and 40°C to 40°C, respectively. The results of their study shows that R502 can be replaced by R507A rather than R404A. For the refrigerants taken into consideration, the efficiency fault in the condenser is largest and the liquid vapour heat exchanger is lowest.

Soni and Gupta, (2013) worked to provide a thorough exergy analysis for the theoretical vapour compression refrigeration cycle using R404A, R407C, and R410A. The research demonstrates that different results are obtained for the effect of evaporating temperatures, condensing temperatures, degree of subcooling, and effectiveness of liquid-vapor heat exchanger on COP, exegetic efficiency, and exergy destruction ration (EDR) of theoretical vapor compression refrigeration cycle. The COP and exegetic efficiency of R407C are better than those of R404A and R410A. The EDR of R410A is higher than that of R407C and R404A.

This analysis was carried out using the condenser temperature between 40 and 50 °C and the evaporator temperature between 50 and 0 °C.

Yeh et al., (2014) based on a finite temperature difference heat transfer method and irreversibility analysis, the effects of subcooling on the coefficient of performance, cooling water pressure drop of the condenser, and heat exchanger area for R1234yf, R1234ze, R22, R134a, and R410A in a single vapor-compression refrigeration system are being studied. The results of their study show that the maximum coefficient of initial cost saving and coefficient of operating cost saving and their corresponding optimum degree of subcooling increase with condensation temperature. At a higher inlet temperature of cooling water, the optimum degree of subcooling turns out to be smaller for all refrigerants. The outcomes are anticipated to make it easier to develop a future vapor-compression refrigeration system that can use different refrigerants.

Dalkilic and Wongwises, (2010) worked to study theoretical performance on a traditional vapor-compression refrigeration systems using mixes of HFC134a, HFC152a, HFC32, HC290, HC1270, HC600, and HC600a were tested in a variety of ratios and compared to CFC12, CFC22, and HFC134a as potential replacements. Taking into account performance coefficient (COP) in comparison to CFC12, CFC22, and HFC134a at a condensing temperature of 50 °C and an evaporation temperature range of -30 °C to 10 °C. The result of their study was refrigeration efficiency, (COP) of the system, increases with increasing Evaporating temperature for a constant condensing temperature in the analysis. And all systems including various refrigerant blends were improved by analyzing the effect of the superheating/subcooling case. Better performance coefficient values (COP) than those of the non-superheating/subcooling case are obtained as a result of their optimization.

Vaibhav et al., (2011) studied characteristics of different refrigerants like R22, R134a, R410A, R407C, and M20 that are used by global manufacturers to meet the challenges of higher efficiency and environmental responsibility while keeping their system affordable have been compared. This was done using a refrigerant property based thermodynamic model of a simple reciprocating system, which can simulate the performance of actual system as closely as possible. The result their study shows that R407C can be a potential HFC refrigerant replacement for new and existing systems presently using R22 with minimum investment and efforts.

Mehmet et al., (2019) study experimental analysis comparing performance of vapour compression refrigerating system until operating with R22 and its performance comparison to new HFC fluids R422A, R417A and R422D. With a semi-hermetic compressor, a coaxial evaporator, an air condenser, and a thermostatic expansion valve, the refrigerator used to evaluate the behavior of R22 substitutive fluid was equipped with the instrumentation required to gather data on temperature, pressure, and mass load of refrigerants. The evaporator was connected to an auxiliary containing water-glycol solution which supplied refrigerating load throughout the different test condition. The result of their study was R22 more energetically efficient other alternative fluid (R22A, R22D and R417) are characterized by ODP=0 in the existing installation they can easily replace R22 without changing lubricant, refrigeration circuit and accessories.

Baskaran et al., (2022) worked on performance investigation on a vapour compression refrigeration system was done using a variety of environmentally friendly refrigerants, including HFC152a, HFC32, HC290, HC1270, HC600a, and RE170. The findings were compared to R134a as a potential replacement alternative. The analysis's alternative refrigerants RE170, R152a, and R600a were shown to have somewhat higher performance coefficients (COP) than R134a at 500°C for condensation and between -300 and 100°C for evaporation, according to the data. Among other options, the refrigerant RE170 was discovered to be a replacement for R134a. In this study, an ideal vapor-compression system is used for the performance analysis of alternative new refrigerants substitute for R134a. The refrigerant RE170 was determined to be the best suitable substitute among those tested for R134a after comparing the performance coefficients (COP) and pressure ratio of the tested refrigerants as well as the primary environmental effects of ozone layer depletion and global warming.

2.4 Computational Fluid Dynamics (CFD) use for refrigerated vehicle body

Computational fluid dynamics (CFD) simulation applied in most disciplines involving to study characteristics of air flow inside insulated body of refrigerated vehicle. Furthermore, temperature spatial variability is also affected by frequent door openings refrigerated food vehicle are subjected to during their travel can studied by using CFD (Artuso et al., 2019)

Shear Stress Transport k-omega (SST k–ω)

The SST (Shear Stress Transport) k-omega turbulence model is a two-equation eddy viscosity model. It is a combination of both the k-epsilon and the k-omega turbulence models, using the former in the free-stream and the latter near the walls.

Turbulence Model

The turbulent flow is the type of viscous flow that is applied to most industries. It is a flow the main turbulence models are grouped into three families.

1. Reynolds-averaged Navier-Stokes (RANS) equations are obtained by time-averaging equations of motion over a coordinate in which the mean flow does not vary.

- Solve time-averaged Navier-Stokes equations
- All turbulent length scales are modeled in RANS
- Extensively used approach for calculating industrial flows.

2. Large Eddy Simulation (LES) solves large-scale flow motion while approximating small scale motions.

- Solves the spatially averaged N-S equations.
- Less expensive than DNS, but the number of computational resource and efforts are still too large for most practical applications.

3. Direct Numerical Simulation (DNS), in which Navier-Stokes equations are solved for all scales of turbulent flow motion, increasing accuracy as well as the time required for the calculation.

- Theoretically, all turbulent flows can be simulated by numerically solving the full Navier-Stokes equations.
- Resolves the whole spectrum of scales. No modeling is required.
- The cost is too excessive
- Not practical for industrial flows and not available in Fluent.

Reynolds-averaged Navier Stokes (RANS), Spalart-Allmara model and Standard k–ε (SKE) model

It's a low-cost RANS model for solving a modified eddy viscosity transport equation. It is useful for aerodynamics and transonic flows over airfoils because it is stable and has good convergence. Its limitation does not promise to apply to all sorts of complex engineering flows. The Standard k–ε e is the most extensively used turbulence model for industrial applications.

It has good convergence and cheap memory requirements. Compressible and incompressible flow are both supported. No-slip walls, unfavorable pressure gradients, severe curvature into a flow, and jet flows are not correct.

RNG *k_ε* and Realizable *k_ε*

Suitable for complex shear flows involving rapid strain, moderate swirl, vortices, and locally transitional flows (e.g., boundary layer separation, massive separation, and vortex shedding behind the bluff body). Offers largely the same benefits and has similar applications as RNG. Possibly more accurate and easier to converge than RNG.

Standard k–ω model

This model is utilized for good convergence, minimal memory requirements, and enhanced accuracy for internal flows, curvatures, separated flows, and jets. However, it is difficult to converge and sensitive to initial conditions.

Shear Stress Transport k-omega (SST k–ω)

The SST (Shear Stress Transport) k-omega turbulence model is a two-equation eddy viscosity model. It is a combination of both the k-epsilon and the k-omega turbulence models, using the former in the free-stream and the latter near the walls. SST k–ω selected because of Frist can be integrated to the wall without using any damping functions. Second accurate and robust for wide range of boundary layer flows with pressure gradient.

2.5 Conclusions from literature review

In the above reviews can be observed that most of researchers where try to study the existing of a refrigerated vehicle with the purpose of predicting the temperature distribution inside it numerically and experimentally. Moreover, a most of the efforts were done to study the exiting refrigerated vehicle by using Computational Fluid Dynamics (CFD) modelling using the CFX module of ANSYS WORKBENCH and also, they have done comparison between CFD and experimental data. Some others worked to investigate dynamic behavior of insulated body of refrigerated vehicle during transport mission also for exiting vehicle. In addition, other study to minimize energy consumption in refrigerated vehicles is to find a light weight and low thermal conductivity material as the external wall of refrigerated vehicles. In general, most researchers try to study the behavior of exiting refrigerated vehicle either by using Computational Fluid Dynamics and experimental method. Most of researchers work on VCRS experimentally by changing different refrigerant to improve performance of the system and reducing global warming.

2.6 Research gap

Fruit transportation in Ethiopia is commonly done by Isuzu car from the product site to different places without refrigeration. This car can be redesigned to be refrigerated by constructing cabin from locally available materials which is the critical part of the refrigerated vehicle. During transportation of product in refrigerated trucks the refrigerated cabin is exposed to temperature in different direction and fluctuation of temperature. The major challenges in cabin design is the effectiveness of the cabin wall in controlling heat loss to the atmosphere. Most literature shows walls of cabin constructed with different wall thickness. No literature worked on varying insulation thickness using ANSYS WORKBENCH software for local weather condition in the design of refrigeration cabin with different materials and thicknesses. This research focuses on the cabin design by varying insulation thickness with similar wall thickness and with different cover material to suitable to the weather condition.

CHAPTER THREE

MATERIALS AND METHODS

3.1 Introduction

In this chapter material used for scale down prototype of the vapor compression refrigeration system for conducting performance test and the methodology used for the simulation study particularly to determine the thickness of the cabin wall that is used to store fruits are described. The data collection methods and selection of materials for the refrigerator components are discussed. The CATIA model of a medium scale Isuzu car that can be used for ANYSYS simulation is developed and the description of the research methodology is shown with the block diagram.

3.2 Materials

Material, measuring device and system components required for developing experimental scale down prototype purchasing from local market. Material used to construct the scale down prototype depend on local availability and data from literature. The main material used in the experiment are presented. The materials required for thesis work are shown in Table 3.1.

Table 3.1 Material used for scale down prototype

No	Material
1	Copper Tube
2	Compressor
3	Refrigerant fluid
4	Insulation (material of body)
5	Capillary tube
6	Thermostat
9	Filter

3.3 Methodology

Different products like fruits, vegetables and other perishable food items by using Isuzu truck in Ethiopia transported from different parts of country to center areas primarily to Addis Ababa which leads highly to wastage of product. The waste of products can be reduced by designing the cargo space of Isuzu car to be used as refrigerator. Theoretical and experimental approach is used as methodology in this study. The research used governing equation of fluid flow & heat transfer and standard refrigeration system correlation to analyze major components of the refrigerator and experimental approach was used to test the performance of scale down prototype. For different analysis and modeling CATIA, ANSYS WORKBENCH, Microsoft excel will be used. The following methodology has been adopted in order to carry out this thesis wok:

(a) Literature Review

Latest literature and research work about on vapor compression refrigeration system on refrigerated trucks and insulation material is surveyed.

(b) Data collection

Meteorological data from Arbaminch to Addis Abeba and insulation material property with thickness from different literatures were collected. Collecting and measuring using primary and secondary data source.

(i) Primary data collection

Design of refrigerated vehicle cabin with dimension of 4.84 m of Length, 2.1 m of Width and 2 m of Height depending on literature reviews.

(ii) Secondary data

The materials needed for constructing the cabin insulation materials and their thermophysical properties are shown in Table 3.2. The thickness of the insulation materials recommended by literation are shown in Table 3.3 up to Table 3.5.

Table 3.2 Material property

Wall material	Density $\left({kg}/{m^3}\right)$	Specific heat $\left({J}/{kg.K}\right)$	Thermal conductivity $\left({W}/{m.℃}\right)$
Fiber glass	1700	1260	0.033
Polyurethane foam	35	1450	0.025
Polywood	650	1760	0.13
Galvanized sheet steel	7850	470	52
Stainless steel sheet	8000	490	16.2
Polyester	1380	1400	0.25

Table 3.3 Constituting of vehicle wall material from literature (Oury et al., 2015)

Wall material	Thickness(mm)
Polyester	1.5
Polyurethane foam	50
Polyester	1.5

Table 3.4 Constituting of vehicle wall material from literature (Jara et al,. 2019)

Wall material	Thickness(mm)
Stainless steel	1
Polyurethane foam	66
Galvanized sheet steel	1

Table 3.5 Constituting vehicle wall from literature (Artuso et al., 2019)

Vehicle wall	Insulation material thickness (mm)
Lateral wall	Fiber glass=1.5 Polyurethane=67 Fiber glass=1.5
Floor wall	Fiber glass=1.5 Polywood=18 Polyurethane=79 Fiber glass=1.5
Roof wall	Fiber glass=1.5 Polyurethane foam=97 Fiber glass=1.5
Front wall	Fiber glass=1.5 Polyurethane foam=67 Fiber glass=1,5
Rear wall	Fiber glass=1,5 Polyurethane foam=67 Fiber glass=1.5

(c) Simulation Concept generation

Input parameter similar thickness to all refrigerated body walls and output parameter temperature of wall. During transportation the refrigerated trucks, is exposed to sun light in different side of walls due to this in this simulation similar wall thickness is applied to all walls of body.

(d) 3D CATIA model

Design of refrigerated truck was carried out using CATIA V5 software depending on different literatures with 4.84mm Length, 2.1mm Width and 2mm Height (Figure 3.1)

(e) Main component design of refrigerated truck

Major component design and selection using governing equation and different literature review for refrigerated truck and scale down prototype was done.

(f) CFD analysis to vary insulation thickness and cover material.

Insulation thickness and cover material was carried out using ANSYS.

(g) Prototype and Experimentation

Scale down prototype constructed depending on different literature and design specification from locally available material for experimentation.

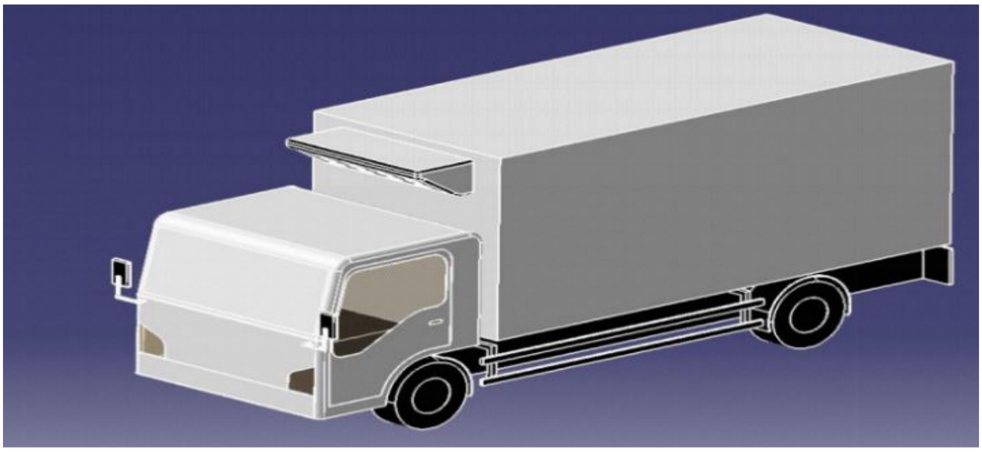

Figure 3.1 3D model of Refrigerated truck

(f) Thesis research method work flow block diagram

The general methodology used for the thesis are indicated in Figure 3.2.

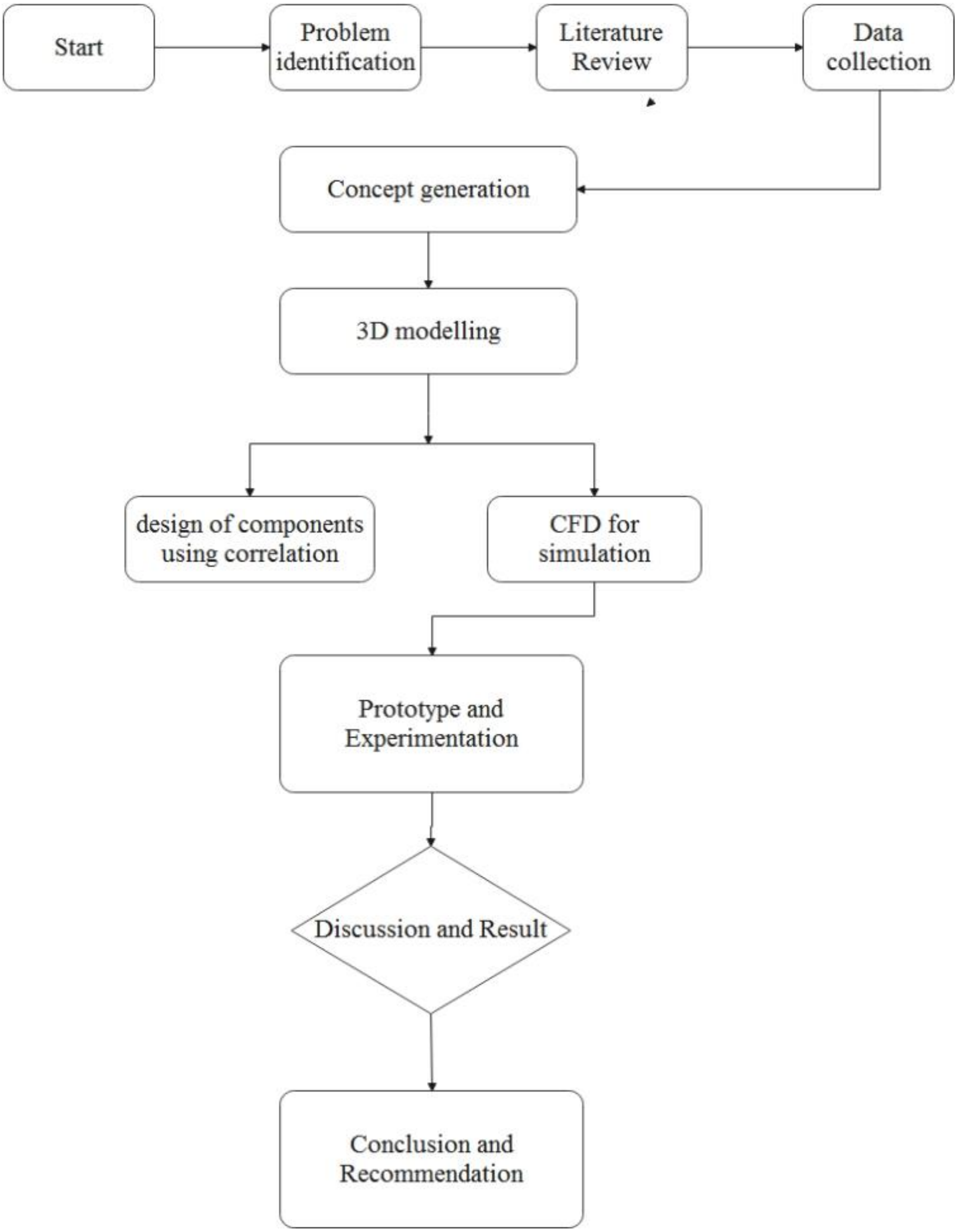

Figure 3.2 Block diagram of methodology

CHAPTER FOUR
DESIGN AND SELECTION OF THE REFRIGERATION SYSTEM MAIN COMPONENTS

4.1 Introduction

In this chapter after estimation of the maximum cooling load or the minimum cabin temperature to cool fruit is determined. Then the appropriate vapor compression system technologies such as compressor, condenser, evaporator and expansion valves were selected are done based on the component selection criteria which found in literature. After selecting and deciding technology & material of components sizing of refrigerated main components were designed using standard correlations. The cabin insulation wall material, the most important part of the refrigeration system, that effectively insulted the refrigerated space from ambient thermal conditions were simulated using ANSYS CFD software for different materials and thickness. Then the influence of the refrigeration system on the performance of the engine was estimated based on the power required to drive the compressor of the VCRS and mass of cabin.

4.2 Selection of Main Components of the Vapor Compression Refrigeration System

The refrigerator type selected for this thesis is refrigerator for transportation of fruits and vegetables from one place to another place on Isuzu car with rear door which works in principle of vapor compression refrigeration system cycle.

4.2.1 Compressor Selection

The compressor is the heart of the refrigeration system. It pumps heat through the system in the form of heat-laden refrigerant. A compressor can be considered a vapor pump. It reduces the pressure on the low-pressure side of the system, which includes the evaporator, and increases the pressure on the high-pressure side of the system. This pressure difference is what causes the refrigerant to flow. All compressors in refrigeration systems perform this function by compressing the vapor refrigerant, which can be accomplished in several ways with different types of compressors. Since compression of refrigerant use same work to be done on it, therefore compressor must be driven by some prime mover (Arora , 2010).

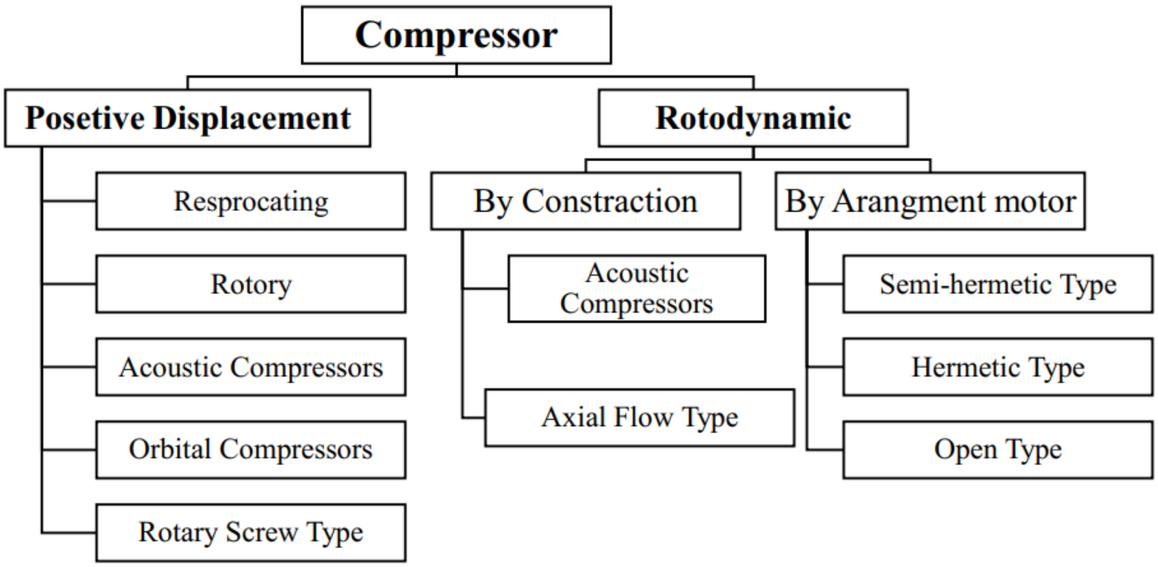

Figure 4.1 Classification of compressor.

The reciprocating compressor uses a piston in a cylinder to compress the refrigerant. Valves, usually reed or flapper valves, ensure that the refrigerant flows in the correct direction. This type of compressor, known as a positive displacement compressor, increases the pressure of the refrigerant by physically decreasing the volume of the container that is holding the refrigerant. In the case of the reciprocating compressor, the volume is decreased as the piston moves up in the cylinder. When the cylinder is filled with vapor, it must be emptied as the compressor turns, or damage will occur.

The rotary compressor is also a positive displacement compressor but are usually very small compared with reciprocating compressors of the same capacity. They are typically used for applications in the small equipment range, such as window air conditioners, household refrigerators, and some residential air-conditioning systems. Rotary compressors are extremely efficient and have few moving parts. They use a rotating drumlike piston that squeezes the refrigerant vapor out the discharge port.

The scroll compressor is one of the latest compressors to be developed and has an entirely different working mechanism. It has a stationary part that looks like a coil spring, and a moving part that matches and meshes with the stationary part. The movable part orbits inside the stationary part and squeezes the vapor from the low-pressure side to the high-pressure side of the system between the movable and stationary parts. Several stages of compression are taking place in the scroll at the same time, making it a very smooth-running compressor with few moving parts. The scroll is sealed on the bottom and top by the rubbing action and at the tip with a tip seal. These sealing surfaces prevent refrigerant from the high-pressure side from pushing back to the low-pressure side while the compressor is running. The scroll compressor is a positive displacement compressor until too much pressure differential builds up; then the scrolls are capable of moving apart, allowing high-pressure refrigerant to blow back through the compressor, preventing overload. The capability to move the mating scrolls apart makes the mechanism more forgiving if a little liquid refrigerant enters the compressor's inlet, because compressor damage is less likely to occur.

The screw compressor is another positive displacement compressor and is used in larger air-conditioning and refrigeration applications. This compressor is made up of two nesting "screws,". A space between the screws gets smaller and smaller as the refrigerant moves from one end to the other. The vapor refrigerant enters the compressor at the point where the screw spacing is the widest. As the refrigerant flows between these rotating screws, the volume is reduced and the pressure of the vapor increases. The screw compressor is popular for use in low-temperature refrigeration applications.

Open type compressor is driven by diesel engine or electric motor with the help of pulley and belt system. The power shaft of compressor (input shaft coupled to motor shaft) extends out through its housing. The compressor may be belt-driven or gear driven. Therefore, a shaft seat is required to prevent the refrigerant from leaving out of compressor housing (John et al., 2016).

The selection of a compressor should be made according to the following system cooling characteristics and where it will be installed.

- Minimum Evaporator Temperature

- Cooling Capacity or Thermal Load
- Refrigerant Type
- Ambient Temperature
- Electrical Power Available
- Compressor and Drive Cooling

In this study open type compressor is selected because this type of compressor has easy maintenance.

4.2.2 Condenser Selection

Condenser is an important devise used the high temperature side of refrigeration system. Its function is to remove heat of the hot vapour refrigerant discharged from the compressor. Hot vapour refrigerant consists of the heat absorbed by evaporator heat of compression added by mechanical energy of compressor motor. The heat from the hot vapour refrigerant in a condenser is removed first by transporting it to walls of the condenser and then from tubes condensing or cooling medium. The cooling medium may be water or air or combination of two cooled. And the condenser performs three main functions when refrigerant flowing through it (Arora, 2010).

1, desuperheating the vapors (the superheated vapour cooled to saturation temperature corresponding to pressure of refrigerant this occur in discharge line or in few coils of condenser).

2, Condensing vapors to liquid (saturated vapour gives up its latent heat and it condensed to saturated liquid refrigerant).

3, Subcooling the liquid (the temperature of refrigerant reduced to below its saturation temperature in order to increase refrigerant effect).

The greatest amount of heat is absorbed in the system when the refrigerant is at the point of changing state (liquid to a vapor). The same thing happens, in reverse, in the condenser. The point where the change of state (vapor to a liquid) occurs is where the greatest amount of heat is rejected. The condenser operates at higher pressures and temperatures than the evaporator and is often located outside. The same principles apply to heat exchange in the condenser as in the evaporator.

The materials a condenser is made of and the medium used to transfer heat make a difference in the efficiency of the heat exchanger.

The selection of condenser depends on types of refrigerants, capacity of refrigerating system and type of cooling medium.

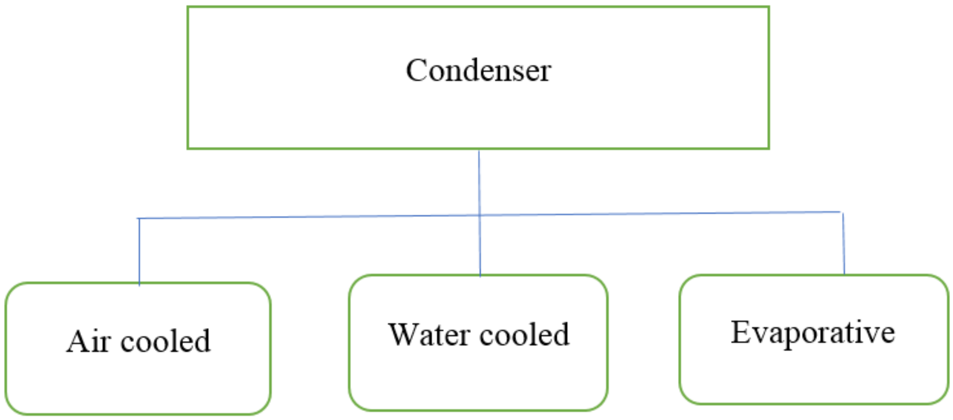

Figure 4.2 Classification of condenser

1**, Air-cooled condenser** is one in which the removal of heat is done by air. Usually consist of pipes with fins attached, but can occasionally have wires, or even a plate, affixed to the refrigerant's piping. These give the condenser a greater surface area and allow for more efficient cooling. Air circulation is achieved either by static means, where air in contact with the pipes becomes hot and rises to be displaced by cooler air. Or, more typically, there is forced convection, where fans pass air over the condenser. Generally copper tube used because of its excellent heat transfer ability.

2, **Water-cooled condenser** normally consist of an outer tube carrying hot vaporized refrigerant which flows over an inner tube containing a counter flow of cool water. These shell-within-tube condensers are very efficient. Water-cooled condensers are more complex than air-cooled condensers as there are design considerations in water flow regulation and corrosion prevention. However, the advantages of water-cooled systems are that water has a higher exchange coefficient than air so heat transfer will be more efficient.

3, **Evaporative condenser** use both air and water in condensing medium to condense hot vapour refrigerant to liquid refrigerant this condenser performs combined functions of water-cooled condenser and cooling tower. In its operation water pumped from the sump to spray header and sprayed nozzles over condenser coils through which hot vapour refrigerant compressor is passing. The heat transfer of refrigerant through the condensing tubes walls and into the water that is wetting outside surface of the tubes.at the same time water a fan draws air from the bottom side of condenser and discharge out of top of the condenser. The air causes the water from surface condenser coil to evaporate and absorbs the latent heat evaporation from remaining water to cool (Khurmi and Gupta 2008).

In this thesis air cooled condenser and tube type condenser is selected because as the heat removing is done by air which means it consume less power, no extra moving parts, no noise, it consists of steel or copper tubing's through which the refrigerant flow. The size of the tube usually ranges from 6 mm to 12 mm outside diameter, depending upon the size of condenser. Generally, copper tubes are used because of their excellent heat transferability. The tubes are usually provided with plate-type fins to increase the surface area of heat transfer. The fins are usually made from aluminum because of its lightweight. The flow of the liquefied refrigerant will be assisted by gravity, so the inlet will be at the top of the condenser and an outlet at the bottom. Rising pipes should be avoided in the design, and care is needed in installation to get the level of the pipes. The fins spacing is quite wide to reduce dust clogging.

4.2.3 Evaporator selection

The evaporator absorbs heat into the system or in a refrigeration system is responsible for absorbing heat into the system from whatever medium is to be cooled. This heat- absorbing process is accomplished by maintaining the evaporator coil at a lower temperature than the medium to be cooled (John et al., 2016).

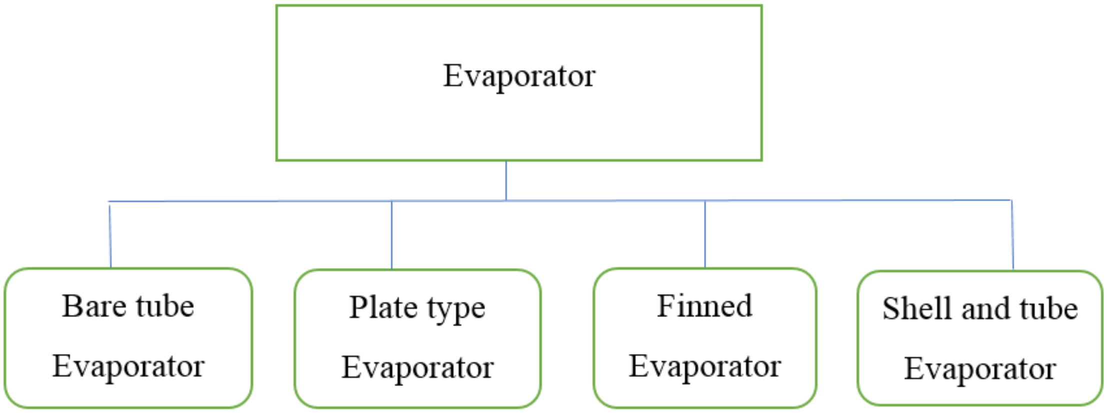

Figure 4.3 Evaporator classification

Bare tube evaporator

In this type of evaporator, the entire surface of coil is in contact with the refrigerant inside. The material used for bare tube evaporator is steel or copper. This type of evaporator is also called prime surface evaporator. The copper tubing is used for small evaporator or small evaporators where the refrigerant other than ammonia is used, while the steel pipes are used with the large evaporators where ammonia is used as the refrigerant. The bare tube evaporator comprises of several turns of the tubing, though most commonly flat zigzag and oval trombone is the most common shapes. The bare tube evaporators are usually used for liquid chilling. In the blast cooling and the freezing operations, the atmospheric air flows over the bare tube evaporator and the chilled air leaving it used for cooling purposes.

Plate type evaporator

In this of evaporator, the coils are either welded on one side of a plate or between the two plates which are welded together at the edge. And usually made up of copper or aluminum is embedded in the plate so as so to form a flat looking surface. Externally the plate type of evaporator looks like a single plate, but inside it, there are several turns of the metal tubing through which the refrigerant flows. The advantage of the plate type of evaporators is that they are more rigid as the external plate provides lots of safety. The external plate also helps to increase the heat transfer from the metal tubing to the substance to be chilled. Further, the plate type of evaporators is easy to clean and can be manufactured cheaply. The Plate evaporator are generally used in house hold refrigerator, home freezers, beverage coolers, iceream cabinets.

Finned evaporator

Finned evaporators are bare tube type of evaporator covered with metallic fins. And finned evaporator, the outer surface area is surrounded by thin metallic plate called fins. These fins are thin metallic plates, usually aluminum or copper, securely attached or banded to the evaporator tubes, with bare tube evaporators. When the fluid (air or water) to be chilled flows over the bare tube evaporator lots of cooling effect from the refrigerant goes wasted since there is less surface for the transfer of heat from the fluid to the refrigerant. The fluid tends to move between the open spaces of the tubing and does not come in contact with the surface of the coil, thus the bare tube are less effective. The fins on the external surface of the bare tube evaporators increase the contact surface of the metallic tubing with the fluid and increase the heat transfer rate, thus the finned evaporators are more effective than the bare tube evaporators. These fins increase the heat transfer efficiency of the evaporator. Finned evaporator are used in air cooling application.

Shell and tube type: The shell and tube types of evaporators are used in the large refrigeration and central air conditioning systems. The evaporators in these systems are commonly known as the chillers. The chillers comprise of a large number of the tubes that are inserted inside the drum or the shell. Depending on the direction of the flow of the refrigerant in the shell and tube type of chillers, they are classified into two types: dry expansion type and flooded type of chillers. In dry expansion chillers, the refrigerant flows along the tube side and the fluid to be chilled flows along the shell side. The flow of the refrigerant to these chillers is controlled by the expansion valve. In the case of the flooded type of evaporators, the refrigerant flows along the shell side and fluid to be chilled flows along the tube. In these chillers, the level of the refrigerant is kept constant by the float valve that acts as the expansion valve also.

In this study bare tube evaporator is selected because they are easier to keep clean and the construction is simple.

4.2.4 Selection expansion device

The expansion device is an important device that divides the high-pressure side of refrigerating system. It is connected between the receiver and the evaporator. The expansion devices perform the different function which includes firstly it reduces the high-pressure liquid refrigerant to low pressure liquid refrigerant before send to the evaporator. Secondly it maintains the desired pressure differences the high- and low-pressure sides of the system, then liquid refrigerant vaporizes at the designed pressure in the evaporator and controls the flow of refrigerants based on load on the evaporator (Arora , 2010).

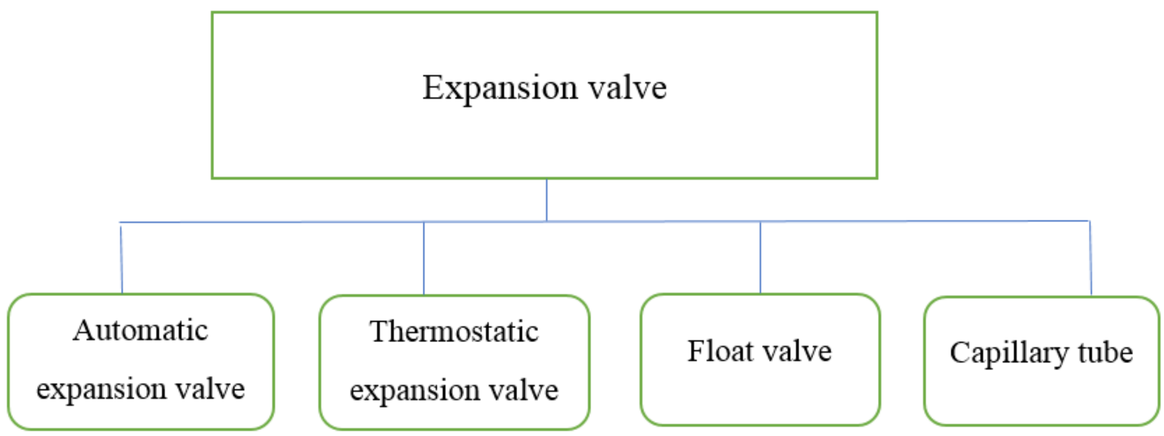

Figure 4.4 Classification of expansion valve

The automatic expansion valve: regulates the flow of refrigerant from the liquid line to the evaporator by using a pressure-actuated diaphragm. It maintains a constant pressure in the evaporator. The setback is that it is not efficient if the load fluctuates hence this type is not suitable for use in air conditioning as the load fluctuates a lot during its operation.

Thermostatic expansion valve: is a precision device that it regulates the rate of flow of liquid refrigerant into the evaporator in exact proportion to the rate of evaporation of liquid refrigerant which is according to the heat load. And also regulate the quantity of refrigerant vapour exhaled by evaporator. Thermostatic expansion valve works according to the temperature of the refrigerant vapour and leaving the evaporator and pressure in the evaporator.

The capillary tube: is used as an expansion device in small capacity hermetic sealed refrigeration unit such as domestic refrigerator, water cooler, room air conditioner and freezer because of their simplicity, reliability, low cost, no moving parts and lasts longer. Capillary tube is a fixed length of small diameter tubing lying between the outlet of the condenser and the inlet of the evaporator. It reduces the pressure of the refrigerant from the high-pressure side to the low-pressure side of the system and controls the flow of refrigerant to the evaporator. In order to use this device, the amount of refrigerant in the system must be properly calibrated at the factory level.

The Float Valve: is actuated by a float that is immersed in the liquid refrigerant. Both low side float and high side-float are used to control the flow of liquid refrigerant. The high side float maintains liquid at constant level in condenser. The low side float helps to maintain a constant level of liquid refrigerant in the evaporator. It opens when there is no liquid in the evaporation. And closes when there is liquid in the evaporation.

In this thesis the selected type of expansion valve is thermostatic expansion valve because ensure complete vaporization of refrigerant in evaporator, eliminate the risk of liquid refrigerant particles from reaching compressor and it can used in large capacity refrigeration system.

4.2.5 Refrigerant selection

The refrigerant is heat carrying medium which during their cycle (compression condensation. Expansion and evaporation) in the refrigeration system absorbs heat from a low temperature system and discards the heat so absorbs to higher temperature system. The suitability of refrigerant for a certain application is determined by its physical, thermodynamic, chemical properties, non - corrosive to mechanical components and be safe free from flammability and non-toxicity. It would not cause ozone depletion or climate change. Since different fluids have the desired traits to different degrees, the choice is a matter of tradeoffs. The desired thermodynamic properties are a boiling point somewhat below the target temperature, the high heat of vaporization, a moderate density in liquid form, a relatively high density in gaseous form, and a high critical temperature. Since boiling point and gas density are affected by pressure, refrigerants may be made more suitable for a particular application by appropriate choice of operating pressures (Khurmi and Gupta 2008).

4.2.5.1 Different types of refrigerants

R-11, Trichloro-monofluoro-methane: synthetic chemical product which has low pressure refrigerant due to this it used exclusively large centrifugal compressor systems of 200TR and above. Ozone depletion factor (ODF) of this refrigerant is equal to 1 and proportion of chlorine by weight is 77.4.

R-12 dichloro-difluoro-methane: popular refrigerant**.** It is colorless, odorless, and liquid with relatively low latent heat value advantage in small refrigerating machine. Ozone depletion factor of this refrigerant is 1. proportion of chlorine by weight is 58.6.

R-113 Trichloro-trifluoro-ethane: has boiling point 46.6℃. It used in commercial and industrial air conditioning with centrifugal compressor with. This refrigerant has the advantage of reaming liquid at room temperature and pressure. therefore, it can be carried in sealed tins rather than cylinder. ODF value is 0.8 amount of chlorine by weight 56.7.

R-22 monochloro-difluoro-methane: man-made refrigerant developed for installation that need a low evaporator temperature.it can applied in air conditioning and household refrigerators and used with reciprocating and centrifugal compressors. Ozone depletion factor of this refrigerant is 0.05 and amount of chlorine by weight is 41.0.

R-134 Tetrafluoro-ethane: most preferred substitute for refrigerant R-22. atom, since refrigerant R134a has no chlorine atom, therefore this refrigerant has zero ozone depleting (ODP) and has 74% less global warming potential (GWP).

R-152 Difluoro –ethane: refrigerant R152 has similar characteristics refrigerant R134a has slight vacuum in evaporator at -25℃ and the discharge temperature is higher because of high ratio of specific heat.

For this study R134a is selected because it is, available, working in the desired temperature nontoxic and non-corrosive.

Table 4.1 Ozone depletion factor of refrigerant.

Refrigerant	ODF	Proportion of chlorine by weight
R11	1.0	77.4
R12	1.0	58.4
R113	0.8	56.7
R22	0.05	41.0
R152a	0	0
R134a	0	0

4.2.6 Selection of Other essential components of refrigeration system

A) Flirter drier

Filter driers are devices used in a HVAC system that are a combination of filter and dryer (or drier). A filter is used to remove any particle such as dirt, metal or chips from entering the refrigerant flow control. The refrigerant flow control device could be thermostatic expansion valve or simply a capillary tube. The filter is sometimes also referred to as a strainer. It is critical that these particles are filtered out and prevented from going into the metering device. It can cause blockage to the passage flow of the refrigerant in the expansion valve and cause improper operation to the system. In this thesis is suction line selected because of which contains a solid core with desiccant and activated alumina to remove moisture and acid while filtering out contaminants. It also has access valves to measure pressure drop across the filter-drier.

B) Receiver

Receiver is a storage vessel designed to hold excess refrigerant which is not in circulation. Refrigeration systems exposed to varying heat loads, or system utilized a condenser flooding valve to maintain head pressure during low ambient temperature will need a receiver to store excess refrigerant. Receiver selection should be based on the vessels ability to hold 100% of the total system refrigerant charge.

C) Thermostat

The thermostat controls the cooling process by monitoring the temperature and then switching the compressor on and off. When the sensor senses that its cold enough inside a refrigerator, it turns off the compressor. If its senses too much heat, it switches the compressor on and begins the cooling process again. For this study cold thermostat is selected to control the refrigerator temperature of the refrigerator. The cold thermostat used to maintain the refrigerator temperature at the required level. The thermostat operates by using a temperature-sensitive gas sealed inside the thermos bulb which is attached to bellows assembly inside the thermostat housing. As the compartment temperature increases, the gas expands which forces the bellows to expand causing points inside the housing to start the compressor. Once the compartment temperature begins to decrease, the sensitive gas will contract until the bellows shrink and separate the two contacts, cutting off the power to the compressor, thus shutting off the refrigeration systems. If for any reason the thermos-bulb would become broken, allowing the sensitive gas to escape, the thermostat would fail in the open position. This would result in no refrigeration and a new thermostat would have to be installed. The cold thermostat has an external adjustment which may increase or decrease the temperature of the compartment approximately 2°C. Never turn the thermostat to the off position (completely-counter clockwise) as this will turn off the refrigeration system altogether (Laguerre and Flick, 2010).

Table 4.2 Selected components of refrigeration system.

Components/system	Selected type of component
Refrigeration cycle	Vapour compression refrigeration system
Refrigerator type	Single rear door
Compressor	Open type
Condenser	Air cooled copper wire and tube type
Evaporator	Copper bare tube evaporator
Expansion valve	Thermostatic expansion valve
Thermostat	Cold thermostat
Filter drier	Suction line type
Insulation	Polyurethane foam
Refrigerant fluid	R134a

4.3 Cooling load demand estimation

The total cooling load for the Isuzu freight cabin are due to

1. Transmission heat gain
2. Estimation heat of respiration load
3. Heat to be extracted from the fruit
4. Entry of unconditioned ambient air
5. Heat gain of solar radiation

Table 4.3 Recommended temperature and relative humidity of different products (Arora, 2010)

Product type	RH	Temp. difference	Remarks
Fruits, vegetables, flowers, etc.	90%	$4-5℃$	Minimum moisture loss
General storage, packed products.	80-85%	$6℃$	product require lower RH
Pharmaceutical, beer, potatoes, onion, tough-skin fruits, etc.	65-80%	$7-9℃$	Product require moderate RH
Prep/cutting rooms, candy, etc.	50-65%	$9-12℃$	Product not affected by RH

Ambient temperature of cities that Isuzu car transports fruits in The Southern and Oromia regions is given in table 4.4.

Table 4.4 Isuzu fruit transportation route cities starting from Arba minch to Adis Abeba and their maximum ambient temperature (https://power.larc.nasa.gov/data.access.viewer)

	Temperature of major cities (°C)											
City	Sep.	Oct.	Nov.	Dec.	Jan.	Feb.	Mar.	April.	May.	June.	July.	Aug.
Arbaminch	26.85	28.15	29.30	29.56	27.44	31.47	32.61	32.57	25.71	25.49	25.09	27.78
Wolaita Sodo	24.65	26.05	26.90	27.55	27.41	29.81	33.37	34.21	28.30	27.08	25.47	25.08
Shashemene	21.46	21.61	21.8	22.82	23.03	25.30	27.57	28.01	24.16	24.64	21.87	21.46
Butajira	20.87	20.06	21.07	22.20	22.91	25.41	27.48	28.01	25.12	26.40	21.29	21.58
Ziway	32.65	25.87	27.40	27.96	28.11	31.11	32.22	32.05	29.49	32.65	26.69	24.90
Mojo	27.22	27.87	33.35	28.05	28.25	32.11	32.94	33.50	30.77	33.33	29.83	27.03
Bishoftu	24.40	24.82	30.02	25.29	26.58	28.80	29.81	31.31	29.33	29.75	26.06	24.86
Adiss Abeba	21.98	22.88	23.33	24.21	25.62	27.04	30.09	30.52	27.80	28.86	23.05	22.85

From above data minimum temperature is 20.06℃ in month of October in Butajira city and the maximum temperature is 34.21℃ occur in Wolaita Sodo city in the month of April. To estimate cooling load, we take maximum temperature of Wolaita Sodo.

Table 4.5 Common fruit that transported by Isuzu car in Ethiopia and their minimum storage temperature(ASHRAE, 2014).

Fruit type	Storage temperature (°C)	Relative humidity (%)
Avocado	13	85 to 90
Banana	13 to 15	90 to 95
Mango	13	85 to 90
Tomato	10 to 13	90 to 95
Orange	10 to 13	85 to 90
Papaya	7 to 13	85 to 90
Pineapple	7 to 13	85 to 90

In this thesis papaya fruit is selected because of minimum storage temperature is 7°C.

4.3.1.1 Transmission heat gain

The process of conduction through the wall or the cabin envelope connecting the outside and the inside of the time heat balance (Koerniawan et al., 2017). The transmission heat load to the cabin is due heat conduction entering through the insulated side walls, ceiling, and floor. In refrigerated vehicle, heat recovery is usually 5-15% through transmission. So, there's a thermal energy flowing into the cabin from the roof, walls and floor of the refrigerated space. Heat always flows from hot to cold, and the inner part of the refrigerated space is much colder than the surrounding environment, so heat always tries to get into the area due to this temperature difference. In this study above heat source of transmission is considered.

Heat transfer through the cabin:

Conduction load should be calculated floor, wall and ceiling.

- The size of our cold storage is 4.84m long, 2.1m wide and 2m high.
- Ambient air is 34.21°c, Inner air 5 °c.
- U over heat transfer coefficient of Walls, roofs and floors, w/m2.
- The floor temperature is 10 °c.

To calculate the transmission load, the formula is (Pual, 2017):

$$Q_{tran} = \frac{UA(T_o - T_i)24}{1000} \tag{4.1}$$

- Q_{tran} is heat load $\left({}^{kWh}/_{day}\right)$
- U is the overall heat transfer coefficient is given by $\left({}^{kWh}/_{day}\right)$
- A is wall, roof and ground surface area (m^2)
- T_i is Internal temperature or air temperature inside the room (° C)
- T_i is External temperature or ambient air temperature (° C)
- 24 is number of hours in a day
- 1000 is conversion from Watt to kW.

The overall heat transfer coefficient is given by (Krishnakumar, 2017).

$$U = \frac{1}{\frac{1}{h_o}+\frac{x_1}{k_1}+\frac{x_2}{k_2}\cdots\frac{1}{h_i}} \tag{4.2}$$

Where

h_o is heat transfer coefficient on the inner surface $\left({W}/{m^2 K}\right)$

h_i is heat transfer coefficient on the inner surface $\left({W}/{m^2 . K}\right)$

x_1, x_2 is thickness of wall and insulating material, respectively (m)

k_1, k_2 is thermal conductivity of wall insulating materials $\left({W}/{m. K}\right)$

With thick wall and low conductivity, the resistance ${x}/{k}$ makes U so small that ${1}/{h_o}$ and ${1}/{h_i}$ have little effect and can be omitted from the calculation (Krishnakumar, 2017).

$$U = \frac{1}{\frac{x_1}{k_1}+\frac{x_2}{k_2}+\frac{x_3}{k_3}} \tag{4.3}$$

Total heat transfer through material Q_{tran} = heat transfer through walls + floor +roof

4.3.1.2 Heat to be extracted from the fruit

Product heat is the heat brought into the cabin from the fresh that are initially at a warmer temperature. When new products enter the cabin, the heat enters the storage and subsequently, the energy is required to cool them (Yuzainee et al., 2019). To specify cooling load based on volume of refrigerated space the following load should be considered: The quantity of heat to be remove from the product placed in the refrigerated space is calculated by using its mass of product, specific heat capacity of product. The quantity of heat of product to be stored above freezing point temperature is given by (Arora, 2010). Heat extracted from the produce as it cools to the storage temperature; in this study calculate the cooling load according to the temperature coming from the new product replacement in the refrigerated cabin.

Papaya fruit for this thesis study because of lower storage temperature.

And the following formula used for this account:

$$Q_{extra} = \frac{mC_p(T_{fru} - T_i)}{3600} \quad (4.4)$$

- Q_{extra} is extracted heat load $\left({kWh}/{day}\right)$
- C_p is specific heat capacity of the product $\left({kJ}/{kg℃}\right)$
- m is mass of newly added products (kg)
- T_{fru} is product input temperature (℃)
- T_i is temperature inside the box (℃)
- 3600 is Convert from kJ to kJ.

4.3.1.3 Estimation heat of respiration load

Another load is the cooling load account from the product respiration. Heat generated by the produce as a natural by-product of its respiration. In this study the product's respiratory temperature on average daily 1.9 ${kJ}/{kg}$, but the rate varies with time and temperature.

To calculate this, we will use the following formula:

$$Q_{RES} = \frac{m * RESP}{3600} \quad (4.5)$$

Where

- Q_{Resp} is fruit product respiration heat load $\left({kWh}/{day}\right)$
- m is quantity of fruit product in the storage cabin (kg)
- RESP is respiratory temperature of the product $\left({kJ}/{kg}\right)$
- 3600 is converts kJ to h.

4.3.1.4 Entry of unconditioned ambient air

The external cooling load is affected by the heat transfer from/to the environment through the cabin envelope which is uncontrolled air flow all little cracks and opening in cabin (Parishwad et al., 2000). Cooling load Account from infiltration therefore it needs to calculate the heat load from the air infiltration (leakage).

$$Q_{inf} = \frac{volume * change * energy(T_o - T_i)}{3600} \quad (4.6)$$

- Q_{inf} is air infiltration heat load $\left({kWh}/{day}\right)$
- Change is number of volume air changes in the day
- Volume is cold Storage Volume (m^3)
- Energy is centigrade degree of energy per cubic meter
- T_o is ambient air temperature (℃)
- T_i is cold room temperature (℃)
- 3600 is only converts from kJ to kWh.

Assuming that the door will create there is 4 volume air changes per day because product entry to the refrigerated space, the volume is calculated as 20.328m^3, each cubic meter of new air 2 ${kJ}/{°C}$, ambient air 34.21°C outside and the air in the refrigerated box 5°C.

4.3.1.5 Miscellaneous load calculation

Service load can be taken as 10 percent of the total load due to loading, unloading of product and door opening. Including safety factor to take into account the errors and variations in the design, also apply a safety factor to the calculation. A deviation of 10% to 30% can be added to calculate this.

4.3.1.6 Total load cooling calculation

To calculate the total cooling load, calculated values were collected. Using equation 4.1 up to 4.6 the transmission load, heat to be extracted from the fruit, estimation heat of respiration load and entry of unconditioned ambient air was calculated and result are summarized in table 4.6.

Table 4.6 Summarized value of cooling load calculation

Calculated terms	Valued in $\left({}^{kWh}/_{day}\right)$
Transmission load	7.97
Product initial heat load	11.36
Product respiration load	2.6
Heat infiltration load	1.32
Miscellaneous load	26.62
Safety factor	30.72

Cooling capacity Calculation

The last thing we need to do is calculate the cooling capacity that is necessary to remove this heat gain from the environment. For this, the calculated total cooling load is divided into 7, based on the operation of the device 7 hours per day. This means that the capacity required by our refrigeration unit should be total cooling load/operation time = $4.391kW$

Total cooling load capacity 4.319kW.

4.4 Design of the major component

In this section thermodynamics and thermal analysis of the refrigeration system components are made based on the specified capacity of the refrigerator for sizing the refrigerator components.

4.4.1 Sizing of the compressor

The refrigerator compressor is one of the four main components that makes the refrigerator work. The compressor's job is to compress and control the flow of refrigerant. The compressor receives low pressure gas from the evaporator and converts it into high pressure gas. As the gas is compressed and the pressure increases and also the temperature increases (wang and shang, 2018).

The following steps are refused in the design of compressor.

- Select discharge and suction pressure of compressor
- Take the inlet state as the exit state of the evaporator.

- Take the entropy of exit state equal to inlet entropy.
- Designate the exit state.
- Read the thermos-physical properties of the refrigerant at the inlet and exit states.
- Calculate the suction pressure.
- Calculate the compressor power requirement.
- Determine the volumetric efficiency.

A) Operating temperature and pressure of compressor

Referring to standard vapor compression refrigeration cycle

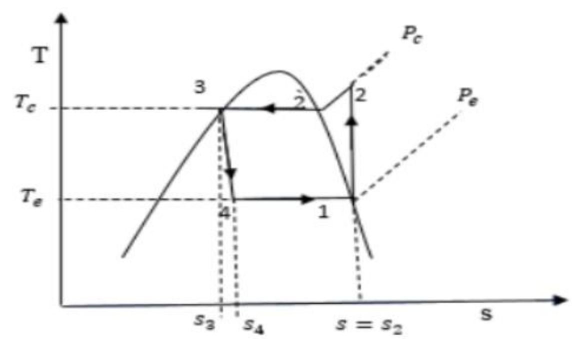

Figure 4.5 Temperatures vs. entropy diagram of an ideal VCRC

Where 1-2 compression process, 2-3 condensation process 3-4 expansion process and 4-1 evaporation process.

- 1-2 isentropic compression: - refrigerant vapor received from the evaporator is compressed isentropically in a compressor by an external source of energy (work in-out), pressure and temperature increase.
- Process 2-3 condensation: - compressor discharges vapor into the condenser where it condensed completely i.e., turns in to liquid. Heat is rejected from the refrigerant to the cooling medium, usually air or water.
- Process 3-4 expansion: - from condenser liquid refrigerant passes through the expansion valve where it is throttled resulting in a drop of temperature and pressure. However, enthalpy remains constant (throttling expansion).

- Process 4-1 evaporation: - liquid refrigerant at a low temperature passes into the evaporator where it extracts heat from the product to be cooled. Due to the absorption of extract heat, the liquid refrigerant turns into vapor and enters into the compressor.

  A simple analysis of VCRS can be carried out using assumptions

  I. Steady flow
  II. Negligible kinetic and potential energy changes across each component
  III. No heat transfers in connecting pipelines.
  IV. The steady flow energy equation is applied to each of the four components.

Heat balance for the open system of closed cycle as given by

$$E_{in} - E_{out} = \Delta E_{system} \tag{4.7}$$

$$Q_{in} - Q_{out} - (Q_{out} - W_{in}) = \Delta E_{system} \tag{4.8}$$

$$Q_e - W_c - Q_c = 0 \tag{4.9}$$

Where: E_{in} is energy entered to the system (kJ)

E_{out} is energy leaves the system (kJ)

Q_{in} is heat gain by evaporator (kJ)

Q_{out} is heat released by condenser (kJ)

Determination of discharge and suction pressure of the compressor

A, Suction pressure (P_e) and evaporator temperature (T_e)

- In basics of physics, heat flows from high temperature to low temperature and to achieve this process there must be temperature difference.so the temperature of refrigerant in evaporator tubes should be less than product inside the refrigerated space 5℃.
- Suction pressure must be greater than atmospheric pressure (1atm=101.3Kpa).
- The selected pressure must be in the range of working of refrigerant fluid.

- Take into consideration heat transfer from environment refrigerated space because of imperfect insulation to compensate this the temperature deference between refrigerant and product inside refrigerated vehicle must be higher as much as possible.
- If higher temperature difference between product inside refrigerated vehicle and evaporator is chosen, the T_e value will be lower the compressor power input will be higher. A compromise between energy cost and initial investment should be made through life-cycle cost analysis. So, it is not recommended much lower evaporator temperature.
- Value of temperature difference between product inside the refrigerated space and evaporator should be 6 and 10°F (3.3 and 15.6). For energy-saving models the temperature difference between the refrigerated space and evaporator should be as low as 4 and 7°F (2.2 to 3.3℃).
- Depend on above consideration assume evaporator temperature $(T_e) = -2℃$ and suction pressure (P_e) evaporator coil working pressure =272.06Kpa (wang and shang, 2018).

B, Discharge pressure (P_c) (condenser coil working pressure) and saturated temperature of the condenser (T_c).

- The temperature of refrigerant at the exit of condenser must be higher than temperature of ambient air of outside (34.21℃) the reason is heat always flows in the direction decreasing temperature and in order to have transfer there must be temperature difference.
- Discharge pressure must be greater than atmospheric pressure (1atm=101.3Kpa)
- Saturated temperature of the condenser T_c must be higher than evaporator temperature.
- The total heat of rejection is equal to net refrigeration at the evaporator (cooling capacity) plus the energy input into the refrigerant by the compressor (heat of compression), so the saturated temperature of condenser should be higher than temperature of product inside the refrigerated space (5℃).
- If the compressor discharge temperature is very high then it may result in breakdown of lubricating oil, causing wear and reduced life of the compressor valves (mainly the discharge valve). When temperature is high undesirable chemical reaction may take place inside the compressor, especially in the presence of water. This may ultimately damage the compressor (Kharagpur, 2008).

- At a constant evaporator temperature as the condensing temperature increases, then the enthalpy of refrigerant at the inlet to the evaporator increases. Since the evaporator enthalpy remains constant at a constant evaporator temperature, the refrigeration effect decreases with increase in condensing temperature. The refrigeration capacity (Q_e) also reduces with increase in condensing temperature as both the mass flow rate and refrigeration effect decrease. So, compressor discharge temperature is not recommended much higher as much as possible.
- A high condensing temperature (T_c) means a higher condensing pressure (P_c) a higher discharge temperature. High T_c and P_c result in higher power input and, more often unsafe operating conditions. Both are undesirable.
- The condenser temperature difference (CTD) for an air-cooled condenser is defined as the difference in saturated condensing temperature corresponding to the refrigerant pressure at the inlet and the air intake dry-bulb temperature $T_2 - T_{air}$ the total heat rejection Q_r of an air-cooled condenser is directly proportional to its CTD. The Q_r of an air-cooled condenser operated at a CTD of 30°F (16.7°C) is approximately 50 percent greater than if the same condenser is operated at a CTD of 15°F (8.3°C). On the other hand, for a specific value of an air-cooled condenser selected with a CTD of 15°F (8.3°C) is larger than a condenser elected with a CTD of 30°F (16.7°C).
- Depend on the above consideration assume the discharge pressure is (condenser coil working pressure) P_c = 1000Kpa and the saturated temperature of the condenser) is = 39.37℃. Therefore, the saturated temperature of the condenser (at) is =39.37℃ and evaporator (at P_e=272.06Kpa) is T_e= -2℃ reads as from the saturated table of refrigerant R134a.

Table 4.7 Properties of R134a at evaporator temperature ($\boldsymbol{T_e} = -\mathbf{2}$°C) and condenser pressure ($\boldsymbol{P_c} = \mathbf{1000}\boldsymbol{kPa}$)

Temp	Pressure	Volume $\left({m^3}/{kg}\right)$	Enthalpy $\left({kJ}/{kg}\right)$			Entropy $\left({kJ}/{kg.K}\right)$		
°C	kPa	v_g	h_f	h_{fg}	h_g	s_f	s_{fg}	s_g
-2	272.06	0.07440	49.27	200.12	249.29	0.1946	0.7380	0.9326
39.37	1000	0.08019	107.32	163.66	271.28	0.3919	0.5237	0.9156

Figure 4.6:P-h diagram of R134a describes the ideal cycle of the vapor compression refrigeration system. Table 4.7: Presents the properties of R134a in the selected condensation and evaporation pressure.

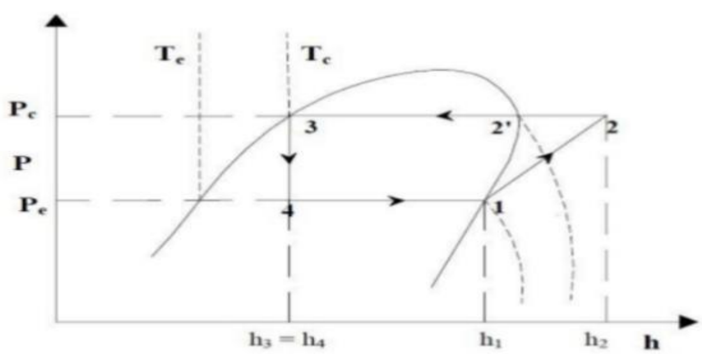

Figure 4.6 Pressures vs. enthalpy diagram of an ideal VCRC (Kharagpur, 2008)

@point1. (From saturated vapor table of R134a @ $P_e = 314.37kPa$

$$h_1 = h_g \text{ and } s_1 = s_g$$

@point2. (From super table of R1314a @ $P_c = 1000kPa$

$$s_1 = s_2$$

From superheated section of the thermodynamics property table

Table 4.8 Properties of superheated R134a at condenser pressure ($P_c = 1000kPa$)

Temp (℃)	Specific volume (v) $\left({m^3}/{kg}\right)$	Specific enthalpy (h) $\left(\frac{kJ}{kg}\right)$	Specific entropy (s) $\left(\frac{kJ}{kg.K}\right)$
P=1000Kpa($T_{sat} = 39.37$)			
Sat.	0.020313	270.99	0.9156
40	0.020406	271.71	0.9179
T_2	v_2	h_2	0.9326
50	0.021796	282.74	0.9525

By interpolating

T_2 *and* h_2 can be calculated

@Point3 (From saturated liquid table of R134a @ $P_c = 1000kPa$

$h_3 = h_4 = h_f$

Coefficient of performance:

The coefficient of performance is an index of the performance of thermodynamic cycle or a thermal system. Because the COP can be greater than 1.COP is used instead of thermal efficiency.

The COP can be determined using the expression given by (Kharagpur, 2008).

$$COP = \frac{input}{desired\ output} = {(h_1 - h_4)}/{(h_2 - h_1)} \tag{4.10}$$

h_1 is specific enthalpy at evaporator outlet ($kJ.kg^{-1}$)

h_2 is specific enthalpy at condenser inlet ($kJ.kg^{-1}$)

h_4 is specific enthalpy at evaporator inlet ($kJ.kg^{-1}$)

COP is ideal coefficient of performance

The cooling effect (q_e) and the cooling capacity of the evaporator ($\boldsymbol{Q_c}$):

Cooling effect refers to the enthalpy difference when the refrigerant passes through the evaporator coil.

$$\text{Cooling effect } (q_e) = h_1 - h_4 \tag{4.11}$$

$$\dot{m}_r = \frac{Q_c}{q_e} \tag{4.12}$$

q_e is cooling effect $(kJ.kg^{-1})$

$\dot{m}_r$ is mass flow rate of refrigerant $(kg.s^{-1})$

Power of compressor (P) cooling capacity is given by

$$P = \dot{m}_r * (h_2 - h_1) \tag{4.13}$$

P is power of compressor in (kW).

Table 4.9 Based on the above equations, the mass flow rate, power of compressor and COP are achieved.

q_e $(kJ.kg^{-1})$	$\dot{m}_r$ $\left(\frac{kg}{s}\right)$	P (kW)	COP
141.97	0.0309	0.828	5.3

4.4.2 Sizing of Evaporator Coil

To design evaporator, coil the following parameters must be consider:

a) It is based on the time taken to extract the required heat from the refrigerator compartment by vaporizing R134a.
b) It depends on the property of the materials for which the evaporator coil is made because of its thermal conductivity. If the thermal conductivity is high rapid heat exchange occurs from

the high-temperature area to low temperature area unless a longer time is required to vaporize the refrigerant. The best material with high thermal conductivity is copper.

c) The performance of the compressor or the working pressure of both condenser and evaporator will affect. If the pressure is high enough it will require longer if not, it needs smaller coils to exchange the required heat in both a condenser and evaporator.

d) Mainly it depends on the overall heat transfer coefficient of the hot and cold fluid. Heat transfer analysis on condenser and evaporator coil

There are three modes of heat transfer in evaporator given by (Theodore et al,. 2008).

There are three modes of heat transfer in evaporator coil

Convection heat transfer $Q_{con} = h_i A(T_{air} - T_e)$ (4.14)

Conduction heat transfer $Q_{cond} = \frac{KA}{t}(T_{sur} + T_e)$ (4.15)

Radiation heat transfer $Q_{rad} = A\varepsilon\sigma\left({T_{sur}}^4 - {T_e}^4\right)$ (4.16)

Overall heat transfer $Q_e = UA\Delta T$ (4.17)

Where h_i is inside convective heat transfer

k is Conduction heat transfer coefficient $(W.m^{-1}K^{-1})$

t is times(s)

T_{air} is air temperature (K)

T_e is evaporator temperature (K)

T_{sur} is surface temperature (K)

A is Area (m^2)

U is overall heat transfer coefficient $(W.m^{-2}K^{-1})$

Thermal analysis for evaporator coils an evaporator should transfer enough heat from as small size as possible. It should be light, compact, safe, and durable. The pressure loss should be as low as possible. The selected evaporator for the design is natural convection bare tube Evaporators. Heat reaches the Evaporator by all three methods of heat transfer. To determine the length of the evaporator the total heat transfer from the evaporator can be written as given by (Cengel and Boles, 2008).

$$Q_c = Q_e = U_o * A_e * F * LMTD \tag{4.18}$$

Where Q_c is total heat transfer from evaporator (kJ)

Q_e is cooling capacity (kJ)

U_o is over all heat transfer $(W.m^{-2}K^{-1})$

A_e is total area of evaporator (m^2)

F is correction factor

LMTD is long mean temperature difference (K)

$$LMTD = \frac{\Delta T_1 - \Delta T_2}{ln^{\Delta T_1}/_{\Delta T_2}} \tag{4.19}$$

a) $\Delta T_1 = T_{air} - T_e(K)$
b) $\Delta T_2 = T_{sur} - T_e(K$

Table 4.10 Standard pipe size for evaporator and condenser

[http://WWW.engineeringpage.com/technology/thermal/tubesize.html]

Tube size	Outer diameter			Wall thickness	
	Inch	mm	BWG	inch	mm
1/4	0.250	0.6350	22	0.028	0.711
			24	0.022	0.559
3/8	0.375	9.525	18	0.049	1.245
			20	0.035	0.889
			22	0.028	0.771
1/2	0.500	12.700	18	0.049	1.245
			20	0.035	0.889
5/8	0.625	15.875	16	0.065	1.651
			18	0.049	1.245
			20	0.035	0.889
3/4	0.750	19.050	12	0.109	2.769
			14	0.083	2.108
			16	0.065	1.651
			18	0.049	1.245
			20	0.035	0.889

From standard pipe sizes for evaporator assume outer diameter = 19.050 mm and Inner diameter = 16.281 mm.

Estimation over all heat transfer coefficient (U_o)

$$1/U_o = \frac{A_o}{A_i h_i} + \frac{A_o \ln\left(d_o/d_i\right)}{2\pi K L} + \frac{1}{h_o} \qquad (4.20)$$

As

$$A_o = \pi d_o L \tag{4.21}$$

And

$$A_i = \pi d_i L \tag{4.22}$$

By substituting the equations

$$1/U_o = \frac{d_o}{d_i h_i} + \frac{d_o ln\left(d_o/d_i\right)}{2K} + \frac{1}{h_o} \tag{4.23}$$

To find U_o first find, h_i and h_o

h_i estimation

$$h_i = Nu * \frac{K}{d_i} \tag{4.24}$$

To find the Nusselt number, the flow property specified depending on Reynolds number as shown.

$$Re = \frac{\dot{m}_{rif}}{\pi d_i \mu} \tag{4.25}$$

If the flow is turbulence flow inside a tube it considered as fully developed turbulent flow inside a tube and governed by the recommended correlation by Dittes and Boelter for cooling of the fluid is given as.

$$Nu = 0.023 Re^{\frac{4}{5}} * Pr^{0.3} \tag{4.26}$$

The inside heat transfer coefficient analysis of evaporator is based on the property of refrigerant fluid at evaporator temperature and pressure. To find the property of fluid after throttling the flash gas percentage after should be calculated by.

$$x = \frac{h_4 - h_f}{h_g - h_f} \tag{4.27}$$

This helps to calculate viscosity and thermal conductivity of fluid as shown in Eqn. (4.28) & (4.29)

$$\mu = \mu_l + x(\mu_v - \mu_l) \tag{4.28}$$

$$K = K_l + x(K_v - K_l) \tag{4.29}$$

At T inside tube saturation vapor R134a.

From the table R134a saturation vapor table at $T_e = -2℃$

- The flash gas percentage after throttling $x = \frac{h_4 - h_f}{h_g - h_f}$
- $\mu = 212.32 kg.m^{-1}s^{-1}$
- $\dot{m}_r = 0.03093 s^{-1}$
- $k = 70.3 * 10^{-3} W.m^{-1}K^{-1}$
- $k_{copper} = 401 W.m^{-1}K^{-1}$
- $C_p = 1.33 kJ.kg^{-1}K^{-1}$
- $Pr = \frac{\mu C_p}{k} = 4.02$
- For $Re = \frac{\dot{m}_{rif}}{\pi d_i \mu} = 11398.21$ turbulence flow inside a tube fully developed turbulent flow inside a tube the recommend correction by Dittes and Boelter for cooling of the fluid is given by based on the given data and equation internal convective heat transfer coefficient becomes.
- $LMTD = 15.8℃$

h_o estimation

h_o can be estimated by the following given by (Cengel and Boles, 2008).

$$Nu = c * Re^m pr^n \left(\frac{pr}{prs}\right)^{0.25} \tag{4.30}$$

$$Re = \frac{V * d_o}{v} \tag{4.31}$$

And

$$pr = \frac{v}{\alpha} = \frac{\mu C_p}{k} \tag{4.32}$$

h_o Becomes

$$h_o = \left(\frac{V * d_o}{v}\right)^m \left(\frac{\mu C_p}{k}\right)^n \left(\frac{\frac{C_p}{k}}{prs}\right)^{0.25} * \frac{k}{d_o} \tag{4.33}$$

Hence, from the table 4.11 Re= 259.58 C=0.51 and m=0.5 also, since, $pr < 10$, n=0.37

It follows the Property of air at an assumed mean temperature of the air at 301K.

- $v = 15.68 * 10^{-6} m^2 s^{-1}$
- $\dot{m}_r = 0.0309\, kgs^{-1}$
- $k = 26.24 * 10^{-3} W.m^{-1} K^{-1}$
- $pr = 0.7 m^2 s^{-1}$
- $u_\infty = 0.5\, m.s^{-1}$
- $prs = 0.708$ T@ -2℃.

Table 4.11 C and M selection table for different Reynold value (Theodore,2008)

Re_D	C	M
1-40	0.75	0.4
40-1000	0.51	0.5
$10^3 - 2 * 10^5$	0.25	0.6
$2 * 10^5 - 10^6$	0.076	0.7

$$Q_e = U_o * A_e * F * LMTD$$

$$A_e = 2\pi L$$

The length of evaporator becomes 26.65m

4.4.3 Sizing of the condenser

Condenser is device used to condense a substance from its gaseous to liquid state, by cooling it by extracting its latent heat and transferred to the surrounding environment.

Types of condensers

1, Air- cooled

2, Water-cooled

3, evaporative

In this section the dimension of condenser diameter and thickness tube are decided, length of tube is calculated based on thermal analysis.

The condenser sized by analyzing following parameters and conditions

Thermal property of condenser material and the refrigerant R134a the higher conductivity it has higher heat transfer will be. In this thesis copper is selected because it's high thermal conductivity (Theodore et al,. 2008).

Surface area to volume ratio has its effect

Surface area $A_s = 2\pi r L$ (4.34)

Where r is radius of coil

L is length of the coil

Volume $V_{eva} = \pi r^2 L$ (4.35)

Surface area to volume ratio

$$\frac{A_s}{V_{eva}} = \frac{2}{r} \tag{4.36}$$

The temperature difference between ambient air and condensing fluid. High-temperature difference required a smaller length compared to low-temperature difference. Merely it depends on the overall heat transfer coefficient of the hot and cold fluid. Heat transfer analysis on the condenser. There are three modes of heat transfers in the condenser are given by (Cengel and Boles, 2008).

Convection heat transfer $Q_{conv} = h_i A(T_{air} - T_e)$ (4.37)

Conduction heat transfer $Q_{cond} = \frac{KA}{t}(T_{Al} - T_e)$ (4.38)

Radiation heat transfer $Q_{Rad} = A\varepsilon\sigma\left({T_{Al}}^4 - {T_e}^4\right)$ (4.39)

Over all heat transfer $Q_e = UA\Delta T$ (4.40)

Where,

$h_i$is inside convective heat transfer $(W.m^{-2}K^{-1})$

K is conduction heat transfer coefficient $(W.m^{-1}K^{-1})$

t= time(s)

A= area (m^2)

T_{air} = air temperature

T_e = evaporator temperature

U = over all heat transfer coefficient $(W.m^{-2}K^{-1})$

The diameter and the thickness of the condenser are decided from literature then the length of the condenser calculated based on the diameter thickness of the condenser. Since inside the condenser tubes, there are two different flow regimes, namely, the Superheated vapor and the two-phase mixture, the lengths of these regions are calculated separately, and some of these lengths gives the total length of the condenser. The superheated vapor, which leaves the compressor, enters the condenser and leaves as a saturated liquid. The total heat that should be removed from the condenser is the heat gain from the evaporator and heat added during compression (Cengel and Boles, 2008).

$$\dot{Q}_{cond} = \dot{W}_{com} + \dot{Q}_{evap} \tag{4.41}$$

The heat rejected from the condenser is in two regions first from the superheated region (single phase region) then from the condensation region (double phase region).

$$\dot{Q}_{cond} = \dot{Q}_{super} + \dot{Q}_{double} = U * A * F * LMTD \tag{4.42}$$

LMTD of condenser calculated by inlet and outlet temperature and F get from graph by using inlet and outlet temperature.

$$LMTD = \frac{\Delta T_1 - \Delta T_2}{ln^{\Delta T_1}/_{\Delta T_2}} \tag{4.43}$$

The temperature of refrigerant R134a at inlet of condenser and outlet of condenser

The temperature of refrigerant R134a at inlet of condenser $T_3 = 44.23℃$

The temperature of refrigerant R134a at outlet of condenser $T_3 = 39.72℃$

The inlet air temperature in the condenser is $T_{air\ inlet} = 28℃$

The outlet air temperature in the condenser $T_{air\ outlet} = 31℃$

For the superheat region $\Delta T_1 = T_3 - T_{air\ inlet} = 16.23℃$

$$\Delta T_1 = T_3 - T_{air\ outlet} = 13.23℃$$

For the condensation region $\Delta T_1 = T_3 - T_{air\ inlet} = 11.72℃$

$$\Delta T_1 = T_3 - T_{air\ outlet} = 8.72℃$$

LMTD for superheat region

LMTD=287.68K

LMTD for condensation region

LMTD=283.15K

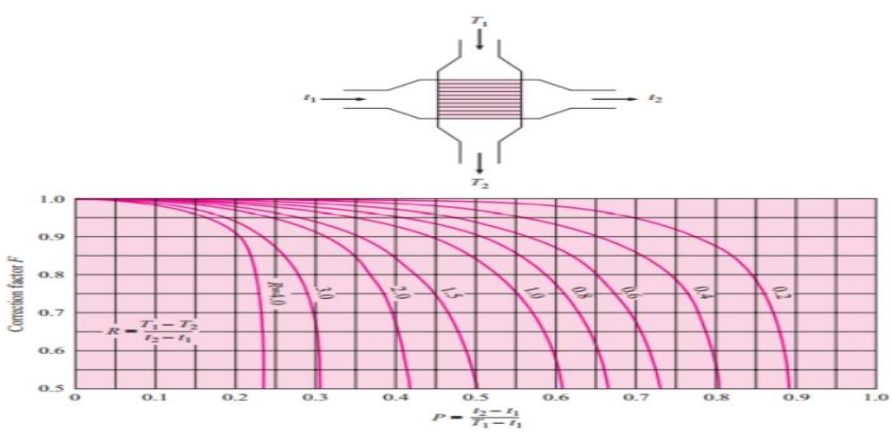

Figure 4.7 Correction factor plot for single pass cross flow exchanger one fluid mixed the other unmixed (Cengel and Ghajar, 2015).

The correction factor for super-heated region is $f = 0.975$

Specification of inner and outer diameter of condenser is 0.01628m and 0.01905m respectively.

Frist estimation of overall heat transfer coefficient (U_o)

$$1/U_o = \frac{A_o}{A_i h_i} + \frac{A_o ln\left({d_o}/{d_i}\right)}{2\pi KL} + \frac{1}{h_o} \tag{4.44}$$

$$A_o = \pi d_o L \tag{4.45}$$

As

$$A_i = \pi d_i L \tag{4.46}$$

And

By substitution equation Eqn. 4.45 and 4.46 in Eqn. 4.44

$$1/U_o = \frac{d_o}{d_i h_i} + \frac{d_o ln\left({d_o}/{d_i}\right)}{2K} + \frac{1}{h_o} \tag{4.47}$$

To find U_o first, we find h_i and h_o

$$h_i = Nu * \frac{K}{d_i} \tag{4.48}$$

Property of R134a from table temperature of

- $\mu = 19.14 * 10^{-6} kg.m^{-1}s^{-1}$
- $\dot{m}_r = 0.309 kg.s^{-1}$
- $k = k_v = 77.7 W.m^{-1}K^{-1}$
- $c_p = 1.073 kJ.kg^{-1}K^{-1}$
- $pr = \frac{\mu cp}{k} = 0.2643$

- $Re = \frac{4m_{rif}}{\pi d_i \mu} = 126318.167$ turbulence frow inside a tube fully developed turbulent flow inside a tube the recommended correlation by Dittes and Boelter for cooling of the fluid is given by.
- $Nu = 0.023 * Re^{\frac{4}{5}} * pr^{0.3}$
- $h_i = Nu * \frac{K}{d_i}$
- $h_i = 0.023 * Re^{\frac{4}{5}} * pr^{0.3} * \frac{K}{d_i}$

Finding h_o

Property of assumed mean temperature of the air at 301K

- $v = 15.69 * 10^{-6} m^2 s^{-1}$
- $\dot{m}_r = 0.0309 kg\ s^{-1}$
- $k = 26 * 10^{-3} W.m^{-1}K^{-1}$
- $c_p = 1.007 * kJ.kg^{-1}K^{-1}$
- $\alpha = 22.5 * 10^{-6}$
- $Pr = 0.708$

The length required at the superheat region (L_{sup})

For the superheat (single -phase) region the condenser heat rejection is equal to

$$\dot{Q}_{sup} = \dot{m}_{rif}(h_2 - h_{3\grave{g}}) = U_o * F * A_c * LMTD$$

$$A_c = \pi d_o L_{sup} + \frac{\dot{Q}_{sup}}{U_o * F * LMTD}$$

$$1/U_o = \frac{d_o}{d_i h_i} + \frac{d_o \ln(d_o/d_i)}{2K} + \frac{1}{h_o}$$

$$L_{sup} = 0.64m$$

Length of the condenser at the double phase region (L_{double})

Heat to be removed from double phase region

$$\dot{Q}_{double} = \dot{m}_{rif}(h_{\grave{2}} - h_3) = U_o * F * A_c * LMTD$$

$$A_c = \pi d_o L_{double} + \frac{\dot{Q}_{double}}{U_o * F * LMTD}$$

$$L_{double} = 20.97m$$

$$L_{total} = L_{sup} + L_{double} = 21.61m$$

.

The total length condenser is 21.61m

4.5 Design of insulation materials for cabin using ANSYS CFD Software

Overall system performance is strongly influenced by insulation thickness due to the heat transfer through the cabinets wall which driven by the temperature difference between inside and outside air. Such corresponding difference to approximate 60% of thermal load and this can be reduced by diminishing the temperature difference. However, this is not practicable since both temperatures are established by energy rating standard. Another option would be to increase the thermal insulation thickness, without reducing highly the useful volume of compartment. Another important thing is internal and external cover of insulation material which may prolong the ageing period of insulation and also the shelf life of fresh raw fruits of are to avoid the increased environmental impact of refrigerated vehicles it would be great interest to reduce their energy consumption, especially by improving and reinforcing insulation.

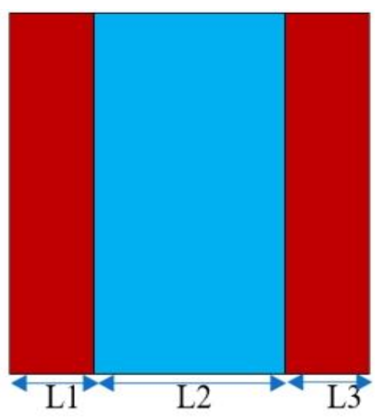

Figure 4.8 Insulation thickness

When selecting suitable thermal insulation material, the required thermal properties are of prime importance. For the functionality and safety of the cabin other important criteria in the choice of insulation are mechanical strength, resistance to ageing, resistance to air and moisture penetration and fire performance. The most common material used cold room and refrigerated vehicle for insulation is polyurethane foam (PUR). PUR insulation has low thermal conductivity values to achieve optimal energy savings with minimal thickness. The excellent mechanical strength values and exceptional durability of PUR insulation fulfil all the requirements of insulation materials used in the building industry (Nce, 2021).

This thesis also focuses on insulation thickness variation and changing different cover material to increase performance using CFD. Thickness of each simulation based on recommended thickness value internationally between 50mm to 150mm for refrigerated trucks. For each simulation maximum ambient temperature of wolaitta sodo is taken which is 34.21℃ and the temperature of inside refrigerated cabin is 5℃.

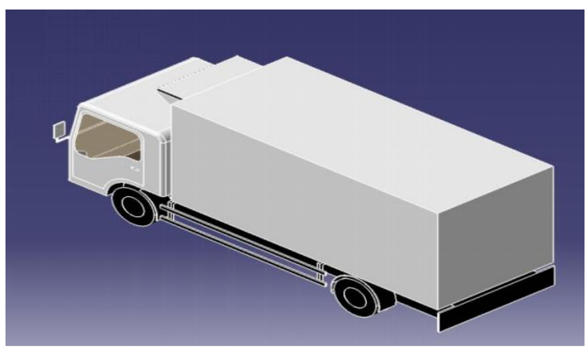

Figure 4.9 Back view of 3D model of Refrigerated truck

Figure 4.10 Side view of 3D model of Refrigerated truck

Figure 4.11 Top view of 3D model of Refrigerated truck

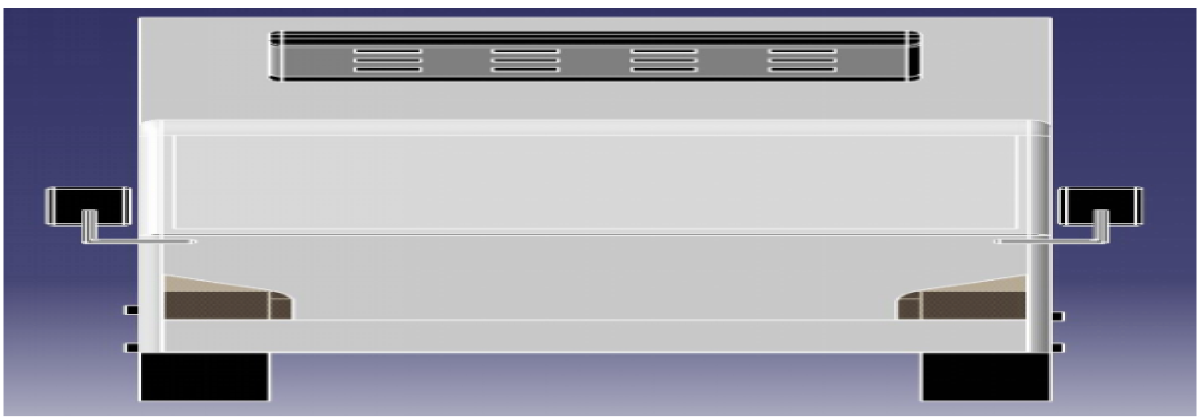

Figure 4.12 Front view of 3D model of Refrigerated truck

Governing equation

Energy, continuity and momentum equation used (Einstein, 2019) .

Continuity equation

$$0 = \frac{\delta \rho}{\delta t} + \frac{\delta}{\delta x_i} \rho(\mu_i) \quad (4.49)$$

Momentum equation

$$\frac{\partial}{\partial t}(\rho \mu_i) + \frac{\delta}{\delta x_i}(\rho \mu_i \mu_f) = \frac{\delta \rho}{\delta x_i} + \frac{\delta \tau_y}{\delta x_i} \quad (4.50)$$

Energy Equation

$$\frac{\partial}{\partial x}(\rho h_{tot}) + \frac{\delta}{\delta x_j}\left(\rho h_{tot}\mu_f\right) + \frac{\delta P}{\delta t} + \frac{\delta}{\delta x_j}\left(\mu_i \tau_y + \lambda \frac{\delta T}{\delta x_f}\right) \tag{4.51}$$

$$\mu\left(\frac{\delta \mu_i}{\delta x_f} + \frac{\delta \mu_f}{\delta x_j} + \frac{2}{3}\delta y \frac{\delta \mu_i}{\delta x_j}\right)$$

$$h_{tot} = h + \frac{1}{2}{\mu_i}^2$$

Governing equation of k_ω SST turbulence model:

$$\rho \frac{Dk}{Dt} = \tau_y \frac{\delta \overline{u_\iota}}{\delta x_j} - \rho\beta * f_\beta * k\omega + \frac{\delta}{\delta x_j}\left[\left(\mu + \frac{\mu t}{\sigma_\epsilon}\right)\frac{\delta k}{\delta x_j}\right]$$

$$\mu_t = \alpha * \rho \frac{k}{\omega}$$

$$\rho \frac{D\omega}{Dt} = \frac{\omega}{k}\tau_y \frac{\delta \overline{u_\iota}}{\delta x_j} - \rho\beta f_\beta \omega^2 + \frac{\delta}{\delta x_j}\left[\left(\mu + \frac{\mu t}{\sigma_\omega}\right)\frac{\delta \omega}{\delta x_j}\right]$$

$$\omega \approx \frac{\epsilon}{k}\alpha\frac{1}{\tau}$$

ω is specific dissipation rate.

Belongs to general 2-equation EVM family fluent 12 supports the standard k_ω model and SST k_ω model

k_ω model prepared mainly because

Frist can be integrated to the wall without using any damping functions.

Second accurate and robust for wide range of boundary layer flows with pressure gradient.

As shown in Figure 4.13 mesh generated of refrigerated cabin and to reduce simulation time body of truck is removed and only body refrigerated cabin used.

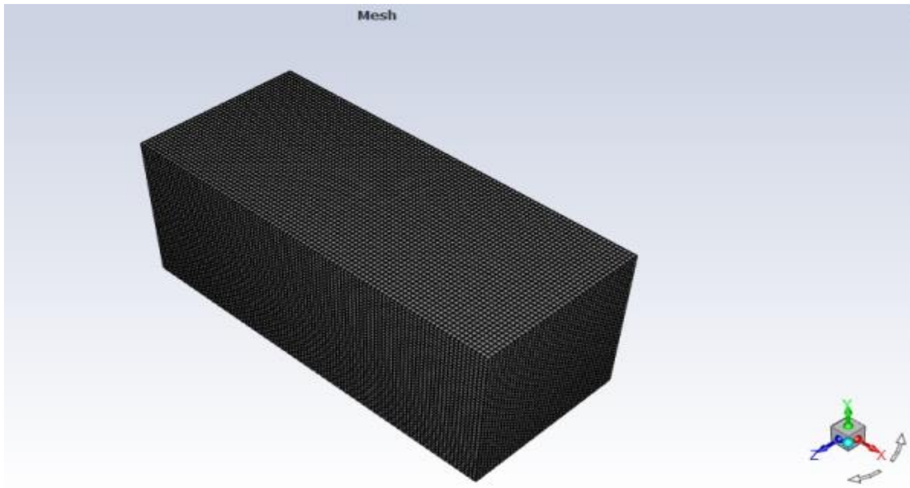

Figure 4.13 Mesh generation

Solver type: pressure based

Velocity formulation: Absolute

Time: Steady

Wall motion: Stationary wall

Shear condition: No slip

Motion: Relative adjacent cell zone

Roughness models: Standard

Mesh quality

According to the user Guide for ANSYS mechanical, mesh quality is determined by the minimum orthogonal quality. Orthogonal quality ratings range from 0 to 1, with lower values signifying worse cells. The minimum orthogonal quality should not be less than 0.01, with the average being much higher, as shown below in Figure 4.16 the mesh quality is greater than 0.01.

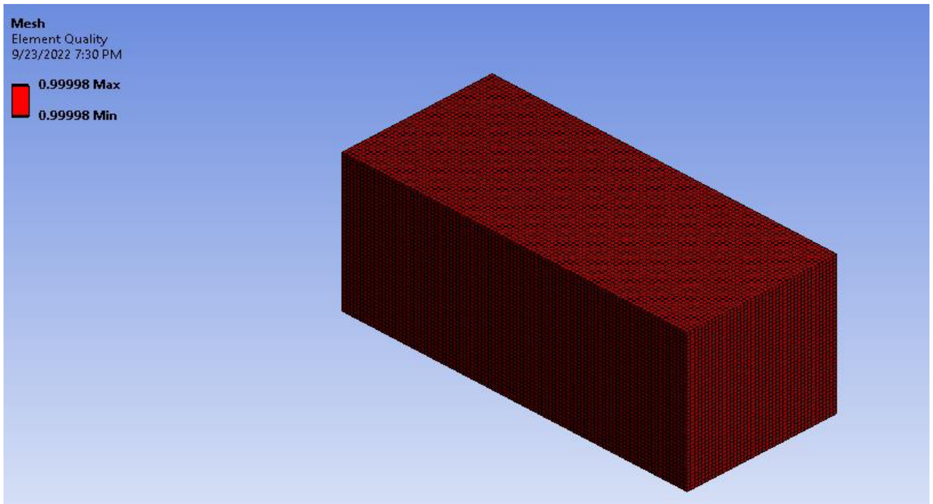

Figure 4.14 Mesh quality

Below the figure 4.16 to 4.20 or simulation case 1 up to 5 is shows the result of wall temperature with different material and thickness.

Table 4.12 Simulation case 1

Wall material	Thickness (mm)		
	Round (1)	Round (2)	Round (3)
Fiber glass	1.5	3.5	5.5
Polyurethane foam	67	69	71
Fiber glass	1.5	3.5	5.5

Round (1)

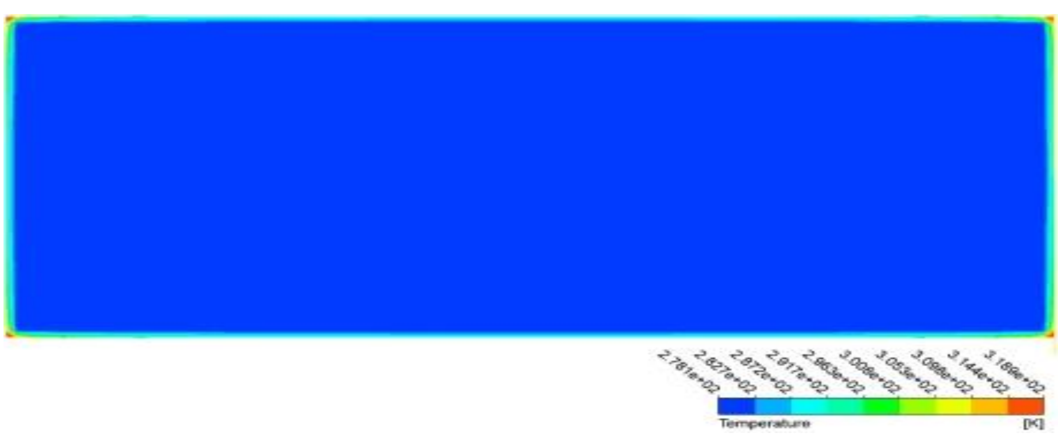

Figure 4.15 Wall temperature

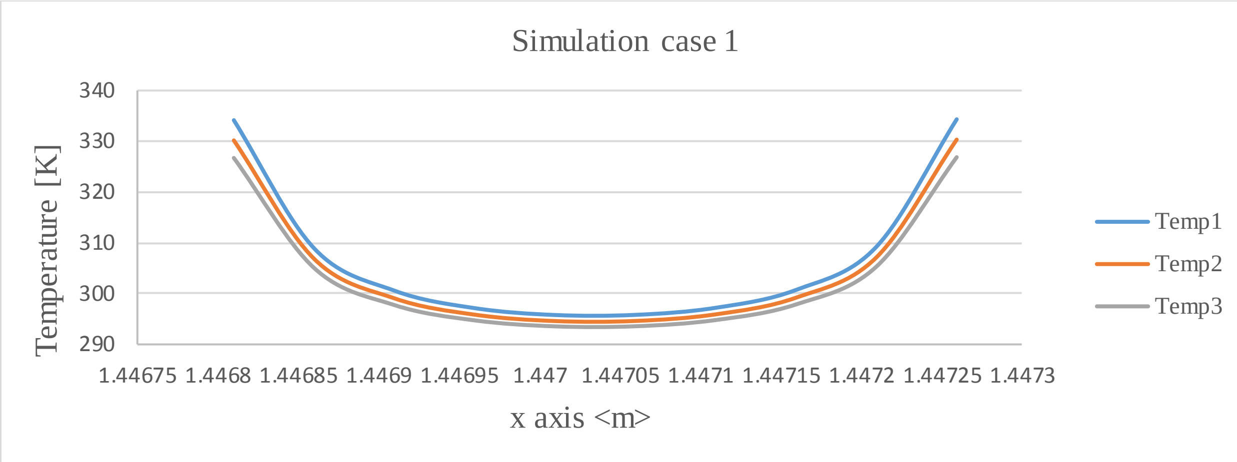

Figure 4.16 Simulation result of case one.

As shown in above simulation indicate that as increase in insulation material thickness decrease in wall temperature. X axis in (m) shows distance of wall to take temperature value. Here the selected point to measure temperature is diagonally and temperature at corner is higher than center of wall due to high heat flux. In this simulation fiber glass used as cover material which has lower density compared to other cover material and thickness 1 $(70mm)$ higher temperature than thickness 2 $(76mm)$ and thickness 2 higher than temperature compered to thickness 3 $(82mm)$. As shown in Figure temperature reaches up to 335℃. The density of material has great factor on load in the refrigerated truck. High wall temperature due to lower simulation thickness. The thickness of all wall is similar.

Table 4.13 Simulation case 2

Wall material	Thickness(mm)		
	Round (1)	Round (2)	Round (3)
Fiber glass	1.5	5.5	3.5
Polyurethane foam	97	101	99
Fiber glass	1.5	5.5	3.5

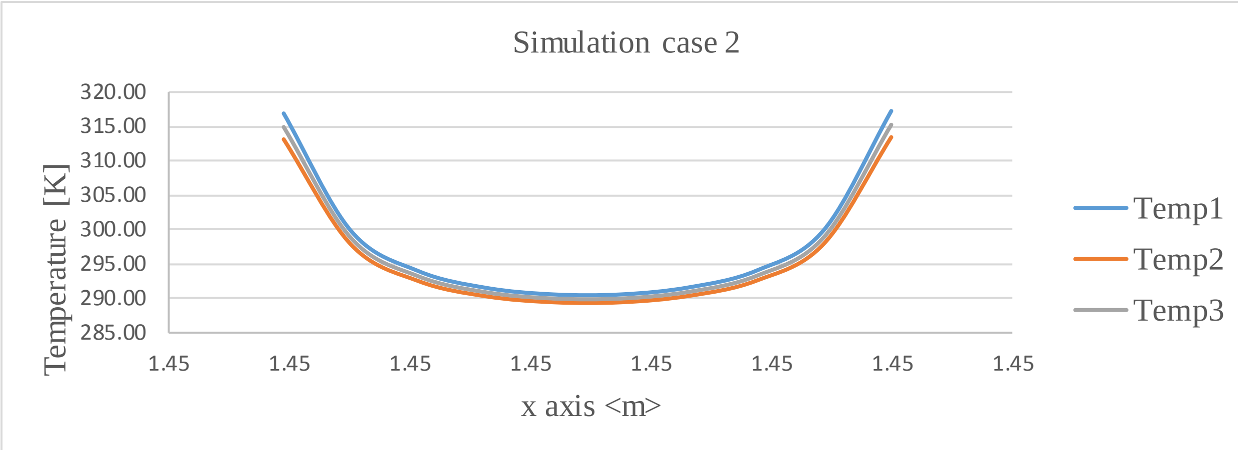

Figure 4.17 Simulation result of case two

In this simulation thickness of insulation material is increased which obtain minimum temperature of wall with minimum energy consumption compared to above simulation (Case1) as shown in figure the temperature of less than 317℃ but increases comparable weight on cabin.

Table 4.14 Simulation case 3

Wall material	Thickness (mm)		
	Round (1)	Round (2)	Round (3)
Fiber glass	1.5	3.5	5.5
Plywood	18	20	22
Polyurethane foam	79	81	83
Fiber glass	1.5	3.5	5.5

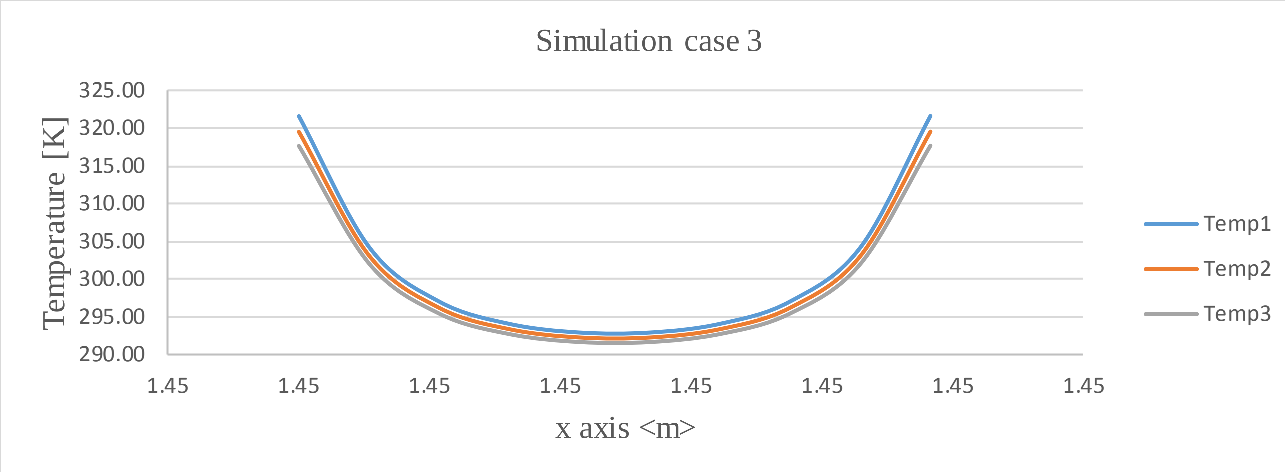

Figure 4.18 Simulation result of case three

This simulation three different material used as cabin material which applied refrigerated vehicle cabin but here in this simulation applied to six walls of refrigerated cabin. The result of simulation shows minimum wall temperature but weight on vehicle is high.

Table 4.15 Simulation case 4

Wall material	Thickness (mm)		
	Round (1)	Round (2)	Round (3)
Polyester	1.5	3.5	5.5
Polyurethane foam	50	52	54
Polyester	1.5	3.5	5.5

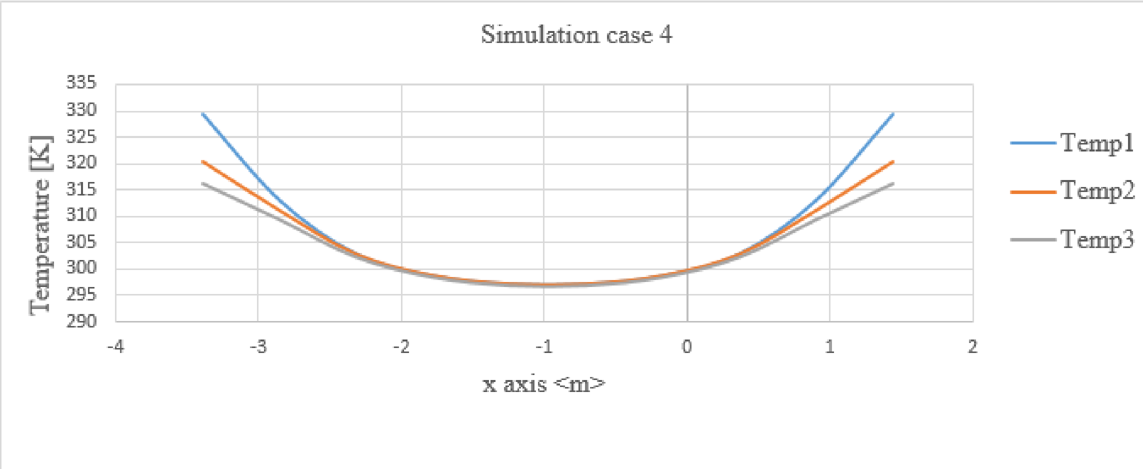

Figure 4.19 Simulation result of case four

In this simulation polyester used as both internal and external cover material of refrigerated cabin with less density. As shown in the above simulation temperature of wall is maximum which is 330℃ and this leads to increase in consumption of energy on refrigerated truck.

Table 4.16 Simulation case 5

Wall material	Thickness (mm)		
	Round (1)	Round (2)	Round (3)
Stainless steel sheet	2	3	1
Polyurethane foam	68	70	66
Galvanizing sheet steel	2	3	1

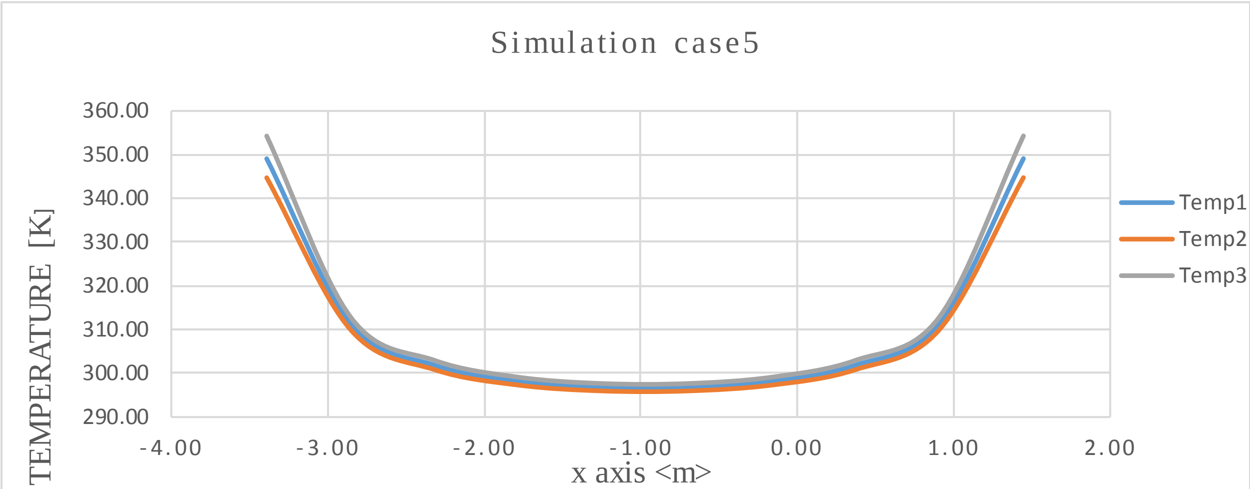

Figure 4.20 Simulation result of case five

In this simulation stainless steel and galvanized sheet used as internal and external cover material of refrigerated cabin respectively. The simulation of shows that high temperature of wall compared to other simulation cases which reaches 354℃ due material high thermal conductivity and density which leads to higher energy consumtion large weight on vehicle.

From above simulation figure 4.18 to 4.22 increase in temperature of wall leads to increase in temperature of refrigerated space which causes rapid deterioration of product, reduce shelf life of product and directly increase energy consumption of refrigerated vehicle. Another thing is higher density of material increase in load on vehicle. Polyester and fiber glass has lower density therefore lower load on vehicle however the thermal conductivity of fiber is lower than polyester so fiber glass temperature which achieve lower temperature of wall. Stainless steel and galvanized sheet steel higher property of material density which highly increase weight of refrigerated cabin and higher thermal conductivity. From above simulation we can understand fiber glass is best cover material depending both in density of material and thermal conductivity. Another thing is temperature at corner is high due to high heat flux.

4.6 Analysis fuel consumption estimation

Estimation of fuel consumption due to addition of vapor compression refrigeration system, and mass on vehicle.

$$F_w = F_{grad} + F_a + F_R \quad (4.52)$$

Where

F_w is wheel force or total running resistance (N)

F_{grad} is gradient force (N)

F_a is acceleration force (N)

F_R is rolling resistance force (N)

$$F_w = m_v g sin\theta + CV^2 + fw = m_v g sin\theta + f w_t \quad (4.53)$$

Power needed for total load (P)

$$P = (m_v g sin\theta + CV^2 + fw)V = (m_v g sin\theta + f w_t)V \quad (4.54)$$

Engine Brake Torque (T_e)

$$T_{ebt}(G)n_{tf} = F_w R = (m_v g sin\theta + f w_r)R \quad (4.55)$$

Engine Brake Power (P_{ebt})

$$P_{ebt} = T_{ebt}(G)n_{tf}\omega_e + (m_v g sin\theta + w_t)V \quad (4.56)$$

f=0.01 for dry asphalt

$$\nabla P_e = T_{ebt}(G)n_{tf}\omega_e - (m_v g sin\theta + w_t)V \quad (4.56)$$

Then brake specific fuel consumption given by

$$BSFC = \frac{\dot{m}_f}{P_e}.3600 \quad (4.57)$$

For modified vehicle

$$P_{ebt} = T_{ebt}(G)n_{tf}\omega_e(m_v g sin\theta + w_t)V + P_{comp} \quad (4.58)$$

$\theta = 0$ or level Road

m_v is mass of vehicle (kg)

g is gravity $\left({m}/{s^2}\right)$

f is coefficient rolling resistance

w_t is total weight of vehicle (N)

T_{ebt} is engine brake torque (Nm)

P_{ebt} is engine brake power (kW)

η_{tf} is efficiency of tractive force

P_{com} compressor power (kW)

V_s Vehicle speed $({m}/{s})$

Table 4.17 Total power and brake specific fuel consumption

P_{re}	18.92kw	P_{ce}	0	P_{Te}	18.94kw	BSFC	2.1
P_{rm}	18.33kw	P_{dm}	0.83kW	P_{Tm}	19.16kw	BSFC	3.44

4.7 Summary of the design results

Main components of refrigerator selected based on specification and literature reviews. Cooling load calculated by considering different loads and the cooling load calculated for actual refrigerated truck is $4.392kW$. The length of evaporator and condenser is $26.65m$ and $21.61m$ respectively. Simulation was done using CFD by varying different cover material and insulation thickness. From the simulation fiber glass best material as cover material and polyurethane foam is selected as insulation material based on literature reviews. The consumption of fuel due to additional power is 1.34 liters per hour.

CHAPTER FIVE

SCALE DOWN PROTOTYPE DESIGN AND FABRICATION

5.1 Introduction

In this chapter scale down prototype design for experimentation, instrumentation for measuring purpose and result and discussion for experimental work is discussed.

5.2 Scale down vapor compression refrigeration system

Checking and comparing the theoretical with experimental results refrigerated box fabricated locally. It is not possible to fabricate exact refrigerated cabin due to high cooling load $4.392\ kW$ and financial problem for experimentation. The components of exact refrigerated cabin due high size of compressor, evaporator and condenser are long. So, use low capacity and fabricate this model after checking performance, for test and validation the model experimentally. Due to higher cost and size of compressor and evaporator minimum size compressor selected for experiment. So, scale down cooling load by 10.

A) Sizing compressor

Evaporator temperature and condenser pressure are the same for model, so cooling effect are the same only difference is mass flow rate of refrigerant and power of compressor.

Mass flow rate ($\dot{m}_r$)

$$\dot{m}_r = \frac{Q_c}{q_e} \tag{5.1}$$

Power of compressor (P) cooling capacity is given by

$$P = \dot{m}_r * (h_2 - h_1) \tag{5.1}$$

Table 5.1 Based on the above equations, the following results are achieved.

$q_e(kJ.kg^{-1})$	$\dot{m}_r\left({kg}/{s}\right)$	$P\left({kJ}/{s}\right)$
141.97	0.00309	0.173

Here specification of 0.173 ${kJ}/{s}$ hermetic sealed reciprocating compressor used due to availability for modeling and refrigerant used is R134a.

B) Sizing of evaporator at cooling capacity

Length of evaporator at the scale down cooling capacity follows the same step above sizing with above one only difference is diameter of coil and mass flow of refrigerant. The outer and inner diameter of evaporator for this cooling assuming 6.35 and 5.64 mm, respectively.

Inside convection heat transfer coefficient (h_i)

$$Re = \frac{\dot{m}_{rif}}{\pi d_i \mu} \tag{5.3}$$

$$Nu = 0.023 Re^{\frac{4}{5}} * Pr^{0.3} \tag{5.4}$$

$$h_i = Nu * \frac{k}{d_i} \tag{5.6}$$

Outer convection heat transfer coefficient (h_o)

$$Re = \frac{V * d_o}{v} \tag{5.7}$$

Assumed velocity air inside refrigerated box is

$$Nu = c * Re^m * pr^n \left(\frac{pr}{prs}\right)^{0.25} \tag{5.8}$$

$$h_o = Nu * \frac{k}{d_o} \tag{5.9}$$

$$Q_e = U_o * A_e * F * LMTD \tag{5.10}$$

For cooling capacity 4392W

$$A_e = \pi d_o L$$

Then length of evaporator becomes $= 3.23m$

C) Length of condenser

Length of condenser at cooling capacity 0.439 kW follows the same step with above design. All properties are the same because of the condenser temperature the only difference is diameter of coil. Outer and inner diameter of condenser for this cooling capacity is assuming 6.35 and 5.64 mm, respectively.

Inside convective heat transfer (h_i)

$$Re = \frac{4\dot{m}_{rif}}{\pi d_i \mu} \tag{5.11}$$

$$Nu = 0.023Re^{\frac{4}{5}} * Pr^{0.3} \tag{5.12}$$

$$h_i = Nu * \frac{k}{d_i} \tag{5.13}$$

Outer convection heat transfer coefficient (h_o)

$$Re = \frac{V * d_o}{v} \tag{5.14}$$

Assumed velocity air inside refrigerated box is

$$Nu = c * Re^m pr^n \left(\frac{pr}{prs}\right)^{0.25} \tag{5.15}$$

$$h_o = Nu * \frac{k}{d_o} \tag{5.16}$$

Heat removed from the condenser in superheated region

$$\dot{Q}_{sup} = \dot{m}_{rif}\left(h_2 - h_{\grave{3}g}\right) = U_o * F * A_c * LMTD \tag{5.17}$$

$$A_C = \pi d_o L_{sup} = \frac{\dot{Q}_{sup}}{U_o * F * LMTD} \tag{5.18}$$

$$L_{sup} = 0.64m$$

Length of condenser in double phase

$$\dot{Q}_{double} = \dot{m}_{rif}(h_{\grave{2}} - h_3) = U_o * F * A_c * LMTD =$$

$$A_o = \pi d_o L_{double} = \frac{\dot{Q}_{double}}{U_o * F * LMTD} \tag{5.19}$$

$$L_{double} = 3.46m$$

$$L_{total} = L_{sup} + L_{double} = 4.2m$$

5.3 Fabrication and assembly of scale down refrigerator

The manufacturing process of scale down refrigerator explained below. Initially, all the components required for the system were gathered and then fabricated locally. The vapor compression refrigeration system prototype was fabricated locally on the basis of the design decision and calculated values of the scale down prototype components. In this section the fabrication of evaporator, expansion valve, condenser, and other components indicated in table 5.2. After prototype fabricated by the specification of the components found in the sizing portion and assembly of parts is made in a way suitable for the experiment. The wire and tube condenser placed at front part of refrigerator. A coper tube evaporator, capillary tube, and filter drier are purchased as specified. Table 5.2 reviews the overall component type of the refrigerator.

Due to availability of material insulation material taken to experimental work is glass wool which has almost similar thermal conductivity with polyurethane foam with 66mm thickness. External cover material is stainless steel with 1mm thickness and internal cover material galvanized sheet with 1mm thickness is used.

Table 5.2 Refrigerator system component description for scale down prototype

No	Components/systems	Type of selected components
1	Refrigeration system	Vapour compression refrigeration system
2	Refrigeration type	Refrigeration system with rear door
3	Condenser	Air cooled wire and tube type
4	Evaporator	Bare tube and natural convection
5	Compressor	1/4 hp compressor (L72CZ) compressor
6	Expansion device	Coiled capillary tube
7	Filter drier	Throw air type
8	Thermostat	Cold thermostat
9	Insulation material	Glass wool

5.3.1 Fabrication of evaporator

Based on selected and size in above copper tube outer diameter of 6.35mm and 5.64mm most of time in refrigerated trucks evaporator placed in inside of front wall. In refrigerated trucks the cabinets have only one part for product storage and also for scale down prototype evaporator placed at inside of front wall and with only one compartment for storage of product.

Figure 5.1 Evaporator

5.3.2 Fabrication of condenser

The air-cooled wire and tube copper condenser are selected in the chapter four and in the sizing section of chapter four the length is designed to be 4.2m long, 6.35 mm diameter. As shown in Figure 5.2, wire and tube condenser with the required diameter, thickness, and length is purchased.

Figure 5.2 Condenser

5.4 Other component of refrigerator

Compressor, capillary tube and filter drier and are purchased due to specification of selection and designing section.

Figure 5.3 Compressor, capillary tube and filter drier.

5.5 Assembly of refrigerator parts

The condenser is placed at the front side of the refrigerator by screwing the condenser in to the body of the refrigerator for support system compressor placed at front part of refrigerator with filter drier by acetylene and oxygen gas wielding. Evaporator wrapped in the internal wall front part of cabinet of the refrigerator this kind of evaporator installation common in refrigerated trucks and gives approximately uniform temperature in the compartment which is very essential for the experimentation. And it brazed with the capillary tube in one end and with the compressor on the other end. Capillary tube brazed with evaporator inlet and filter drier. Finally, the compressor is assembled by brazing it with the evaporator outlet and condenser inlet. The electrical system is installed with the connection of the thermostat which sensed the outlet temperature of the evaporator to auto-start and stops the compressor.

Leakage Test

Leakage tests are done before and after charging refrigeration gas into the system. After the system fully assembled it evacuated from the air and tested for leakage by plugging pressure gage and measuring vacuum pressure of an hour, it maintains the same pressure which means no linkage in the system. The R134a gas has charged in to the system with the required pressure the second leakage test is done after working for 10 hours and the pressure reads shows that there is no leakage in the system.

Experimental Setup

Figure 5.4 shows the refrigerator proposed to the experiment. Conventionally, an air-cooled wire and tube type condenser is attached to the front of the refrigerator. The refrigerant flowing inside the tube rejects heat to the ambient due to the natural convection. It is a known fact that with the higher ambient temperature, the condenser temperature and condenser pressure settle on the higher side.

Figure 5.4 Scale down prototype

Instrumentation

As shown in figure 5.5 K-type Thermocouple thermometers (HT-9815 and WL-362) are used for the measurement of temperature. Timer used to take calibration with time interval.

Figure 5.5 Temperature measuring instrument (a) Digital thermocouple thermometer (b) k type thermometer (c) timer (d) k type thermocouple thermometer

Calibration of Thermocouple

As shown in Figure 5.6 thermocouples are calibrated with a digital thermometer. The calibration has two steps first the thermocouples have inserted in the water ice bath at 0 °C along with mercury thermometers and readings are taken. For better results, this process done by boiling the water the readings are recorded. After the recording completed the deviation of thermocouple thermometers is calculated. Calibration of thermocouples are explained in appendix.

Figure 5.6 Calibration temperature measuring instrument with ice.

5.6 Temperature measurement

The evaporator temperature is measured at three points at the inlet, middle, and outlet of the evaporator. The temperature of the compartment and papaya which took as the load on the refrigerator are taken at different points.

Figure 5.7 Papaya fruit for experimentation

Figure 5.8 Papaya inside refrigerator

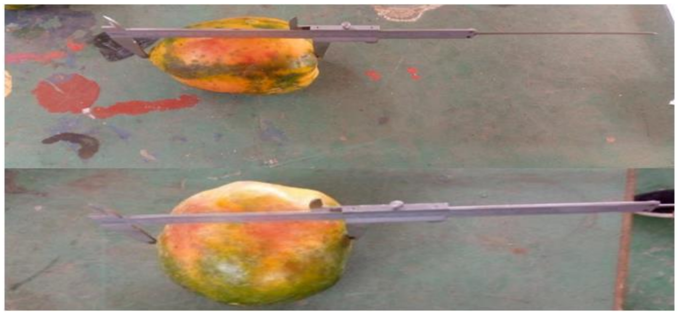

Figure 5.9 Papaya fruit used for on load test.

For on load test the diameter and length of papaya fruit is 110cm and 140cm respectively.

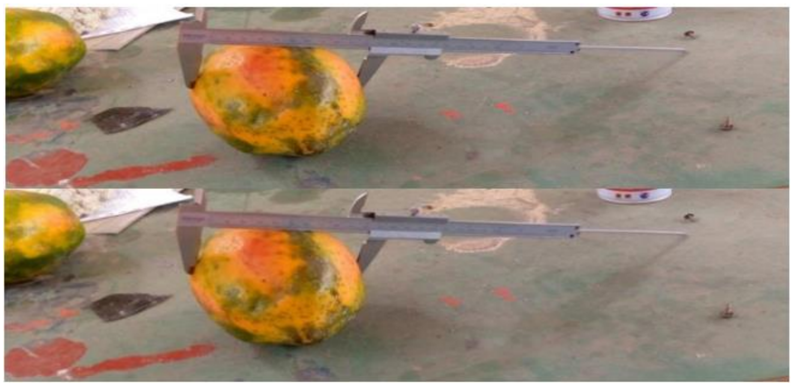

Figure 5.10 Papaya fruit used for full load test.

Full load test the diameter and length of papaya fruit is 115cm and 145cm respectively.

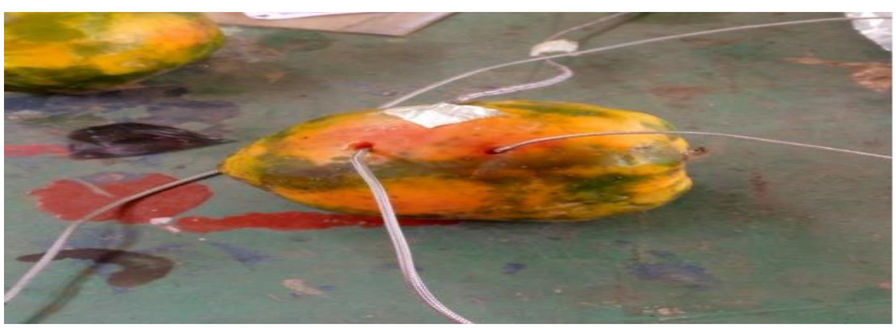

Figure 5.11 Papaya fruit with different depth for full load test.

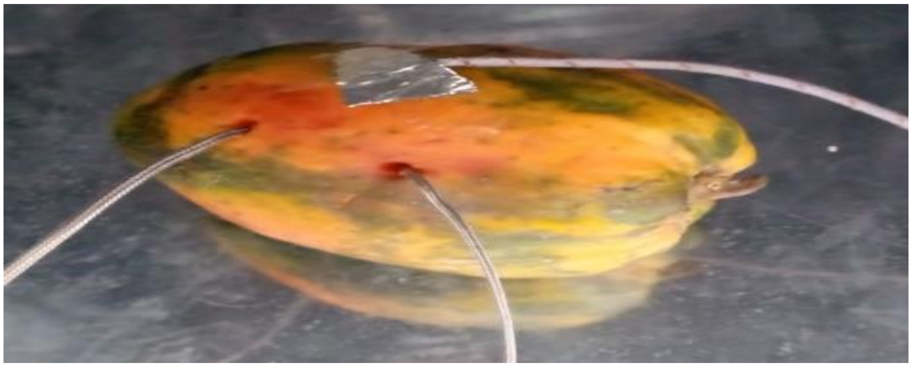

Figure 5.12 Papaya fruit with different depth for on load test.

CHAPTER SIX
EXPERMENTAL PERFORMANCE TEST OF REFRIGERATION SYSTEM

6.1 Introduction

In this chapter, the result and its implication obtained from investigating the experimental performance of fabricated refrigerator with and without load are presented and discussed. Experimentation was carried out to investigate the performance of the fabricated refrigerator with and without load by measuring surface temperature of the condenser, evaporator, compartment, product, and ambient temperature. By using of papaya fruit as load.

No load and full load test

Here papaya taken to calculate cooling load and for experimental work because of low storage temperature. Experimental work was done first only one papaya taken to work experiment outside by exposing refrigerator to ambient temperature of adama the three-thermocouple wire used to read temperature of papaya at different depth as shown in figure to know how long time taken to come to storage temperature. The temperature measurement is taken in the inlet, middle, and outlet of the condenser and evaporator. For the both tests (no-load and load) temperature measurement taken at the start and end of the compressor and every five minutes between the start and the stop of the compressor. in the on-load test, the refrigerator is loaded with papaya at room temperature around 25 ℃ and the temperature change is measured by inserting thermocouple in the papaya at different depth and the result is taken to calculate the refrigeration effect of the refrigerator.

6.2 Experimental performance of the VCRS

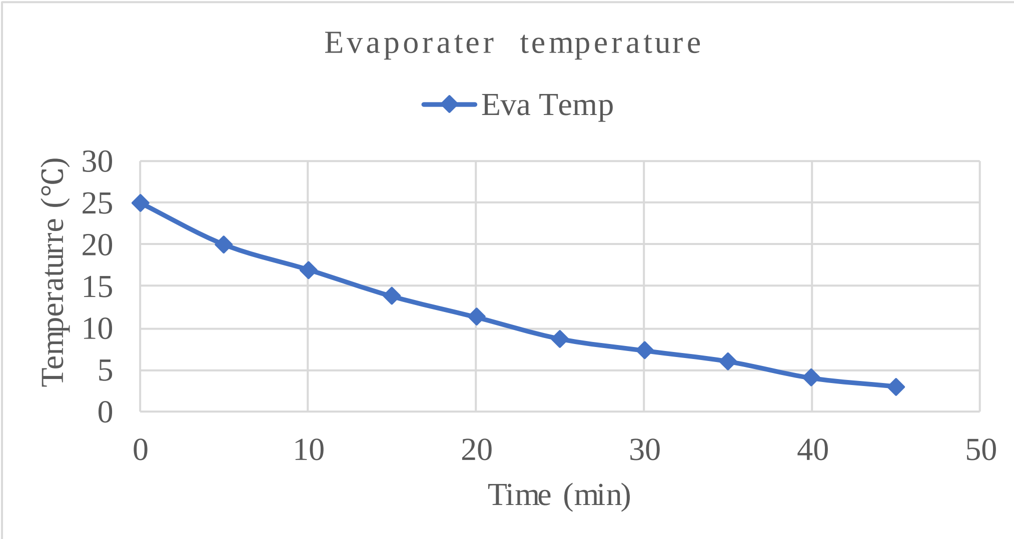

Figure 6.1 Temperature of evaporator at middle starting from atmospheric temperature

After 45-minute temperature of evaporator coil at the middle becomes 3°C without load of average value.

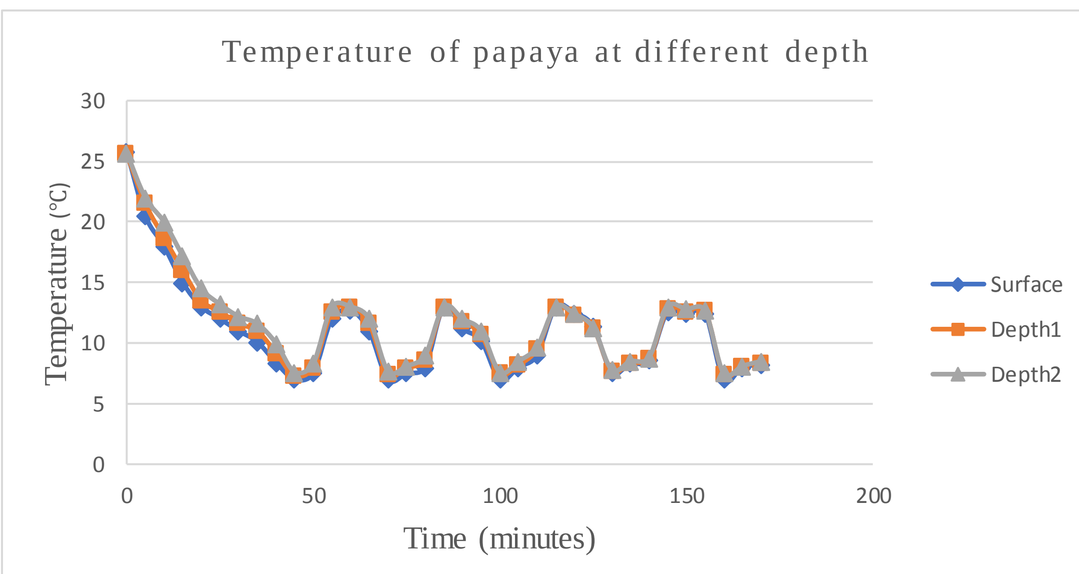

Figure 6.2 Temperature of papaya at different depth for no load test

Free load test only one papaya taken to know performance of refrigerator for three hours. Which take 45 minutes to come to storage temperature as shown in above figure temperature at surface lower and increase at depth 1 to 2. The temperature varies between 13 and 7 ℃ storage temperature of papaya fruit.

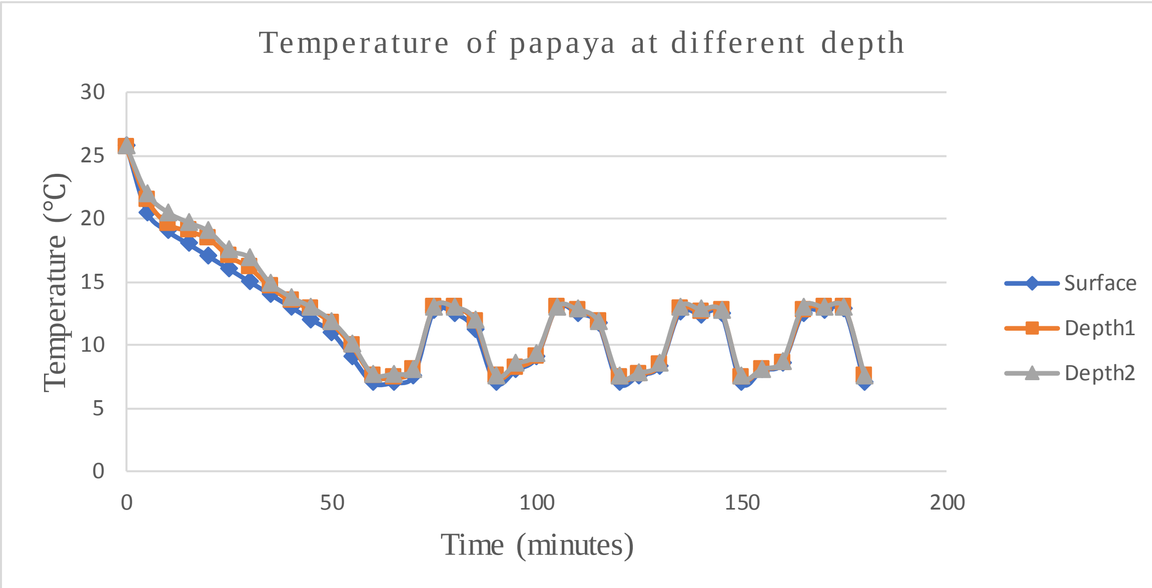

Figure 6.3 Temperature of papaya at different depth for full load test

Full load test which indicates performance of refrigerator. The temperature of papaya comes to storage temperature after 60 minutes. At different depth of papaya fruit as indicated in graph of experimental result temperature of papaya different from surface to internal depth. At the surface temperature lower increase at depth 2 and 1 and comes to storage temperature after 60 minutes.

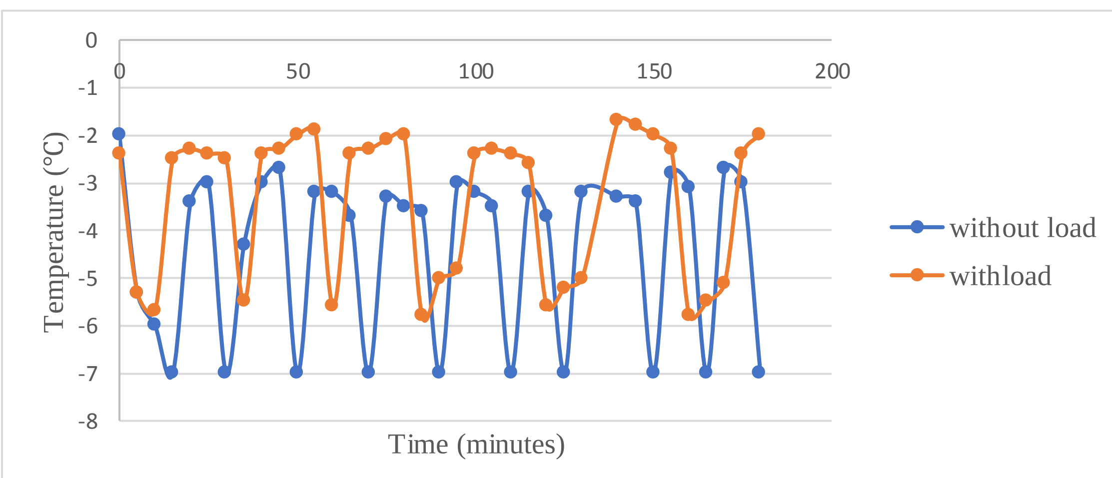

Figure 6.4 Inlet temperature of evaporator with and without load

The measurement taken at every five minutes on off compressor. The evaporator temperature at inlet in full load test is higher than that of no-load test this in turn increases the compressor outlet temperature (42℃ from 39.37℃).

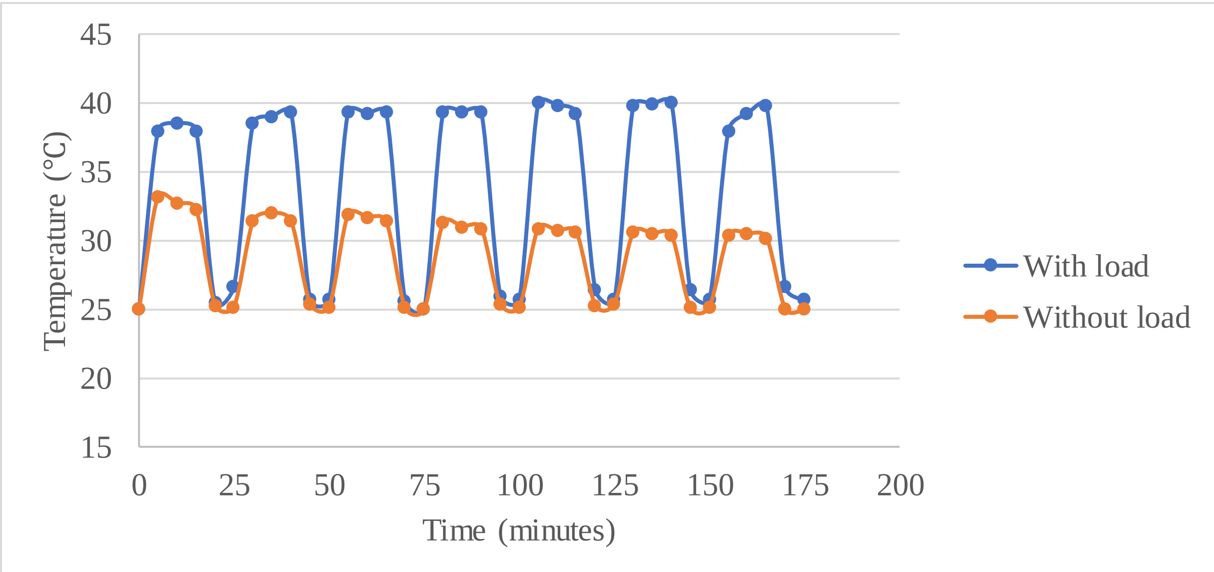

Figure 6.5 Middle temperature of condenser with and without load

Temperature of middle of condenser as shown in above figure temperature with full load shows higher than temperature without load. When the load refrigerator increases cases complete evaporation of refrigerant and superheated at the compressor inlet this causes to increase the condensing temperature and pressure.

6.3 Dimensional similarity

Let the heat flux taken to determine dimensional similarity due to similarity thickness of wall. And thermal conductivity of glass wool and polyurethane foam almost similar with small difference 0.023 $^{W}/_{m.K}$ and 0.025 $^{W}/_{m.K}$ respectively. Due to availability of insulation material the glass wool used in scale down prototype and its approximate similarity of thermal conductivity.

$$\frac{q}{A} = \frac{K\Delta T}{\Delta x} \tag{5.20}$$

$$\frac{q}{A} = \frac{K_1 \Delta T_1}{\Delta x} = \frac{K_2 \Delta T_2}{\Delta x} = \frac{K_1}{K_2} \Delta T_1 + T_\infty = T_2 \tag{5.21}$$

$$T_2 = \frac{K_1}{K_2}(T_1) + T_\infty \left(1 - \frac{K_1}{K_2}\right) \tag{5.22}$$

Where,

ΔT_1 is temperature of scale down prototype

ΔT_2 is temperature of refrigerated trucks

Roof wall selected to determine area because it's possible to estimate another wall also based one of the walls.

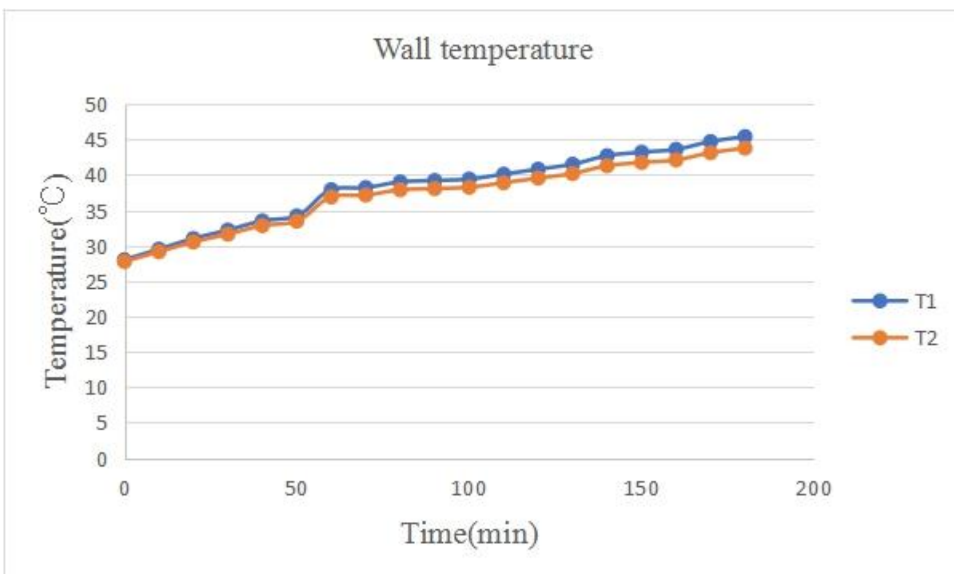

Figure 6.6 Temperature of wall

Wall temperature of experimental work and simulation shows small difference which is 4.1℃.

CHAPTER SEVEN
CONCLUSION AND RECOMMENDATION

7.1 Conclusions

In this thesis, a vapor compression refrigeration system was designed Isuzu car of cargo dimension $4.84m * 2.1m * 2m$ which has a cooling capacity of $4.392kW$ and $0.828kW$ compressor power input and cyclically operating R134a refrigerant working with -2 and 39.37℃ temperature of the evaporator and condenser, respectively in the pipe circuit. For cabin model was design using CATIA V5 and the refrigeration components were by considering the mass and type for selected fruit done using correlations. The design was evaporator and condenser length of $26.65m$ and $21.61m$ respectively with COP 5.3. One tenth scale down model of the designed cabinet size (or cargo size) Isuzu car the experiment was conducted out door condition to evaluate the experimental performance. The major findings were the size of evaporator and condenser is $3.23\ m$ and $4.2m$. After constructing the refrigeration system, refrigerant leakage and pressure tests were done to ensure that the refrigerator is ready for the experiment. Experimental performance investigation of the system was done as designed condition without load and with load of papaya. Papaya fruit without load only one papaya to show the performance of refrigerator and it takes 45 minutes to become storage temperature. Full load test shows papaya fruit takes 60 minutes to become storage temperature. Fuel consumption analysis shows additional fuel consumption of the refrigerated Isuzu truck is 1.34 liter per hour greater than the unrefrigerated Izusu car existing.

Fiber glass, polyester and stainless steel with Galvanized sheet steel is used insulation cover material and different thickness of insulation are simulated using ANSYS WORKBENCH with 2mm thickness difference in material the result of the simulation shows fiber glass best insulation cover material due to its thermal conductivity and density of material. The dimensional similarity shows small difference of wall temperature which is 4.1℃.

7.2 Recommendation

- Temperature at the corner of cabin is high due to high heat flux this need further simulation to control heat transfer improvement.
- To reduce aerodynamic drag force the corner surface of cabin can be round the CATIA model rather than using a rectangular design.

.

REFERENCES

Adekomaya, Oludaisi, Tamba Rotimi Sadiku, and Zhongie Huan (2017), "Minimizing Energy Consumption in Refrigerated Vehicles through Alternative External Wall." *Renewable and Sustainable Energy Reviews67:8993.*http://dx.doi.org/10.1016/j.rser.2016.09.007.

Ahamed, J U, R Saidur, and H Masjuki (2011), "A Review on Exergy Analysis of Vapor Compression Refrigeration System." *Renewable and Sustainable Energy Reviews* 15(3): 1593–1600. http://dx.doi.org/10.1016/j.rser.2010.11.039.

Ajayi, O et al. 2019. "ScienceDirect ScienceDirect ScienceDirect Investigation O 3 – Nanofluid on the Investigation of of the the Effect Effect of of R134a / Al 2 O 3 – Nanofluid on the Performance of a Domestic Vapour Compression Re." *Procedia Manufacturing* 35: 112–17. https://doi.org/10.1016/j.promfg.2019.05.012.

Arora, Akhilesh, and S C Kaushik (2008), "Theoretical Analysis of a Vapour Compression Refrigeration System with R502 , R404A and R507A ´ Orique d ' Un Syste ` Me Frigorifique a ` Compression de Analyse the Vapeur Au R502 , R404A et R507A." 31: 998–1005.

Artuso, Paolo et al. 2019. "Dynamic Modeling and Thermal Performance Analysis of a Refrigerated Truck Body during Operation." *International Journal of Refrigeration* 99: 288–99. https://doi.org/10.1016/j.ijrefrig.2018.12.014.

ASHRAE. 2014. *REFRIGERATION SI Edition*.

Baskaran, A et al. (2022), "Exergy Performance Investigation of Eco-Friendly Refrigerant Mixtures as an Alternative to R134a in a Domestic Refrigerator." 2022.

Brecht, Jeffrey K et al. "Protecting Perishable Foods During Transport by Truck and Rail."

C P Arora (2010),. *Refrigeration and Air Conditioning Text Book.*

Dalkilic, A S, and S Wongwises (2010), "A Performance Comparison of Vapour-Compression Refrigeration System Using Various Alternative Refrigerants." *International Communications in Heat and Mass Transfer* 37(9): 1340–49. http://dx.doi.org/10.1016/j.icheatmasstransfer.2010.07.006.

Design, Industrial, South Africa, Ibogun Campus, and Ogun State (2017), "All Rights Reserved."

Einstein, Albert. 2019. "The K-ω Shear-Stress Transport (SST) Turbulence Model." : 57–66.

G.V. Parishwad, CH.Prasad, R.K.Bharwaj and V.K.Nema (2000), "Estimation Of Cooling Load."

Garimella, Srinivas, Ashlie M Brown, and Ananda Krishna (2011), "Waste Heat Driven Absorption / Vapor-Compression Cascade Refrigeration System for Megawatt Scale , High-

Flux , Low-Temperature Cooling ` Me Frigorifique a ` Absorption a ` Compression de Vapeur Syste ´ Par La Chaleur Re ´ Cupe ´ Re ´ e Pour Le Refroidisse." *International Journal of Refrigeration* 34(8): 1776–85. http://dx.doi.org/10.1016/j.ijrefrig.2011.05.017.

Getahun, Samuel (2018), "Experimental and Numerical Investigation of Airflow Inside Refrigerated Shipping Containers." : 1164–76.

Glouannec, Patrick, Benoit Michel, Guillaume Delamarre, and Yves Grohens (2014), "Experimental and Numerical Study of Heat Transfer across Insulation Wall of a Refrigerated Integral Panel Van." *Applied Thermal Engineering* 73(1): 194–202. http://dx.doi.org/10.1016/j.applthermaleng.2014.07.044.

Gupta, B L, Mayank Bhatnagar, and Jyotirmay Mathur (2014),"Optimum Sizing of PV Panel , Battery Capacity and Insulation Thickness for a Photovoltaic Operated Domestic Refrigerator." *SUSTAINABLE ENERGY TECHNOLOGIES AND ASSESSMENTS* 7: 55–67. http://dx.doi.org/10.1016/j.seta.2014.03.005.

Gupta, Jyoti Soni1 and R C (2013), "PERFORMANCE ANALYSIS OF VAPOUR COMPRESSION REFRIGERATION SYSTEM WITH R404A, R407C AND R410A."

Hammond, E C, and J A Evans (2014) ,"ScienceDirect Application of Vacuum Insulation Panels in the Cold Chain Analysis of Viability Application de Panneaux d ' Isolation Sous Vide Dans La Chaine Du Froid e Analyse de La Viabilit E." *International Journal of Refrigeration* 47(0): 58–65. http://dx.doi.org/10.1016/j.ijrefrig.2014.07.010.

Ilorkar, Ashutosh V., Amol M. Andhare, Alok Kumar Jha, and Mohan G. Trivedi (2019), "The Design and Development of Milk Vending E-Vehicle Using Vapour Compression Refrigeration System." *International Journal of Mechanical and Production Engineering Research and Development* 9(Special Issue): 17–23.

Imtiaz, Fawaz, Md. Samiul Alam Bhuiyan, and Md. Ashiqur Rahman (2020), "Assessment of Thermal Performance of Transport Refrigeration Vehicles by Modifications in the Compartment Design and Storage Pattern." *Proceedings of International Exchange and Innovation Conference on Engineering & Sciences (IEICES)* 6(November): 284–91.

Investigation, Experimental, O F Phase, Material Integrated, and Vapor Compression (2020), "MATERIAL INTEGRATED VAPOR COMPRESSION."

Islam, Mehran, Asif Kabir, Arnab Mustafiarka, and Ashiqur Rahman (2019), "Assessment of the Transport Refrigeration System in Bangladesh and Numerical Simulation of the Refrigeration Performance Assessment of the Transport Refrigeration System in Bangladesh and Numerical Simulation of the Refrigeration Performance." 030013(July).

Jae, Won, Kookjeong Seo, and Yongchan Kim (2012), "Development of an Optimization Strategy for Insulation Thickness of a Domestic Refrigerator-Freezer ´ Veloppement d ' Une Strate ´ Gie d ' Optimisation de l ' e ´ Paisseur De ´ Rieur d ' Un Re ´ Frige ´ Rateur / Conge ´ Lateur de l ' Isolation a Domestiqu." *International Journal of Refrigeration* 36(3): 1162–72. http://dx.doi.org/10.1016/j.ijrefrig.2012.11.013.

James, Christian (2019), Sustainable Food Supply Chains *Food Transportation and Refrigeration Technologies — Design and Optimization*. Elsevier Inc. http://dx.doi.org/10.1016/B978-0-12-813411-5.00013-2.

Jara, Paúl B.Torres et al. (2019), "Thermal Behavior of a Refrigerated Vehicle: Process Simulation." *International Journal of Refrigeration* 100: 124–30. https://doi.org/10.1016/j.ijrefrig.2018.12.013.

Jara, Paúl Torres et al. (2019), "Thermal Behavior of a Refrigerated Vehicle : Process Simulation Comportement Thermique d ' Un Véhicule Frigorifique : Simulation de Processus." *International Journal of Refrigeration* 100: 124–30. https://doi.org/10.1016/j.ijrefrig.2018.12.013.

John A. Tomczyk, Eugene Silberstein, William C. Whitman, William M. Johnson. (2016), *Refrigeration and Air Conditioning Technology*.

Kharagpur (2008), *Refrigeration and Air Condtioning*.

Krishnakumar, T (2017),"Design of Cold Storage for Fruits and Vegetables." (2002).

Laguerre, O, and D lick (2010),"Temperature Prediction in Domestic Refrigerators : Deterministic and Stochastic Approaches ´ Vision de La Tempe ´ Rature a ` l ' Inte ´ Rieur Des Re ´ Frige ´ Rateurs Pre ´ Terministes et Stochastiques Domestiques : Approches De." *International Journal of Refrigeration* 33(1): 41–51. http://dx.doi.org/10.1016/j.ijrefrig.2009.09.014.

Loads, Cooling, Irma Handayani Lubis, and Donny Koerniawan (2017),"Cooling Load Estimation in the Building Based On Heat Sources Cooling Load Estimation in the Building Based On Heat Sources."

Mehmet ALTINKAYNAK, Engin OLGUN, Arzu ŞENCAN ŞAHİN*, and 1Isparta (2019), "Comparative Evaluation of Energy and Exergy Performances of R22 and Its Alternative R407C, R410A and R448A Refrigerants in Vapor Compression Refrigeration Systems." 2019(3): 659–67.

Micheaux, T Lafaye De et al (2016), "Experimental and Numerical Investigation of the Infiltration Heat Load during the Opening of a Refrigerated Truck Body To Cite This Version : HAL Id : Hal-01287034."

Nce, A L L I A (2021), "Physical Properties of Polyurethane Insulation." *Australian Modern Building Alliance* Paper 1: 1–12.

Oury, Alexandre, Patrick Namy, and Mohammed Youbi-idrissi (2015),"Aero-Thermal Simulation of a Refrigerated Truck Under Open and Closed Door Cycles."

Pual (2017) ,"Pual,2017.Pdf"

R.S.Khurmi and J.K.Gupta (2008), "Refrigeration and Air Conditioning."

Rech, Sergio, Elisa Finco, and Andrea Lazzaretto (2020), "A Multicriteria Approach to Choose the Best Renewable Refrigeration System for Food Preservation." *Renewable Energy* 154: 368–84. https://doi.org/10.1016/j.renene.2020.02.115.

S. A. Tassou*, G. De-Lille, Y. TG (2010), "Food Transport Refrigeration – Approaches to Reduce Energy Consumption and Environmental Impacts of Road Transport." *Applied Thermal Engineering* 29(8–9): 1467–77. http://dx.doi.org/10.1016/j.applthermaleng.2008.06.027.

Senguttuvan, Santhosh et ,.al (2020), "Enhanced Airflow in a Refrigerated Container by Improving the Refrigeration Unit Design." *International Journal of Refrigeration*. https://doi.org/10.1016/j.ijrefrig.2020.08.019.

So, Jun-hwi, Sung-yong Joe, Seon-ho Hwang, and Soojin Jun (2021), "Analysis of the Temperature Distribution in a Refrigerated Truck Body Depending on the Box Loading Patterns." : 1–20.

Sruti, N M K S, P R Jenaneswari, and E Yu Anisimova (2020), "Improvement of Insulation Material for Cool Box Application Improvement of Insulation Material for Cool Box Application."

Taylor, Publisher (2007), "Two Fundamental Problems of Refrigerator Thermal Insulation Design." (December 2014): 37–41.

Thavamani, Jeyaraj, and Senthil (2022), "Performance Analysis of Retrofitted Domestic Vapor Compression Refrigeration System Using Hydrocarbon Refrigerants." *International Journal of Ambient Energy* 0(0): 1–25. https://doi.org/10.1080/01430750.2020.1751284.

Theodore L.Bergman Adriennes S.Lavine(2008), *Fundmentals of Heat and Mass Transfer*.

Thiessen, Susan et al (2018), "AC PT US CR."

Vaibhav Jain, S. S. Kachhwaha2, R.Mishra (2011), "Comparative Performance Study of Vapour Compression Refrigeration System with R22/R134a/R410A/R407C/M20." 2(2): 297–310.

Venkataraman, et al. (2020), "Coupling of Engine Exhaust and Fuel Cell Exhaust with Vapour Absorption Refrigeration / Air Conditioning Systems for Transport Applications : A Review." *Thermal Science and Engineering Progress* 18(March): 100550. https://doi.org/10.1016/j.tsep.2020.100550.

Verma, Sankarshan, and Harjit Singh (2020), "Why and Which Insulation Materials for Refrigerators ! Why and Which Insulation Materials for Refrigerators !" (April).

wang and shang (2018), *HANDBOOK OF AIR CONDITIONING AND REFRIGERATION*.

Xiaofeng, Xu, and Zhang Xuelai (2020), "Jo Ur Na l P Re Of." *Journal of Food Engineering*: 110286. https://doi.org/10.1016/j.jfoodeng.2020.110286.

Yeh, Min-Hsiung Yanga and Rong-Hua (2014), "Theoretical Analysis of Optimal Subcooling for Single Theoretical Analysis of Optimal Subcooling for Single Vapor-Compression Refrigeration." (March 2015): 37–41.

Yunus A. Cengel and Afshin J. Ghajar (2015), *HEAT AND MASS TRANSFER*.

Yunus A.Cengel and A.Boles Michael (2008), *THERMODYEMICS*.

Yuzainee, M Y, N H Noor Zafira, and J Nurulnadiah (2019), "Cooling Load Calculation for Efficient Cold Storage of Fresh-Cut Yam Bean." (4): 6506–13.

Zhang, Xiang et al (2017),"Computational Fluid Dynamic Study of Thermal Effects of Open Doors of Refrigerated Vehicles." (September): 1–13.

Https://power.larc.nasa.gov/data.access.viewer.
Http://WWW.engineeringpage.com/technology/thermal/tubesize.htm.

APPENDICES

Appendix A

Table A.1: Pressure vs. Enthalpy carve of R134a.

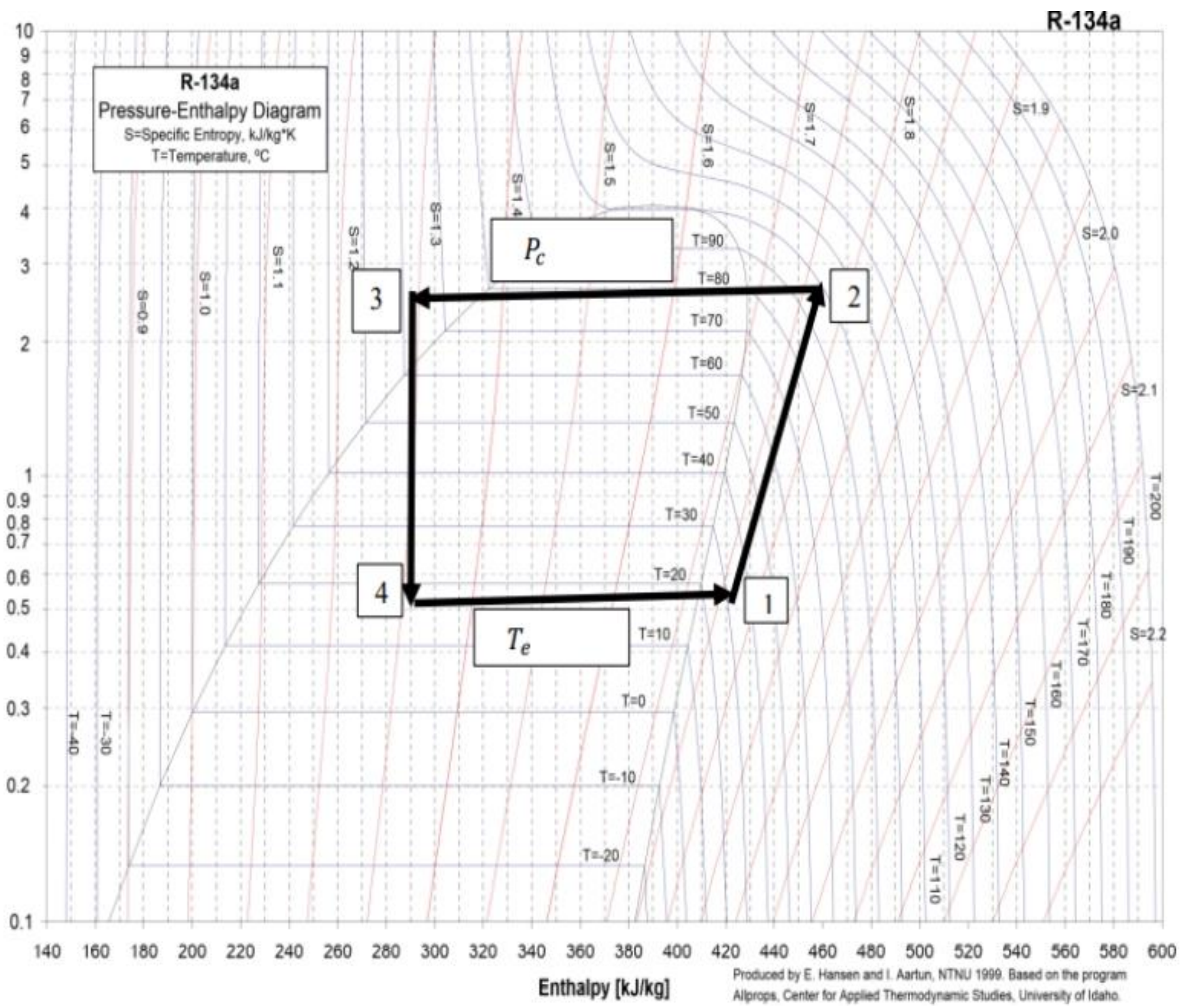

Appendix B

Table B.1: Saturation properties of refrigerant R134a

Temp	Pressure	volume(m^3/kg)		enthalpy (kJ/kg)			entropy (kJ/kg.K)		
deg C	kPa	vf	vg	hf	hfg	hg	sf	sfg	sg
-40	51.2	0.0007054	0.3611	0.00	225.86	225.86	0.0000	0.9687	0.9687
-36	62.9	0.0007112	0.2977	5.04	223.35	228.39	0.0214	0.9418	0.9632
-26	101.7	0.0007265	0.1896	17.76	216.92	234.68	0.0738	0.8777	0.9515
-24	111.3	0.0007297	0.1741	20.33	215.60	235.93	0.0841	0.8653	0.9495
-22	121.7	0.0007329	0.1601	22.91	214.26	237.17	0.0944	0.8531	0.9476
-20	132.7	0.0007362	0.1474	25.49	212.92	238.41	0.1046	0.8411	0.9457
-18	144.6	0.0007396	0.1359	28.09	211.55	239.64	0.1148	0.8292	0.9440
-12	185.2	0.0007499	0.1074	35.92	207.39	243.31	0.1451	0.7941	0.9392
-10	200.6	0.0007535	0.0996	38.55	205.97	244.52	0.1550	0.7827	0.9377
-8	216.9	0.0007571	0.0924	41.19	204.53	245.72	0.1650	0.7714	0.9364
-6	234.3	0.0007608	0.0859	43.84	203.08	246.92	0.1749	0.7602	0.9351
-4	252.7	0.0007646	0.0799	46.50	201.61	248.11	0.1848	0.7490	0.9338
-2	272.2	0.0007684	0.0744	49.17	200.12	249.29	0.1946	0.7380	0.9326
0	292.8	0.0007723	0.0693	51.86	198.60	250.46	0.2044	0.7271	0.9315
2	314.6	0.0007763	0.0647	54.55	197.07	251.62	0.2142	0.7162	0.9304
4	337.7	0.0007804	0.0604	57.25	195.53	252.78	0.2239	0.7055	0.9294
6	362.0	0.0007845	0.0564	59.97	193.95	253.92	0.2336	0.6948	0.9284
8	387.6	0.0007887	0.0528	62.69	192.36	255.05	0.2432	0.6842	0.9274
12	443.0	0.0007975	0.0463	68.19	189.11	257.29	0.2625	0.6632	0.9256
16	504.3	0.0008066	0.0408	73.73	185.74	259.47	0.2816	0.6424	0.9240
20	571.7	0.0008161	0.0360	79.32	182.28	261.60	0.3006	0.6218	0.9224
24	645.8	0.0008261	0.0319	84.98	178.70	263.68	0.3196	0.6014	0.9210
28	726.9	0.0008367	0.0283	90.70	175.00	265.69	0.3385	0.5811	0.9196
30	770.2	0.0008421	0.0266	93.58	173.09	266.67	0.3479	0.5710	0.9189
36	911.9	0.0008595	0.0224	102.33	167.17	269.50	0.3761	0.5407	0.9168
38	963.2	0.0008657	0.0211	105.29	165.12	270.41	0.3855	0.5307	0.9162
40	1016.6	0.0008720	0.0200	108.27	163.01	271.28	0.3949	0.5206	0.9155
42	1072.2	0.0008786	0.0189	111.26	160.88	272.14	0.4043	0.5105	0.9147
44	1130.1	0.0008854	0.0178	114.28	158.69	272.97	0.4136	0.5004	0.9140
48	1252.9	0.0008997	0.0160	120.39	154.16	274.55	0.4324	0.4800	0.9125
52	1385.4	0.0009150	0.0143	126.60	149.41	276.01	0.4513	0.4595	0.9108
56	1528.2	0.0009317	0.0128	132.92	144.40	277.32	0.4702	0.4387	0.9089
60	1681.8	0.0009498	0.0114	139.36	139.13	278.49	0.4892	0.4176	0.9068
70	2116.8	0.0010038	0.0087	156.14	124.37	280.51	0.5376	0.3624	0.9000
80	2633.2	0.0010773	0.0064	174.25	106.42	280.67	0.5880	0.3014	0.8894
90	3244.2	0.0011936	0.0046	194.78	82.49	277.27	0.6434	0.2272	0.8706
100	3972.4	0.0015357	0.0027	225.15	34.39	259.54	0.7232	0.0921	0.8153

Table B.2: Saturation properties of refrigerant R134a (concluded)

Pressure	Temp deg	volume (m^3/kg)		Energy(kJ/kg)		enthalpy (kJ/kg)			entropy (kJ/kg.K)		
kPa	C	vf	vg	uf	ug	hf	hfg	hg	sf	sfg	sg
60	-36.9	0.0007098	0.3112	3.8	209.1	3.9	223.9	227.8	0.0164	0.9481	0.9645
80	-31.1	0.0007185	0.2376	11.2	212.5	11.2	220.2	231.5	0.0472	0.9100	0.9572
100	-26.4	0.0007259	0.1926	17.2	215.2	17.3	217.2	234.5	0.0720	0.8799	0.9519
120	-22.3	0.0007324	0.1621	22.4	217.5	22.5	214.5	237.0	0.0928	0.8550	0.9478
140	-18.8	0.0007383	0.1402	27.0	219.6	27.1	212.1	239.2	0.1110	0.8337	0.9446
160	-15.6	0.0007437	0.1235	31.1	221.4	31.2	209.9	241.1	0.1270	0.8150	0.9420
180	-12.7	0.0007487	0.1104	34.9	223.0	35.0	207.9	242.9	0.1415	0.7982	0.9397
200	-10.1	0.0007534	0.0999	38.3	224.5	38.5	206.0	244.5	0.1547	0.7831	0.9378
220	-7.6	0.0007578	0.0912	41.5	225.9	41.7	204.3	245.9	0.1668	0.7693	0.9361
240	-5.4	0.0007620	0.0839	44.5	227.2	44.7	202.6	247.3	0.1780	0.7566	0.9347
260	-3.2	0.0007661	0.0777	47.3	228.4	47.5	201.0	248.6	0.1885	0.7448	0.9333
280	-1.2	0.0007699	0.0724	50.0	229.5	50.2	199.5	249.7	0.1984	0.7338	0.9322
300	0.7	0.0007737	0.0677	52.5	230.5	52.8	198.1	250.9	0.2077	0.7234	0.9311
320	2.5	0.0007773	0.0636	54.9	231.5	55.2	196.7	251.9	0.2165	0.7137	0.9301
340	4.2	0.0007808	0.0600	57.3	232.5	57.5	195.4	252.9	0.2248	0.7044	0.9293
360	5.8	0.0007842	0.0567	59.5	233.4	59.8	194.1	253.8	0.2328	0.6956	0.9284
400	8.9	0.0007907	0.0512	63.7	235.1	64.0	191.6	255.6	0.2477	0.6793	0.9270
500	15.7	0.0008060	0.0411	73.0	238.8	73.4	186.0	259.3	0.2803	0.6438	0.9241
600	21.6	0.0008200	0.0343	81.0	241.9	81.5	180.9	262.4	0.3081	0.6138	0.9219
700	26.7	0.0008332	0.0294	88.3	244.5	88.8	176.2	265.1	0.3324	0.5876	0.9200
800	31.3	0.0008459	0.0256	94.8	246.8	95.5	171.8	267.3	0.3541	0.5643	0.9184
900	35.5	0.0008581	0.0227	100.9	248.9	101.6	167.7	269.3	0.3739	0.5431	0.9170
1000	39.4	0.0008701	0.0203	106.5	250.7	107.4	163.7	271.0	0.3920	0.5237	0.9157
1200	46.3	0.0008935	0.0167	116.7	253.8	117.8	156.1	273.9	0.4245	0.4886	0.9131
1400	52.4	0.0009167	0.0141	126.0	256.4	127.3	148.9	276.2	0.4533	0.4573	0.9106
1600	57.9	0.0009401	0.0121	134.5	258.5	136.0	141.9	277.9	0.4792	0.4287	0.9080
1800	62.9	0.0009640	0.0106	142.4	260.2	144.1	135.1	279.2	0.5031	0.4020	0.9051
2000	67.5	0.0009888	0.0093	149.8	261.6	151.8	128.3	280.1	0.5252	0.3767	0.9020
2500	77.6	0.0010569	0.0069	167.1	263.5	169.7	111.2	280.9	0.5755	0.3170	0.8925
3000	86.2	0.0011413	0.0053	183.1	263.4	186.6	92.6	279.2	0.6215	0.2578	0.8792

Appendix C

Table C.1: Properties of refrigerant R134a

Temp.,* °C	Absolute Pressure, MPa	Density, kg/m³ Liquid	Volume, m³/kg Vapor	Enthalpy, kJ/kg Liquid	Enthalpy, kJ/kg Vapor	Entropy, kJ/(kg·K) Liquid	Entropy, kJ/(kg·K) Vapor	Specific Heat c_p, kJ/(kg·K) Liquid	Specific Heat c_p, kJ/(kg·K) Vapor	c_p/c_v Vapor	Velocity of Sound, m/s Liquid	Velocity of Sound, m/s Vapor	Viscosity, μPa·s Liquid	Viscosity, μPa·s Vapor	Thermal Cond., mW/(m·K) Liquid	Thermal Cond., mW/(m·K) Vapor	Surface Tension, mN/m	Temp.,* °C
−103.30a	0.00039	1591.2	35.263	71.89	335.07	0.4143	1.9638	1.147	0.585	1.163	1135.	127.	2186.6	6.63	—	—	28.15	−103.30
−100.00	0.00056	1581.9	25.039	75.71	337.00	0.4366	1.9456	1.168	0.592	1.161	1111.	128.	1958.2	6.76	—	—	27.56	−100.00
−90.00	0.00153	1553.9	9.7191	87.59	342.94	0.5032	1.8975	1.201	0.614	1.155	1051.	131.	1445.6	7.16	—	—	25.81	−90.00
−80.00	0.00369	1526.2	4.2504	99.65	349.03	0.5674	1.8585	1.211	0.637	1.151	999.	134.	1109.9	7.57	—	—	24.11	−80.00
−70.00	0.00801	1498.6	2.0528	111.78	355.23	0.6286	1.8269	1.215	0.660	1.148	951.	137.	879.6	7.97	125.8	—	22.44	−70.00
−60.00	0.01594	1471.0	1.0770	123.96	361.51	0.6871	1.8016	1.220	0.685	1.146	904.	139.	715.4	8.38	121.1	—	20.81	−60.00
−50.00	0.02948	1443.1	0.60560	136.21	367.83	0.7432	1.7812	1.229	0.712	1.146	858.	142.	594.3	8.79	116.5	7.12	19.22	−50.00
−40.00	0.05122	1414.8	0.36095	148.57	374.16	0.7973	1.7649	1.243	0.740	1.148	812.	144.	502.2	9.20	111.9	8.19	17.66	−40.00
−30.00	0.08436	1385.9	0.22596	161.10	380.45	0.8498	1.7519	1.260	0.771	1.152	765.	145.	430.4	9.62	107.3	9.16	16.13	−30.00
−28.00	0.09268	1380.0	0.20682	163.62	381.70	0.8601	1.7497	1.264	0.778	1.153	756.	145.	418.0	9.71	106.3	9.35	15.83	−28.00
−26.07b	0.10132	1374.3	0.19016	166.07	382.90	0.8701	1.7476	1.268	0.784	1.154	747.	146.	406.4	9.79	105.4	9.52	15.54	−26.07
−26.00	0.10164	1374.1	0.18961	166.16	382.94	0.8704	1.7476	1.268	0.785	1.154	747.	146.	406.0	9.79	105.4	9.53	15.53	−26.00
−24.00	0.11127	1368.2	0.17410	168.70	384.19	0.8806	1.7455	1.273	0.791	1.155	738.	146.	394.6	9.88	104.5	9.71	15.23	−24.00
−22.00	0.12160	1362.2	0.16010	171.26	385.43	0.8908	1.7436	1.277	0.798	1.156	728.	146.	383.6	9.96	103.6	9.89	14.93	−22.00
−20.00	0.13268	1356.2	0.14744	173.82	386.66	0.9009	1.7417	1.282	0.805	1.157	719.	146.	373.1	10.05	102.6	10.07	14.63	−20.00
−18.00	0.14454	1350.2	0.13597	176.39	387.89	0.9110	1.7399	1.286	0.812	1.159	710.	146.	363.0	10.14	101.7	10.24	14.33	−18.00
−16.00	0.15721	1344.1	0.12556	178.97	389.11	0.9211	1.7383	1.291	0.820	1.160	700.	147.	353.3	10.22	100.8	10.42	14.04	−16.00
−14.00	0.17074	1338.0	0.11610	181.56	390.33	0.9311	1.7367	1.296	0.827	1.162	691.	147.	344.0	10.31	99.9	10.59	13.74	−14.00
−12.00	0.18516	1331.8	0.10749	184.16	391.55	0.9410	1.7351	1.301	0.835	1.164	682.	147.	335.0	10.40	99.0	10.76	13.45	−12.00
−10.00	0.20052	1325.6	0.09963	186.78	392.75	0.9509	1.7337	1.306	0.842	1.166	672.	147.	326.3	10.49	98.0	10.93	13.16	−10.00
−8.00	0.21684	1319.3	0.09246	189.40	393.95	0.9608	1.7323	1.312	0.850	1.168	663.	147.	318.0	10.58	97.1	11.10	12.87	−8.00
−6.00	0.23418	1313.0	0.08591	192.03	395.15	0.9707	1.7310	1.317	0.858	1.170	654.	147.	309.9	10.67	96.2	11.28	12.58	−6.00
−4.00	0.25257	1306.6	0.07991	194.68	396.33	0.9805	1.7297	1.323	0.866	1.172	644.	147.	302.2	10.76	95.3	11.45	12.29	−4.00
−2.00	0.27206	1300.2	0.07440	197.33	397.51	0.9903	1.7285	1.329	0.875	1.175	635.	147.	294.7	10.85	94.3	11.62	12.00	−2.00
0.00	0.29269	1293.7	0.06935	200.00	398.68	1.0000	1.7274	1.335	0.883	1.178	626.	147.	287.4	10.94	93.4	11.79	11.71	0.00
2.00	0.31450	1287.1	0.06470	202.68	399.84	1.0097	1.7263	1.341	0.892	1.180	616.	147.	280.4	11.03	92.5	11.96	11.43	2.00
4.00	0.33755	1280.5	0.06042	205.37	401.00	1.0194	1.7252	1.347	0.901	1.183	607.	147.	273.6	11.13	91.6	12.13	11.14	4.00
6.00	0.36186	1273.8	0.05648	208.08	402.14	1.0291	1.7242	1.353	0.910	1.187	598.	147.	267.0	11.22	90.7	12.31	10.86	6.00
8.00	0.38749	1267.0	0.05284	210.80	403.27	1.0387	1.7233	1.360	0.920	1.190	588.	147.	260.6	11.32	89.7	12.48	10.58	8.00
10.00	0.41449	1260.2	0.04948	213.53	404.40	1.0483	1.7224	1.367	0.930	1.193	579.	146.	254.3	11.42	88.8	12.66	10.30	10.00
12.00	0.44289	1253.3	0.04636	216.27	405.51	1.0579	1.7215	1.374	0.939	1.197	569.	146.	248.3	11.52	87.9	12.84	10.02	12.00
14.00	0.47276	1246.3	0.04348	219.03	406.61	1.0674	1.7207	1.381	0.950	1.201	560.	146.	242.5	11.62	87.0	13.02	9.74	14.00
16.00	0.50413	1239.3	0.04081	221.80	407.70	1.0770	1.7199	1.388	0.960	1.206	550.	146.	236.8	11.72	86.0	13.20	9.47	16.00
18.00	0.53706	1232.1	0.03833	224.59	408.78	1.0865	1.7191	1.396	0.971	1.210	541.	146.	231.2	11.82	85.1	13.39	9.19	18.00
20.00	0.57159	1224.9	0.03603	227.40	409.84	1.0960	1.7183	1.404	0.982	1.215	532.	145.	225.8	11.92	84.2	13.57	8.92	20.00
22.00	0.60777	1217.5	0.03388	230.21	410.89	1.1055	1.7176	1.412	0.994	1.220	522.	145.	220.5	12.03	83.3	13.76	8.65	22.00
24.00	0.64566	1210.1	0.03189	233.05	411.93	1.1149	1.7169	1.420	1.006	1.226	512.	145.	215.4	12.14	82.4	13.96	8.38	24.00
26.00	0.68531	1202.6	0.03003	235.90	412.95	1.1244	1.7162	1.429	1.018	1.231	503.	144.	210.4	12.25	81.4	14.15	8.11	26.00
28.00	0.72676	1194.9	0.02829	238.77	413.95	1.1338	1.7155	1.438	1.031	1.238	493.	144.	205.5	12.36	80.5	14.35	7.84	28.00
30.00	0.77008	1187.2	0.02667	241.65	414.94	1.1432	1.7149	1.447	1.044	1.244	484.	143.	200.7	12.48	79.6	14.56	7.57	30.00
32.00	0.81530	1179.3	0.02516	244.55	415.90	1.1527	1.7142	1.457	1.058	1.251	474.	143.	196.0	12.60	78.7	14.76	7.31	32.00
34.00	0.86250	1171.3	0.02374	247.47	416.85	1.1621	1.7135	1.467	1.073	1.259	465.	142.	191.4	12.72	77.7	14.97	7.05	34.00
36.00	0.91172	1163.2	0.02241	250.41	417.78	1.1715	1.7129	1.478	1.088	1.267	455.	142.	186.9	12.84	76.8	15.19	6.78	36.00
38.00	0.96301	1154.9	0.02116	253.37	418.69	1.1809	1.7122	1.489	1.104	1.276	445.	141.	182.5	12.97	75.9	15.41	6.52	38.00
40.00	1.0165	1146.5	0.01999	256.35	419.58	1.1903	1.7115	1.500	1.120	1.285	436.	140.	178.2	13.10	75.0	15.64	6.27	40.00
42.00	1.0721	1137.9	0.01890	259.35	420.44	1.1997	1.7108	1.513	1.138	1.295	426.	140.	174.0	13.24	74.1	15.86	6.01	42.00
44.00	1.1300	1129.2	0.01786	262.38	421.28	1.2091	1.7101	1.525	1.156	1.306	416.	139.	169.8	13.38	73.1	16.10	5.76	44.00
46.00	1.1901	1120.3	0.01689	265.42	422.09	1.2185	1.7094	1.539	1.175	1.318	407.	138.	165.7	13.52	72.2	16.34	5.51	46.00
48.00	1.2527	1111.3	0.01598	268.49	422.88	1.2279	1.7086	1.553	1.196	1.331	397.	137.	161.7	13.67	71.3	16.59	5.26	48.00
50.00	1.3177	1102.0	0.01511	271.59	423.63	1.2373	1.7078	1.569	1.218	1.345	387.	137.	157.7	13.83	70.4	16.84	5.01	50.00
52.00	1.3852	1092.6	0.01430	274.71	424.35	1.2468	1.7070	1.585	1.241	1.360	377.	136.	153.8	13.99	69.5	17.10	4.76	52.00
54.00	1.4553	1082.9	0.01353	277.86	425.03	1.2562	1.7061	1.602	1.266	1.377	367.	135.	149.9	14.16	68.5	17.36	4.52	54.00
56.00	1.5280	1073.0	0.01280	281.04	425.68	1.2657	1.7051	1.621	1.293	1.395	358.	134.	146.1	14.33	67.6	17.63	4.28	56.00
58.00	1.6033	1062.8	0.01212	284.25	426.29	1.2752	1.7041	1.641	1.322	1.416	348.	133.	142.3	14.51	66.7	17.91	4.04	58.00
60.00	1.6815	1052.4	0.01146	287.49	426.86	1.2847	1.7031	1.663	1.354	1.438	338.	132.	138.6	14.71	65.8	18.19	3.81	60.00
62.00	1.7625	1041.7	0.01085	290.77	427.37	1.2943	1.7019	1.686	1.388	1.463	328.	131.	134.9	14.91	64.9	18.48	3.57	62.00
64.00	1.8464	1030.7	0.01026	294.08	427.84	1.3039	1.7007	1.712	1.426	1.490	318.	129.	131.2	15.12	63.9	18.78	3.34	64.00
66.00	1.9334	1019.4	0.00970	297.44	428.25	1.3136	1.6993	1.740	1.468	1.522	308.	128.	127.5	15.35	63.0	19.09	3.12	66.00
68.00	2.0234	1007.7	0.00917	300.84	428.61	1.3234	1.6979	1.772	1.515	1.557	298.	127.	123.9	15.59	62.1	19.40	2.89	68.00
70.00	2.1165	995.6	0.00867	304.29	428.89	1.3332	1.6963	1.806	1.567	1.597	287.	126.	120.3	15.85	61.2	19.72	2.67	70.00
72.00	2.2130	983.1	0.00818	307.79	429.10	1.3430	1.6945	1.846	1.626	1.642	277.	124.	116.7	16.12	60.3	20.05	2.46	72.00
74.00	2.3127	970.0	0.00772	311.34	429.23	1.3530	1.6926	1.890	1.693	1.695	267.	123.	113.1	16.41	59.3	20.39	2.24	74.00
76.00	2.4159	956.5	0.00728	314.96	429.27	1.3631	1.6905	1.941	1.770	1.757	256.	121.	109.4	16.73	58.4	20.74	2.03	76.00
78.00	2.5227	942.3	0.00686	318.65	429.20	1.3733	1.6881	2.000	1.861	1.830	246.	120.	105.8	17.08	57.5	21.09	1.83	78.00
80.00	2.6331	927.4	0.00646	322.41	429.02	1.3837	1.6855	2.069	1.967	1.917	235.	118.	102.1	17.46	56.6	21.46	1.63	80.00
85.00	2.9259	886.2	0.00550	332.27	427.91	1.4105	1.6775	2.313	2.348	2.231	207.	113.	92.7	18.59	54.3	22.41	1.15	85.00
90.00	3.2445	836.9	0.00461	343.01	425.48	1.4392	1.6663	2.766	3.064	2.832	178.	108.	82.6	20.15	—	—	0.72	90.00
95.00	3.5916	771.6	0.00374	355.43	420.60	1.4720	1.6490	3.961	4.942	4.424	145.	102.	70.9	22.59	—	—	0.33	95.00
100.00	3.9721	646.7	0.00265	374.02	407.08	1.5207	1.6093	—	—	—	105.	94.	53.0	28.86	—	—	0.03	100.00
101.03c	4.0560	513.3	0.00195	389.79	389.79	1.5593	1.5593	∞	∞	∞	0.	0.	—	—	∞	∞	0.	101.03

*temperatures are on the ITS–90 scale a = triple point b = normal boiling point c = critical point

Table C.2: Superheated properties of refrigerant R134a

T °C	v m³/kg	u kJ/kg	h kJ/kg	s kJ/kg-K	v m³/kg	u kJ/kg	h kJ/kg	s kJ/kg-K	v m³/kg	u kJ/kg	h kJ/kg	s kJ/kg-K
	P = 0.50 MPa (T_{sat} = 15.71°C)				P = 0.60 MPa (T_{sat} = 21.55°C)				P = 0.70 MPa (T_{sat} = 26.69°C)			
Sat.	0.041118	238.75	259.30	0.9240	0.034295	241.83	262.40	0.9218	0.029361	244.48	265.03	0.9199
20	0.042115	242.40	263.46	0.9383								
30	0.044338	250.84	273.01	0.9703	0.035984	249.22	270.81	0.9499	0.029966	247.48	268.45	0.9313
40	0.046456	259.26	282.48	1.0011	0.037865	257.86	280.58	0.9816	0.031696	256.39	278.57	0.9641
50	0.048499	267.72	291.96	1.0309	0.039659	266.48	290.28	1.0121	0.033322	265.20	288.53	0.9954
60	0.050485	276.25	301.50	1.0599	0.041389	275.15	299.98	1.0417	0.034875	274.01	298.42	1.0256
70	0.052427	284.89	311.10	1.0883	0.043069	283.89	309.73	1.0705	0.036373	282.87	308.33	1.0549
80	0.054331	293.64	320.80	1.1162	0.044710	292.73	319.55	1.0987	0.037829	291.80	318.28	1.0835
90	0.056205	302.51	330.61	1.1436	0.046318	301.67	329.46	1.1264	0.039250	300.82	328.29	1.1114
100	0.058053	311.50	340.53	1.1705	0.047900	310.73	339.47	1.1536	0.040642	309.95	338.40	1.1389
110	0.059880	320.63	350.57	1.1971	0.049458	319.91	349.59	1.1803	0.042010	319.19	348.60	1.1658
120	0.061687	329.89	360.73	1.2233	0.050997	329.23	359.82	1.2067	0.043358	328.55	358.90	1.1924
130	0.063479	339.29	371.03	1.2491	0.052519	338.67	370.18	1.2327	0.044688	338.04	369.32	1.2186
140	0.065256	348.83	381.46	1.2747	0.054027	348.25	380.66	1.2584	0.046004	347.66	379.86	1.2444
150	0.067021	358.51	392.02	1.2999	0.055522	357.96	391.27	1.2838	0.047306	357.41	390.52	1.2699
160	0.068775	368.33	402.72	1.3249	0.057006	367.81	402.01	1.3088	0.048597	367.29	401.31	1.2951
	P = 0.80 MPa (T_{sat} = 31.31°C)				P = 0.90 MPa (T_{sat} = 35.51°C)				P = 1.00 MPa (T_{sat} = 39.37°C)			
Sat.	0.025621	246.79	267.29	0.9183	0.022683	248.85	269.26	0.9169	0.020313	250.68	270.99	0.9156
40	0.027035	254.82	276.45	0.9480	0.023375	253.13	274.17	0.9327	0.020406	251.30	271.71	0.9179
50	0.028547	263.86	286.69	0.9802	0.024809	262.44	284.77	0.9660	0.021796	260.94	282.74	0.9525
60	0.029973	272.83	296.81	1.0110	0.026146	271.60	295.13	0.9976	0.023068	270.32	293.38	0.9850
70	0.031340	281.81	306.88	1.0408	0.027413	280.72	305.39	1.0280	0.024261	279.59	303.85	1.0160
80	0.032659	290.84	316.97	1.0698	0.028630	289.86	315.63	1.0574	0.025398	288.86	314.25	1.0458
90	0.033941	299.95	327.10	1.0981	0.029806	299.06	325.89	1.0860	0.026492	298.15	324.64	1.0748
100	0.035193	309.15	337.30	1.1258	0.030951	308.34	336.19	1.1140	0.027552	307.51	335.06	1.1031
110	0.036420	318.45	347.59	1.1530	0.032068	317.70	346.56	1.1414	0.028584	316.94	345.53	1.1308
120	0.037625	327.87	357.97	1.1798	0.033164	327.18	357.02	1.1684	0.029592	326.47	356.06	1.1580
130	0.038813	337.40	368.45	1.2061	0.034241	336.76	367.58	1.1949	0.030581	336.11	366.69	1.1846
140	0.039985	347.06	379.05	1.2321	0.035302	346.46	378.23	1.2210	0.031554	345.85	377.40	1.2109
150	0.041143	356.85	389.76	1.2577	0.036349	356.28	389.00	1.2467	0.032512	355.71	388.22	1.2368
160	0.042290	366.76	400.59	1.2830	0.037384	366.23	399.88	1.2721	0.033457	365.70	399.15	1.2623
170	0.043427	376.81	411.55	1.3080	0.038408	376.31	410.88	1.2972	0.034392	375.81	410.20	1.2875
180	0.044554	386.99	422.64	1.3327	0.039423	386.52	422.00	1.3221	0.035317	386.04	421.36	1.3124
	P = 1.20 MPa (T_{sat} = 46.29°C)				P = 1.40 MPa (T_{sat} = 52.40°C)				P = 1.60 MPa (T_{sat} = 57.88°C)			
Sat.	0.016715	253.81	273.87	0.9130	0.014107	256.37	276.12	0.9105	0.012123	258.47	277.86	0.9078
50	0.017201	257.63	278.27	0.9267								
60	0.018404	267.56	289.64	0.9614	0.015005	264.46	285.47	0.9389	0.012372	260.89	280.69	0.9163
70	0.019502	277.21	300.61	0.9938	0.016060	274.62	297.10	0.9733	0.013430	271.76	293.25	0.9535
80	0.020529	286.75	311.39	1.0248	0.017023	284.51	308.34	1.0056	0.014362	282.09	305.07	0.9875
90	0.021506	296.26	322.07	1.0546	0.017923	294.28	319.37	1.0364	0.015215	292.17	316.52	1.0194
100	0.022442	305.80	332.73	1.0836	0.018778	304.01	330.30	1.0661	0.016014	302.14	327.76	1.0500
110	0.023348	315.38	343.40	1.1118	0.019597	313.76	341.19	1.0949	0.016773	312.07	338.91	1.0795
120	0.024228	325.03	354.11	1.1394	0.020388	323.55	352.09	1.1230	0.017500	322.02	350.02	1.1081
130	0.025086	334.77	364.88	1.1664	0.021155	333.41	363.02	1.1504	0.018201	332.00	361.12	1.1360
140	0.025927	344.61	375.72	1.1930	0.021904	343.34	374.01	1.1773	0.018882	342.05	372.26	1.1632
150	0.026753	354.56	386.66	1.2192	0.022636	353.37	385.07	1.2038	0.019545	352.17	383.44	1.1900
160	0.027566	364.61	397.69	1.2449	0.023355	363.51	396.20	1.2298	0.020194	362.38	394.69	1.2163
170	0.028367	374.78	408.82	1.2703	0.024061	373.75	407.43	1.2554	0.020830	372.69	406.02	1.2421
180	0.029158	385.08	420.07	1.2954	0.024757	384.10	418.76	1.2807	0.021456	383.11	417.44	1.2676

Appendix D

Thermophysical properties of air at atmospheric pressure

T (K)	ρ (kg/m^3)	C_p (kJ/kg K)	μ (kg/m s $\times 10^5$)	ν (m^2/s $\times 10^6$)	k (W/mk)	α (m^2/s $\times 10^4$)	Pr
100	3.9010	1.0266	0.6924	1.923	0.009246	0.02501	0.770
150	2.3675	1.0099	1.0283	4.343	0.013735	0.05745	0.753
200	1.7687	1.0061	1.3289	7.49	0.01809	0.10165	0.739
250	1.4128	1.0053	1.488	9.49	0.02227	0.13161	0.722
300	1.1774	1.0057	1.983	15.68	0.02624	0.2216	0.708
350	0.9980	1.0090	2.075	20.76	0.03003	0.2983	0.697
400	0.8826	1.0140	2.286	25.90	0.03365	0.3760	0.689
450	0.7833	1.0207	2.284	28.86	0.03707	0.4222	0.683
500	0.7048	1.0295	2.671	37.90	0.04038	0.5564	0.680
550	0.6423	1.0392	2.848	44.34	0.04360	0.6532	0.680
600	0.5879	1.0551	3.018	51.34	0.04649	0.7512	0.680
650	0.5430	1.0635	3.177	58.51	0.04953	0.8578	0.682
700	0.5030	1.0752	3.322	66.25	0.05230	0.9672	0.684
750	0.4709	1.0856	3.481	73.91	0.05509	1.0774	0.686
800	0.4405	1.0978	3.625	82.29	0.05779	1.1951	0.689
850	0.4149	1.1095	3.765	90.75	0.06028	1.3097	0.692
900	0.3925	1.1212	3.899	99.3	0.06269	1.4271	0.696
950	0.3716	1.1321	4.023	108.2	0.06525	1.5610	0.699
1000	0.3524	1.1417	4.152	117.8	0.06752	1.6779	0.702
1100	0.3204	1.160	4.44	136.6	0.0732	1.969	0.704
1200	0.2947	1.179	4.92	159.1	0.0782	2.251	0.707
1300	0.2707	1.197	4.93	182.1	0.0837	2.583	0.705
1400	0.2515	1.214	5.17	205.5	0.0891	2.920	0.705
1500	0.2355	1.230	5.40	229.1	0.0946	3.262	0.705
1600	0.2211	1.248	5.63	254.5	0.100	3.609	0.705

Appendix E

Thermocouple calibration

Thermocouples are sensors used to measure temperature by forming a junction between two wires of separate metals. One end of the junction is called the measurement “hot” junction and the other end is called the reference “cold” junction. When there is a temperature variation in the joint, voltage is created and this voltage can be converted into temperature with a thermocouple reference table or data logger. Thermocouples can be calibrated using a reference thermometer in a temperature calibration test by comparing both measurement values of a reference thermometer and other thermometers. The thermocouple used in this study is a K-type four channel thermocouple and a constant high temperature bath was used for the calibration. A laboratory digital thermocouple was used as a reference for the calibration and the results of the temperature measurement of both the reference and the K-type thermocouple is shown in Table E.1

Table E.1: Water temperature measuring test by using K-type thermocouples and digital thermometer

Time, (minutes)	Digital thermometer reading, T_1 (^{0}c)	K-type thermocouple reading, T_2 (^{0}c)	Uncertainty(^{0}c) $T_1 - T_2$	Percentage uncertainty (%) $\frac{T_1 - T_2}{T_1} * 100\%$
1	26.9	26.6	0.3	1.1
2	29.1	28.9	0.2	0.6
3	30.4	30.2	0.2	0.6
4	32.8	32	0.8	2.4
5	35.4	34.3	1.1	3.1
6	37.6	37	0.6	1.5
7	39.4	38.8	0.6	1.5
8	42	41.1	0.9	2.1
9	45.9	45.5	0.4	0.8
10	51	49.7	1.3	2.5
11	51.5	51.4	0.1	0.2
12	54	53	1	1.8
13	57	56.5	0.5	0.8
14	58.5	57.7	0.8	1.3
15	61.7	61	0.7	1.1
16	62.5	62	0.5	0.8
17	65.6	64.7	0.9	1.3
18	67.4	66.8	0.6	0.8
19	68.7	68.4	0.3	0.4
20	68.7	68.5	0.2	0.2
21	71.4	71.3	0.1	0.1
22	73.7	73.1	0.6	0.8
23	76.2	75.3	0.9	1.1
24	77.7	77.3	0.4	0.5
25	78.9	78.6	0.3	0.3
26	80.5	79.9	0.6	0.7
27	81.3	80.9	0.4	0.4
28	82.4	82	0.4	0.4
29	83.3	83	0.3	0.3
30	84.3	84.2	0.1	0.1
		Average	0.502857	0.9

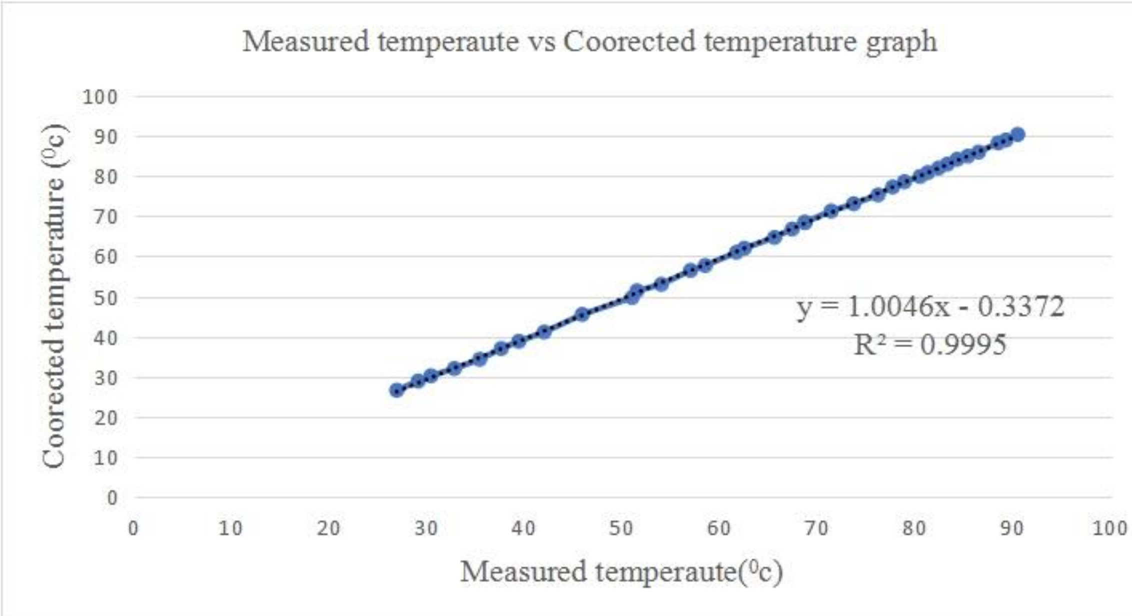

Four-Channel Digital Thermometer Specifications

- Serial number: HT-9815
- Temperature range:0-800℃
- Power supply: 9V

Weight: approx. 250g